Novel *in vitro* Microfluidic Platform for Studying Osteocyte Mechanobiology

by

Liangcheng Henry Xu

A thesis submitted in conformity with the requirements
for the degree of Doctor of Philosophy

Institute of Biomedical Engineering
University of Toronto

Novel in vitro Microfluidic Platform for Studying Osteocyte Mechanobiology

Liangcheng Henry Xu

Doctor of Philosophy

Institute of Biomedical Engineering
University of Toronto

2021

Abstract

Osteocytes are the major mechanosensing cells during bone remodeling. Current bone mechanotransduction research use macro-scale devices such as flow chambers; however *in vitro* microfluidic devices provide an optimal tool to better understand this biological process with its flexible design and high-throughput capabilities. Our recent work on co-culture platform has demonstrated the feasibility of building more complex microfluidic devices for osteocyte mechanotransduction studies. However, there still lacks a robust system where multi-physiological flow conditions are applied to bone cells during intercellular communication. I aim to improve the *in vitro* experimental platform for osteocyte mechanotransduction studies by 1) designing a novel multi-shear stress co-culture microfluidic device to study osteocyte intercellular communication; 2) testing the novel OCY454 osteocyte cell line to enable *in vitro* studies of osteocyte-osteoblast cross-talk; and 3) investigate magnetically actuated beams as a new method for *in vitro* fluid flow stimulation of osteocytes. I demonstrated that osteocytes seeded in the novel microfluidic device respond to different levels of fluid shear stress in each channel by varying amount of secreted RANKL. Furthermore, co-cultured osteoclast precursors had suppressed differentiation when next to osteocytes stimulated with high fluid shear stress.

This microfluidic device can provide a new platform for researchers to further understand how mechanically stimulated osteocytes affect the bone remodelling process without complicated *in vivo* models. I also validated the response of OCY454 osteocytes to fluid shear stress, demonstrating changes in key indicators such as extracellular sclerostin level and intracellular calcium response, as well as capability to drive effector cell differentiation. This new cell line can help unlock further understanding of the role sclerostin plays in bone remodelling, and potentially give rise to novel pharmaceutical targets that can be used for treatment of bone diseases. Using novel magnetically actuated micro-beams, I experimented with a new method of generating localized fluid shear stress on osteocytes. This novel magnetic actuator can help us better understand how intercellular communication propagates within an osteocyte network when stimulated with localized shear stress. With development of new *in vitro* technical approaches to study osteocyte mechanotransduction, a better understanding of the bone remodeling process can be obtained.

Acknowledgments

Here I want to acknowledge individuals that have had tremendous impact on me throughout my PhD career. I would like to first thank my supervisor Dr. Lidan You for all her support and supervision. Lidan generously provided me with academic support in all the projects I was involved in, and she was able to offer guidance every time I run into difficulties or impedances during my research. Lidan provided a very encouraging research environment, allowing us to attempt different research directions and chase after the questions that we are really interested in. I am very grateful to have her as a supervisor throughout my PhD career. As well, I would like to thank my committee members Dr. Edmond Young and Dr. Eric Diller. They have guided me away from stray path and provided their expertise whenever I needed them. I would also like to thank my colleagues in the You lab for being an important part of my journey here. I want to thank Kevin Middleton for all his coaching during the first years of my program, showing me the ways around the lab and the ropes to becoming a successful PhD candidate; I want to thank Vivian Ma for all her compassionate support and counselling, answering all the biological questions that I ever had; I want to thank Christina Mei for her help and support during all my experiments, acting as both an assuring teammate and a reassuring friend; and I want to thank Delphine Lin for her patience and understanding, always being there to help in whatever way she can during a hectic period of time. I would also like to thank the other graduate students in You lab, Madeleine Bareau, Tony Ouyang, and Chao Liu, for creating such a welcoming and supportive environment in MB308, where I am very proud to call my second home for the past 5 years. Special thanks to all the undergraduate students that have worked with me either in the summer, during their thesis, or in a capstone group. They have helped me develop valuable leadership experience, and in many cases made significant contribution to my own research project. Throughout my time here in IBBME, I have been fortunate enough to have made many friends outside my research lab. Erika, Ben, Rick, Sheldon, Onaizah (wrote a paper together), and Buddhisha (iARC co-chair), you have all enriched my life here in UofT, and I am very fortunate to have known every single one of you.

Lastly, I would like to thank my parents, my family, and my girlfriend. My parents have been the cornerstone of my PhD career. They have selflessly provided for me both financially and emotionally without objection, and I am so lucky and grateful for them to support my education.

My grandparents were always there to calm me down and remind me of the finer things in life. My cousins Xuan and Julie, who were great roommates and companions at a time when we are each finding our own path. And last but not least my girlfriend Danchen, for providing me with a shoulder to cry on, a story to laugh about, and a partner to count on. You have all been an important part of my life, and I am truly thankful that you have all been here by my side for the past 5 years.

Table of Contents

Contents

Acknowledgments iv

Table of Contents vi

List of Figures x

List of Appendices xii

Chapter 1 1

1 Introduction 1

1.1 Background on Bone cells 1

1.1.1 Osteocyte pericellular microenvironment 3

1.2 *In vitro* Devices 5

1.2.1 Platform for *in vitro* Studies of Mechanobiology in other systems 5

1.2.2 Platform for Osteocyte *in vitro* Studies 6

1.2.3 Platform for Osteoblast *in vitro* Studies 8

1.2.4 Platform for Osteoclast *in vitro* Studies 9

1.3 Thesis Objectives 10

Chapter 2 12

2 Multi-shear Co-culture Microfluidic Platform for Osteocyte Mechanotransduction Studies 12

2.1 Introduction and Background 12

2.2 Methods 13

2.2.1 Design and fabrication of co-culture platform 13

2.2.2 Cell culture and seeding in co-culture platform 14

2.2.3 Calcium response quantification 15

2.2.4 ELISA quantification of RANKL expression 15

2.2.5 Osteoclast-osteocyte co-culture experiment 16

2.2.6 Particle flow velocimetry....16
2.2.7 Statistics....16
2.3 Experimental Results....17
2.3.1 Flow rate validation....17
2.3.2 Ca^{2+} Response from osteocytes....18
2.3.3 RANKL released from osteocytes....19
2.3.4 Osteoclast differentiation in co-culture....20
2.3.5 Effect of zoledronic acid on osteoclast differentiation in co-culture....22
2.4 Discussion....23
2.5 Conclusion....25
Chapter 3....26
3 Validating OCY454 Cell Model for Osteocyte Mechanotransduction Studies....26
3.1 Introduction and Background....26
3.2 Methods....27
3.2.1 Cell Culture....27
3.2.2 Parallel Plate Flow Chamber Experiments....28
3.2.3 Sclerostin and RANKL/OPG ELISA....28
3.2.4 Intracellular Calcium Response Quantification....29
3.2.5 Fluid Flow and Quantification of ATP Synthesis....29
3.2.6 Osteoblast Conditioning Experiment....29
3.2.7 Quantification of extracellular ALP activity....29
3.2.8 Calcium Deposit Quantification....30
3.2.9 Osteoclast Conditioning Experiment and TRAP Staining....30
3.2.10 Statistics....30
3.3 Experimental Results....30

3.3.1 Sclerostin Expression under OFF 30
3.3.2 Intracellular Calcium Response after Fluid Flow 31
3.3.3 ATP Release after Fluid Flow 32
3.3.4 Flow Stimulated OCY454 Affects Osteoblast Activity 34
3.3.5 OCY454 Affects Osteoclast Differentiation 37
3.4 Discussion 37
3.5 Conclusion 40
Chapter 4 41
4 Magnetically Actuated Beam for Osteocyte Stimulation 41
4.1 Introduction and Background 41
4.2 Methods 43
4.2.1 Design and fabrication 43
4.2.2 Experimental design 45
4.2.3 Finite element simulations and analysis 49
4.2.4 Analytical model 50
4.2.5 Cell culture 51
4.2.6 Intracellular calcium imaging 51
4.3 Contribution to Overall Project 52
4.4 Experimental Results and Discussion 52
4.5 Conclusion 56
Chapter 5 58
5 Summary 58
5.1 Contributions 58
5.2 Limitations 59
5.3 Future Directions 61

References.....63
Appendices.....85
Appendix I: Mechanical Stimulation of Tendon Cells.....85
Copyright Acknowledgements.....90

List of Figures

Figure 2.1: Basic co-culture microfluidic design.

Figure 2.2: Calcium response results from MLO-Y4 osteocytes seeded in the co-culture device.

Figure 2.3: Quantification of soluble RANKL collected from osteocytes channel.

Figure 2.4: Quantification of osteoclast differentiation when co-cultured with osteocytes.

Figure 2.5: Osteoclast differentiation under the treatment of ZA.

Figure 3.1: Sclerostin and RANKL/OPG Expression from OCY454 Cells.

Figure 3.2: OCY454 Calcium response.

Figure 3.3: Total ATP level from OCY454.

Figure 3.4: Osteoblast activity.

Figure 3.5: Osteoclast activity.

Figure 4.1: The fabrication process for the magnetically-actuated beam.

Figure 4.2: Schematics showing the magnetic actuator.

Figure 4.3: Experimental setup to test magnetic actuator.

Figure 4.4: Simulation results for magnetic beam flow generation.

Figure 4.5: Osteocyte calcium response under magnetic actuator stimulation.

Figure 4.6: Sample calcium response curves resulting from magnetic actuation.

Figure I.1: Sample data from strain sensor.

Figure I2: Example of mechanical testing result for a dog tendon.

Figure I.3: Gene expression changes for primary tendon cells

List of Appendices

Appendix I: Mechanical Stimulation of Tendon Cells

Chapter 1

1 Introduction

Bone remodelling is an important process that is responsible for bone growth and recovery from bone tissue injuries, thus understanding the mechanism underlying the process is crucial to finding clinical solutions for bone disorders such as osteoporosis [1]. It is known that mechanical loading is one of the key factors affecting bone remodeling [2]. Current research efforts in the field have been focused on understanding the molecular signaling pathways between the different major cell groups in bone remodelling, namely osteocytes, osteoblasts, and osteoclasts. The central dogma of bone remodelling has been unmasked, where it is understood that osteoblasts act as bone formation cells, osteoclasts act as bone resorption cells, and osteocytes are the mechanosensory cells responsible for regulating osteoclast and osteoblast activity [3]. Although advances in molecular techniques have led a great deal of insight into the various key signalling factors in play during bone remodelling, there still lacks development of *in vitro* tools and platforms where bone remodelling can be studied in the proper environmental context. There is a need to take a look at current existing *in vitro* devices and tools for studying bone cells, and prospect for future directions in which these platforms can take to further advance understanding of bone cell biology.

1.1 Background on Bone cells

As the bone resorption cells, multi-nucleated osteoclasts are derived from haematopoietic lineage precursor cells and its differentiation is promoted by very key bone remodelling factors such as macrophage colony stimulating factor (M-CSF) and receptor activator of nuclear factor kappa-B ligand (RANKL) [4]. Osteoclasts function by forming a tight seal around a resorption area, and degrade underlying bone matrix by increasing the acidity of the sealed region through releasing hydrogen ions. A common way to identify properly differentiated osteoclasts is through staining of tartrate resistant acid phosphatase (TRAP), a highly expressed and localized enzyme within the osteoclast [5]. It has been shown that a mutation in the gene for encoding RANKL and its receptor resulted in high bone mass, showing a disruption of the balance in the bone remodelling process [6]. Although mainly acting as the bone forming cell, osteoblasts also excrete main signalling factors that promote osteoclastogenesis, making it an important component in

balancing the bone remodelling process. Derived from stromal mesenchymal stem cell, the differentiation of osteoprogenitor cells into osteoblasts is regulated by the Wnt and Smad-dependent bone morphogenetic protein (BMP) pathways [7]. It is known that parathyroid hormones (PTH) increases osteoblast numbers and thus improve bone formation, thus clinically established as a treatment of osteoporosis [8]. Once osteoblast has completed its function, it can either become apoptotic, or become the osteocytes that are embedded in the bone matrix. It has recently been discovered that osteocyte is the main mechanosensory cell in bone tissue, and its ablation lead to malfunctioned bone remodelling process which can result in increased bone fragility [9]. It is understood that osteocyte act as a regulator for osteoblast by secreting inhibitors to osteoblastogenesis such as sclerostin [10], but furthermore it has been revealed that apoptotic osteocytes also recruit osteoclast precursors through upregulation of RANKL, showing that osteocyte is the key signalling cell group in the whole bone remodelling process controlling both the bone-forming and bone-resorbing rates [11]. Understanding how osteocytes respond to different loading conditions would be essential to the developments of therapeutic targets for bone related diseases, while probing for the molecular signalling pathways between osteocytes and other bone cells can help map a more complete picture of the bone remodelling process. Previously published literature on osteocytes and their role during bone remodelling is heavily based on well-established flow chamber platforms and transferring of conditioned media to simulate intercellular communication [12–15]. Although these systems are useful for preliminary studies to understand basic cellular behaviour, they lack the representation of real-time intercellular signalling events that occur *in vivo*. Furthermore, conditional media based experiments have a very fundamental problem in that they only represent a uni-directional signalling event, whereas co-culture *in vitro* models would allow secretory factors from both cell populations to affect each other, coalescing multiple signalling events into intercellular signalling networks. This allows researchers to fully capture the relationship between different cell populations that would not appear in conditioned media based studies.

Current *in vivo* studies of osteocyte has been focused on using transgenic reporter mice to study the expression of important osteocyte factors, the most prominent one been the Sost gene and its protein product sclerostin [16]. Mechanical unloading experiments done using mice models showed that weightlessness induced osteocyte apoptosis, which lead to uncontrolled bone resorption and loss of bone strength [17]. It has been shown *in vivo* that the protein sclerostin is

an important protein in bone remodelling signalling pathways, and its expression levels are reduced in osteocytes when stimulated by mechanical loading [18]. Similarly, osteocyte response to mechanical unloading is based on antagonizing wnt/β-catenin signaling that is also mediated by the protein sclerostin [19]. Furthermore, the correlation between sclerostin and the process of bone remodelling has also been identified *in vivo* through mechanical loading experiments, where sclerostin levels significantly decreased post loading through the β-catenin signaling pathway [20]. In recent years, there have been a significant increase in the number of *in vitro* osteocyte studies due to the availability of stable osteocyte-like cell lines such as MLO-Y4 [21] and progenitor cell line MLO-A5 [22]. These cell lines provided the necessary tool required to probe for cellular response of osteocytes to mechanical stress, as well as molecular signalling pathways in the whole bone remodelling process. The effect of prominent signalling factors such as RANKL has been identified to be of crucial importance in bone homeostasis and control of osteoblast and osteoclasts *in vitro* [23]. Even less known molecules such as the sphingosine-1-phosphate has been found to be responsible for mechanical activation of osteocytes in studies using MLO-Y4 cells [24]. As stated previously, sclerostin is a crucial marker of cell response to mechanical loading, however the traditional MLO-Y4 cells do not express sclerostin as a soluble factor [25]. This issue has been recently solved by the establishment of a novel osteocyte-like cell line, the OCY 454 by Dr. Pajevic's group, and using *in vitro* methods they have shown that sclerostin expression of OCY 454 mimics those observed *in vivo* when mechanically stimulated [26]. There is a need now to validate whether OCY 454 osteocytes can be a candidate cell model for *in vitro* studies of osteocyte-osteoblast intercellular communication during bone remodelling.

Although many insights have been made into the bone remodelling process and the functions of the three major cell groups, there is still a lack of fundamental understanding of how these cells respond directly to different levels of mechanical stimuli. As it is known that mechanical loading is the key stimulus factor affecting the bone remodelling process [27], there is motivation to adapt various *in vitro* platforms and tools that can aid in discovering the role of mechanical loading not just in the overall bone remodelling process, but its distinctive effect on the communication between the different bone cells.

1.1.1 Osteocyte pericellular microenvironment

Osteocytes *in vivo* are situated in lacuna-canaliculi networks, where cell processes extend through canaliculi to for cell-cell connections that allow for the propagation of signals,

particularly from stimulation due to mechanical loading. It has been suggested that the pericellular matrix surrounding the osteocyte plays an important role in how osteocytes sense mechanical loading from the tissue level. Several different views and models have been establish to explain how osteocytes can "read" the mechanical cues through various input mechanisms.

The immediate and most common cellular function when it comes to mechanical sensing is the strain on its cytoskeleton. Although it has been shown that cellular strain caused by fluid shear stress at 2, 8, and 16 dynes/cm^2 correlated with increases in intracellular calcium release [28], finite element modelling and *in vivo* studies have provided evidence for significant strain amplification at the lacuna level when using standard tissue level strain [29,30]. Cellular responses are only observed *in vitro* when osteocytes experience strains near 10%, which deviates significantly from physiological levels [31]. These studies show that simple cytoskeleton compression might not be all there is to the mechano-sensing capabilities of osteocytes.

Researchers have identified that the pericellular matrix of the osteocyte might contain the answer to the strain amplification previously identified. Work done by You et al. proposed a model where fluid drag force is sensed by coupling of pericellular matrix with the cell's actin cytoskeleton. This coupling allows for up to 100 fold amplification of the strain sensed by the osteocyte [32]. This was later validated experimentally, where tethering elements was identified in the pericellular space surrounding the osteocyte process, which could be adhesion proteins attached to collagen fibre that is responsible for sensing the drag force within the fluid [33,34]. Recent studies have also observed remodelling at the pericellular level surrounding the osteocyte, where both the extracellular matrix and the bone tissue are remodeled to better adapt the osteocyte for strain-sensing purposes [35,36].

Osteocyte primary cilia has also been suggested to be a key component for mechano-sensing functions [37]. It has been shown *in vitro* that the lengthening of the primary cilia through fenoldopam and lithium showed a significant increase in osteopontin and cAMP expression [38]. Studies have also proven that intracellular calcium fluctuations exist in osteocyte primary cilium and are modulated by TRPV4 [39], further strengthening the role of osteocyte primary cilia play in mechano-sensing functions. Although *ex vivo* studies have quantified that only a low

percentage of osteocytes contain a primary cilia [40], due to the nature of signal propagation through osteocyte networks during mechanical loading [41], these limited osteocytes identified with primary cilium can still play a pivotal role in the overall mechano-sensing function of the cell.

1.2 *In vitro* Devices

1.2.1 Platform for *in vitro* Studies of Mechanobiology in other systems

Microfluidic application in understanding effect of fluid shear stress is not uncommon in biomedical literature. Simple single channel devices have been used to understand cell adhesions and angiogenic sprouting and other biological phenomenon at varying levels of fluid shear stress [42–46]. These simple designs are difficult to scale up, especially when studying different levels of shear stress simultaneously. Typical single channel designs would require an equal scale-up of the fluidic pump equipment, which can be extreme costly. One way to mitigate this cost is to implement a dual inlet design, where a gradient of shear stress level can be achieved across the width of the channel [47]. However, these devices will also mix the signalling factors secreted by underlying cells, and become impractical when implementing oscillatory fluid flow motion that mimics *in vivo* flow patterns for bone tissue. Hence varying the geometric design of the microfluidic device becomes a promising approach to create microfluidic platforms that can be used to study different fluid shear stress levels all at once.

Previous study has designed a pressure driven microfluidic device where fluidic valves were used to separate different cell culture chambers. By inputting varying forms of pressure gradient, different levels of shear stress applied to the cells can be modulated. This platform was used to study effect of different pressure and shear stress on the alignment of valvular endothelial cells [48]. However, this device required a complex pressure gradient controller to operate, and does not allow for decoupling of shear stress and fluid pressure for individual analysis.

Another type of unique design to achieve a gradient of shear stress levels is to adapt a circular culture chamber. Although these types of circular design is ideal for creating large array of varying shear stress levels, they are more suitable for single-cell cultures adjacent to the shear stress channel [49]. When osteocytes are cultured in the circular gradient, fluid flow will displace signalling factors from different osteocyte population and cause unwanted mixing that will

increase the uncertainty of the co-cultured effect. For the desired intercellular signalling event between osteocyte and other bone cells, osteocyte networks under different shear stress levels must be cultured in separate chambers.

Perfusion ports formed by an array of pillar are an excellent way to separate different microfluidic chambers without completely blocking fluid flow. With properly designed Young's modulus, they will be easy to fabricate for a standard PDMS-glass device. The perfusion port feature has been used to design microfluidic devices that contain different levels of fluid shear stress for endothelial cells [50], which provides promising proof that they can be adapted for other biological systems. However, novel designs for osteocyte intercellular signalling will have to take into consideration challenges with co-culturing different bone cells. Similarly, due to unwanted mixing of signalling factors, specific osteocyte fluid shear stress regions must be isolated from one another.

Due to the analogy of electric circuits to microfluidic circuits, varying levels of fluid shear stress can also be achieved by designing arrays of parallel chambers with different hydraulic resistance. Dash et al. demonstrated a simple design where each culturing chamber (with individual outlets) has a unique shear stress level [51]. This would satisfy our need for separation of different osteocyte chambers while achieving large variations in shear stress levels. Similar design was also used to study the effect of different fluid shear stress levels on stem cell differentiation [52]. Detailed design protocols for these multi-shear devices are now available in the literature [53]. Future integration with co-culture features would make this an ideal platform for studying bone remodelling when osteocytes are stimulated with varying levels of fluid shear stress.

1.2.2 Platform for Osteocyte *in vitro* Studies

Many research studies have studied bone cell mechanotransduction under different simulated physiological conditions using macro-scale devices [54]. *In vitro* microfluidic devices provide an optimal tool to further understand this biological process with its flexible design, physiologically-relevant dimensions and cell-medium ratio, combined with high-throughput capabilities. It has been already shown that osteocyte proliferation on PDMS substrate is almost identical to glass slides, with the exception of protein expression levels which only stabilizes after 72 h of culturing [55]. Demonstrating proper osteocyte proliferation on PDMS will allow *in*

vitro study of the effect of substrate stiffness on osteocyte function and its signalling to other bone cells. Furthermore, improved proliferation and conservation of phenotype for MLO-Y4 osteocytes have been observed in collagen coated microfluidic channels, laying foundational proof that similar microfluidic platforms are ideal *in vitro* systems to study osteocyte cellular response to mechanical loading [56]. Initial application of micro-scale cultures of osteocytes involved studying the effect of cell spreading using micro-contact printed islands [57,58]. These experiments looked at the how cell cultured on islands or networks using defined patterns can be more sensitive to fluid flow than monolayers of osteocytes. Both results showed significant increase of intracellular calcium response, and these results will allow insight into the patterned layout of *in vivo* osteocytes that exist in a network of lacuna in the bone matrix, and perhaps provide *in vitro* solutions to create a more realistic culture environment to further study osteocyte biology. Although the novelty of using micro-contact printing to study these types of cell patterns is low, in the context of osteocyte networks it provided an ideal tool for building the next step culture platform.

Currently, *in vitro* platforms have found that oscillatory fluid flow (OFF) conditions significantly change osteocyte behaviour, and promotes better bone formation *in vitro* [59]. However, these experiments relied on the well-studied flow chambers, where large cover glass slides were used as the cell seeding platform. Although stimulated with physiological levels in terms of shear stress magnitude and frequency, monolayer cultures of osteocyte at centimeter scale are still very different from physiological conditions, where osteocytes grow in 3D layers of osteons and experience shear stress from fluid pockets. In an attempt to mimic *in vivo* lacuna-canaliculi, a large micro-array of chambers connected to micro-channels were designed according to dimensions similar to that of micro-canals in the bone matrix [60]. Osteocytes are seeded in individual chambers before sealing the device and studying the effect of fluid flow on cell processes, which extended into the micro-channels to be exposed to fluid flow. Although it is the first time single-cell study on osteocytes was done in a microfluidic device, there is still much to improve upon its design. The design did not take into consideration the difficulty in seeding individual cells, and unfortunately did not use microfluidic flow to assist in cell isolation. Furthermore, the device was designed to be sealed after cell seeding, which greatly limited the amount of pressure the device can handle without proper bonding between the glass and the PDMS. Another design attempting at recreating 3D osteocyte environment *in vitro* using packed

biphasic calcium phosphate beads as a basic structural layout where cultured osteocytes are seeded within the gaps [61]. Although this approach achieve a 3D culture environment for the osteocytes, there was no way to quantify or modulate the fluid shear stress experienced by the osteocyte network. Due to randomness of the bead packing, cultured osteocytes will experience a wide range of shear stress. To better mimic the *in vivo* osteocyte network under mechanical stimulation, novel experimental tools must be explored in an attempt to generate controlled and localized fluid shear stress pockets where intercellular signalling propagation between osteocytes within the same network can be studied.

The current forefront of microfluidic platforms for osteocytes focused on co-culturing of osteocytes and osteoclasts to look at the molecular interactions between them under various flow conditions [62]. The design utilized small micro-channels as communication ports between osteocytes and osteoclasts cultured in different flow channels. Signalling molecular cues from osteocytes under physiological flow can then be detected by parallel osteoclasts to elicit a cellular response. It is the first of its kind in terms of a co-culture system between two bone cells, and the simplicity of design provided opportunity to expand such a platform to tri-cell culture in order to simultaneously study molecular signalling between all three bone cell groups. High-throughput capabilities as well as multi-shear stress features can also be add to generate arrays of co-culture micro-systems where more applications such as on chip drug screening and cell differentiation assay can be done.

1.2.3 Platform for Osteoblast *in vitro* Studies

Since the discovery of osteocyte as the main mechanosensory cell, there is a general lack of development for *in vitro* platforms that create more physiological environments to study the other bone cells. In terms of osteoblast research, there have been very few advancements in its understanding *in vitro* using newly developed platforms. Again using intracellular calcium fluctuation as the standard for measuring cell response to shear stress, a simple microfluidic flow channel was developed to study osteoblasts [63]. As expected, higher magnitude of calcium "flickering" was observed under OFF compared to steady and pulsatile flow. The structural design of the micro-channels are very simple, showing that adaptation of these micro-scale platforms for studying osteoblast is still at a very early stage. Application of microfluidic design parameters created a multi-shear stress micro-platform for studying an array of different

mechanical load simultaneously, and calcium responses from osteoblast shows that they are very sensitive to different magnitudes of shear stress [64]. It is very surprising that this type of large array platforms for high-throughput studies of cell response was developed for osteoblast, but has not yet been developed for osteocytes. From these studies it can be seen that there is a gap between osteocyte research and micro-scale platforms that can be fulfilled by simply adapting existing platforms for other cell types to osteocytes. However, there is still a need to create the physiological osteocyte networks similar to the previously developed patterns through micro-contact printing.

Due to the vital role of mechanical loading on bone remodelling, bone cell survival, and their functions, the main focus of *in vitro* platform development for bone cells has been on mechanical stimuli related tools. There is also other tools on micro-platforms developed for osteoblasts that can be used for other bone cell applications. Gradient generators in microfluidic devices is very common, and it provides a very useful tool to study cell response to chemical cues and chemotaxis. By incorporating a gradient generator into a co-culture device, an upstream cell group, in this case macrophages, can be stimulated to produce physiologically relevant cues that can then be applied to downstream osteoblasts [65]. The physical separation of the cells prevent any cell-cell contact, isolating soluble factors and their signalling effects. As one can imagine, a hierarchy of multi-layer of cells can be established, where stimulation of upstream osteocytes will produce soluble factors that control second layer osteoblasts function, which in turn will secret factors such as RANKL and M-CSF to influence the third layer osteoblasts, creating a complete signalling gradient of the whole bone remodelling process. Such a platform will bring researchers one step closer to understanding physiological responses *in vitro*. Another interesting application of micro-scale devices on osteoblasts is using dielectrophoresis to isolate cells into individual micro-chambers. This combined with previously mentioned osteocyte isolation chamber can produce a more robust single-cell culture system that can closely reciprocate osteocyte responses when they are properly aligned in networks [66].

1.2.4 Platform for Osteoclast *in vitro* Studies

When it comes to study of bone cells on *in vitro* platforms, osteoclasts are the least studied cells in this context. Most research has been focused on dissecting the differentiation pathway leading to this multi-nucleated cell, and there is definitely a need to understand how functions of

osteoclasts can be affected by different micro-environmental factors. Very recent research has started to look at osteoclast bone resorption rate in a microfluidic environment. Microfluidic channel coated with adhesion molecules and an artificial bone matrix was used to confirm whether osteoclasts can perform normal resorption functions in such micro-environments. Other *in vitro* osteoclast experiments include generating large osteoclast cultures from bone marrow cells [67], or studying the effect of vibration frequency on osteoclast bone resorption [68]. However, there is a significant need to push for micro-scale tools to be developed to study osteoclast functions in a more physiological setting compared to the standard large monolayer cultures. Again, previously introduced platforms for both osteoclast and osteocyte can be adapted to osteoclasts, as the micro-environment for all three bone cells is very similar *in vivo*.

1.3 Thesis Objectives

There are very limited applications of microfluidic platforms for bone cell studies. Due to the importance of mechanobiology to bone remodelling, it is very important to establish and improve methodologies that can assist in the *in vitro* experimentation of bone cells. I want to develop a new generation of microfluidic devices that can be used for specifically osteocyte mechanotransduction studies, and help us better understand the bone remodelling process. To do this, I have three main aims:

1) Design and valid a multi-shear stress co-culture microfluidic device for osteocyte mechanotransduction studies.

2) Evaluate whether OCY 454 osteocyte cell model is a good candidate in bone remodelling studies.

3) Adapt magnetically actuated micro-beams to be used as a tool for localized fluid stimulation of osteocyte networks.

This thesis document describes approaches and experimental results that I have achieved towards each of these three objectives. Chapter 2 will focus on the multi-shear stress microfluidic device, while Chapter 3 will talk about validation of the novel OCY 454 osteocyte cell line. Meanwhile, Chapter 4 will be focused on using novel magnetically actuated beams as a tool to generate localized fluid shear stress on osteocyte cultures. Contents from Chapter 3 had been published in

the Journal of Orthopaedic Research [69] and work in Chapter 4 had been published in the PLOS One journal [70]. All research and results in Chapter 2 had been submitted for publication in Integrative Biology and is currently under review.

Chapter 2

2 Multi-shear Co-culture Microfluidic Platform for Osteocyte Mechanotransduction Studies

2.1 Introduction and Background

Current research on osteocyte's role in bone remodelling has been utilizing both *in vivo* animal models [71,72] as well as *in vitro* flow chamber models [73]. Animal models provide a comprehensive tool for studying overall tissue and whole organ system response to mechanical loading, while allowing for accurate compression loading of limbs that mimic exercise conditions [18,74]. However, it is difficult to study signalling pathways *in vivo*, as isolating the effect of each factor proves to be difficult and prone to high variance between samples. Furthermore, it is challenging to translate animal models to human tissue behaviour, and often extensive validation experiments are needed. On the other hand, *in vitro* models provide a more simplistic tool to evaluate single-cell population response to specific levels of mechanical loading in the form of fluid shear stress. Studies using the traditional *in vitro* flow chamber devices have observed the role of RANKL/OPG in osteocyte regulation of osteoclast [75,76], as well as osteocyte regulation of breast cancer metastasis [77,78]. Although lacking the comprehensive tissue level response from *in vivo* models, *in vitro* platforms often excel at pinpointing specific functions of signalling factors and how they coordinate with each other to produce the overall response from a population of cells. Troubles arise when using these macro-scale flow chambers, which require extensive pumping equipment that are difficult to scale up. Most importantly, flow chambers lack physiologically-relevant microenvironment typically experienced by cells *in vivo*, and with its reliance on conditioned media it is not possible for real-time signalling between different cell populations. Hence development of innovative *in vitro* platforms is needed to provide more efficient tools for studying osteocyte mechanobiology.

The rise of microfluidic devices in modelling biological systems has provided novel experimental tools for studying various cell-cell interactions such as mesenchymal stromal cells (MSCs)-endothelial communication during vasculature formation [79,80], or endothelial-epithelial interaction in a lung-on-a-chip [81,82]. In relation to osteocytes, microfluidic devices can be used to simulate different physiological loading conditions (e.g., shear stress, strain, pressure, etc.), accurately controlling their levels and observing specific responses via secretome

of osteocytes. They are also ideal for primary cell studies, allowing large numbers of experimental samples with limited number of cells. With flexible designs for high-throughput capabilities, microfluidic devices are optimal tools for testing potential signalling factors and provide additional drug screening capabilities before clinical experiments are needed. Our recent work on osteocyte-osteoclast co-culture platform has demonstrated the feasibility of building more complex microfluidic devices for bone cell mechanotransduction studies, while maintaining its biological relevance [83]. However, there lacks a robust system where multi-physiological flow conditions are applied to osteocytes to study their intercellular communication, where different levels of fluid shear stress is tested on the same device. In particular, we hope to design for physiological fluid shear stress range between 0.1 -2 Pa [84]. Here we describe a multi-shear co-culture microfluidic device that can be used to study mechanically stimulated osteocyte and their interaction with other bone cells. We validated in our device the changing levels of osteocyte response to different levels of fluid shear stress, and confirmed a corresponding change in downstream cell response via osteoclast formation. Moreover, we demonstrated the capability for the microfluidic device to be used for studying drug effect on osteoclast interaction with mechanically stimulated osteocytes. This platform can be developed further into a large array of smaller devices to achieve a gradient of physiological loading conditions for high-throughput experiments on osteocyte mechanotransduction studies, as well as a drug screening tool.

2.2 Methods

2.2.1 Design and fabrication of co-culture platform

The microfluidic device is designed based on standard fluidic principles that utilize changing dimensions to create different flow rates in chambers connected in a parallel circuit (sharing the same inlet). Average wall shear stresses (τ_A) in each osteocyte chamber are calculated using parallel-plate assumptions based on the following equation:

$$\tau_A = \frac{6U_A\mu}{h} \tag{1}$$

where U_A is the average flow velocity, μ is the dynamic viscosity, and h is the height of the chamber. By changing the length of channels leading up to each chamber, we can proportionally vary the average velocity without effecting the flow profile experienced by the cells (which is

dependent on chamber width and height). The experimental design is consisted of 3 parallel osteocyte chambers each paired with an adjacent osteoclast chamber (Figure 2.1A). The relationship between shear stress in each parallel channel is governed by the following equation:

$$\Delta P = Q \times R_{Hydraulic} \quad (2)$$

Where ΔP is the pressure drop, Q is the flow rate, and $R_{Hydraulic}$ is the hydraulic resistance of each channel. Since all channels share a common inlet and opens to atmospheric pressure on all outlets, ΔP is equal for all channels and any variation in $R_{Hydraulic}$ would modify the flow rate, which is directly correlated to wall shear stress from equation (1). $R_{Hydraulic}$ for a rectangular cross-section channel is governed by the following equation:

$$R_{Hydraulic} = \frac{12\mu L}{wh^3(1 - \frac{0.63h}{w})}$$

Diffusion channels between the two chambers allow for bidirectional transport of signaling molecules between the two cell populations. A sample device is shown in Figure 2.1C to demonstrate physical size and layout.

Fabrication of the microfluidic devices is based on standard soft lithography techniques [85]. Briefly, a photomask containing the pattern for the device is generated using a laser-etched chromium-lined glass plate. The photomask is then used to transfer the design onto a SU-8 2050 coated silicon wafer using UV exposure. The silicon wafer containing the imprinted design is then used as a negative mold for repeated device fabrication. Polydimethylsiloxane (PDMS) at a 10:1 base to curing agent ratio is mixed and poured onto the negative mold before curing at 60°C for 24 hrs. The cured PDMS is cut from the negative mold, and inlets and outlets were cut using 3 mm diameter biopsy punches before bonded to glass slides after plasma treatment of the bonding surfaces to form the final microfluidic device. Fabricated microfluidic device is sterilized using 70% ethanol and UV light before cell seeding.

2.2.2 Cell culture and seeding in co-culture platform

All cells and devices are incubated in 37°C and 5% CO_2 conditions both during incubation period. MLO-Y4 osteocytes are cultured in Alpha Minimum Essential Medium (αMEM) containing 2.5% calf serum (CS), 2.5% fetal bovine serum (FBS), and 1% Penicillin-

Streptomycin (PS). RAW264.7 pre-osteoclasts are cultured in Dulbecco's Modified Eagle Medium (DMEM) containing 10% FBS, 2% Glutamine, and 1% PS. MLO-Y4 cells are trypsinized at 80% confluence before seeded into the microfluidic device at 250k/mL density. Osteocyte chambers in all devices are coated with 0.15 mg/ml type I collagen for 1 hr before cell seeding. Air-liquid barriers formed along the posts between the two chambers prevent osteocytes from escaping to the osteoclast chamber. Osteocytes are cultured for 24 hrs in the device before RAW264.7 cells are added to adjacent chambers. RAW264.7 cells are supplement with 10 ng/mL of recombinant RANKL protein to assist with differentiation. Inlets and outlets of osteocyte chamber are temporarily sealed to prevent pre-osteoclasts from crossing over to the osteocyte chamber. Flow experiments are conducted using a custom-made fluidic pump. Oscillatory fluid flow (OFF) at 1 Hz is applied to the osteocyte chambers for 2 hrs per flow session. Microfluidic device is maintained at 37°C and 5% CO_2 condition during OFF stimulation.

2.2.3 Calcium response quantification

MLO-Y4 osteocytes are seeded inside osteocyte chambers at 250k/mL and grown to 80% confluence before imaging. Osteocytes are stained with Fura-2 AM (Ex: 340 nm/380 nm, Em: 510 nm) live calcium indicator 1 hr before experiment. Devices are maintained on a heated imaging stage, where baseline intracellular calcium fluctuations are measured for 1 min before applying OFF stimulation. Intracellular calcium signals captured during 6 min of flow stimulation are compared to baseline values, and only signals 2-fold or higher are registered as positive calcium response. Response rates are calculated based on number of positive response over total number of cells observed. Average response magnitude is calculated from all positively responding osteocytes.

2.2.4 ELISA quantification of RANKL expression

At 80% confluence, MLO-Y4 cells cultured in the osteocyte chamber are stimulated with OFF for 2 hr and incubated within the device for 24 hrs. Conditioned media (CM) from the osteocyte chambers are extracted and used for standard ELISA quantification of RANKL. Briefly, CM from experiment was added to capture antibody coated 96-well plate, and visualized using secondary antibody bonded to streptavidin-Horseradish peroxidase. Results are read by SpectraMax i3 plate reader at 450 nm.

2.2.5 Osteoclast-osteocyte co-culture experiment

MLO-Y4 cells and RAW264.7 cells are seeded into respective chambers before beginning the 7 day co-culture period. OFF (1 Hz, 2 hrs) is applied to the osteocyte chamber every other day beginning from day 1. Growth media in both osteocyte and osteoclast chambers are changed once every 24 hrs. For zoledronic acid (ZA) experiments, appropriate concentration of ZA is added to fresh osteoclast growth media before daily media changes. At the end of day 7, cells in microfluidic devices are fixed and stained for tartrate resistant acid phosphatase (TRAP) to visualize osteoclast formation. TRAP positive cells are counted from 6 random positions within each osteoclast chamber and added together for quantification. Images were taken at 6 random locations within the osteoclast chamber; no image processing was conducted before manual counting of TRAP positive osteoclasts. A TRAP positive cell is selected when it has both a pink hue and 3 or more nucleus. Experiments were terminated after day 7, as osteocyte confluency levels reached above 100% and some cells were starting to migrate to the adjacent co-culture chamber. Since we were interested in studying intercellular signalling via soluble factors, direct cell-cell connection was not desired.

2.2.6 Particle flow velocimetry

Microfluidic devices were linked up to the custom in-house oscillatory fluid flow pump and filled with floating cell bodies. After turning on the pump, videos at 30 fps for 30 secs were taken at each channel to capture the flow cell bodies. Random streak lines across each channel at the peak of the oscillatory flow were used to calculate the average peak velocity.

2.2.7 Statistics

A minimum of three individual experiments were run with a minimum of 2 samples per experimental group. Each microfluidic device consist of 3 samples, one for each fluid shear stress value at 0.5 Pa, 1 Pa, and 2 Pa. Flow devices have undergone respective OFF stimulation, while no flow groups are consisted of cells seeded within the microfluidic device without OFF stimulation during the entire duration of the experiment. Student's t-test (2-tail, non-paired for calcium response; 2-tail, paired for all other results) was used to test significance between flow

and no flow groups ($\alpha = 0.05$) using mean values from each experimental trials. The *n* value represents the total number of device samples from all experiments.

2.3 Experimental Results

2.3.1 Flow rate validation

To validate the experimental flow velocities inside the microfluidic devices, we conducted particle flow velocimetry. We were able to confirm that the average experimental flow velocity is consistent with those intended for the design (Figure 2.1B). Flow velocities are significantly different between each of the osteocyte chambers, ensuring that different osteocyte populations are experiencing drastically different fluid flow shear stresses. The results also confirmed there is no leakage in the setup, which would result in a loss of flow velocity and require manual adjustment to the inlet flow rates of the OFF pump in order to achieve the desired flow velocities within the microfluidic device.

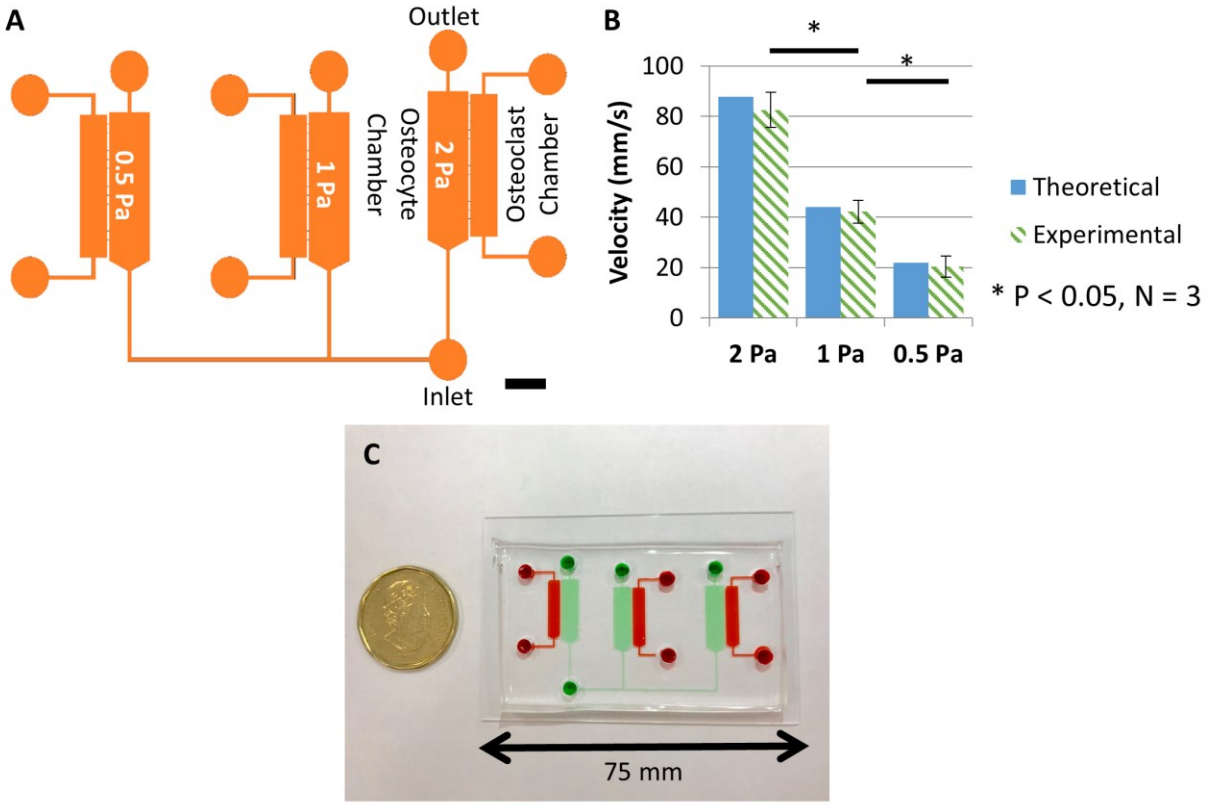

Figure 2.1: Basic co-culture microfluidic design. A) Schematic showing the layout of the device, consisting of 3 pairs of osteocyte-osteoclast chambers. Each pair of

chamber was connected by 20 μm wide and 300 μm long diffusion channels. All three pairs of chambers shared a common inlet, utilizing a single flow input source for the entire device. Scale bar = 4 mm. B) Flow validation results showing that experimental flow velocities were close to theoretical values designed for the devices. These flow velocities were based on a set pump flow rate and correlated directly with the intended shear stresses. C) Picture showing device post fabrication. The green dye highlighted the osteocyte chambers and their inlet/outlet, while the red dye showed the individual osteoclast chambers.

2.3.2 Ca^{2+} Response from osteocytes

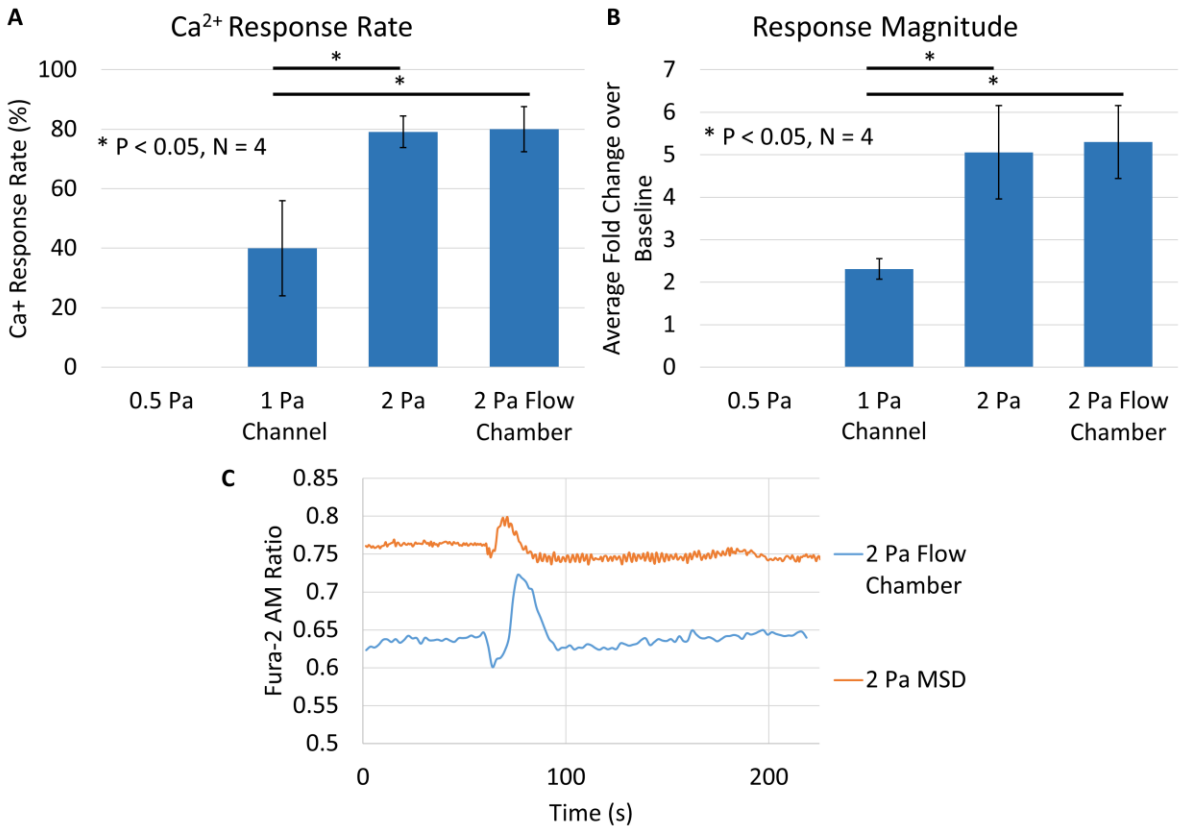

Figure 2.2: Calcium response results from MLO-Y4 osteocytes seeded in the co-culture device. A) Calcium response rate of osteocytes seeded in the co-culture device. Response rate is based on number of positive response compared to total number of cells imaged. Response rates increased as shear stress increased. Response rate in 2 Pa osteocyte chamber were similar to response rate observed from traditional flow chamber devices. B) Average response magnitude also increased with higher shear stress level, where magnitudes observed in the 2 Pa osteocyte chamber are again similar to values obtained from traditional flow chambers. C) Representative calcium response curves from the 2 Pa channel in the microfluidic device vs. standard 2

Pa flow chamber, showing consistency in the spatiotemporal response pattern between the two platforms.

We observed a significant difference in calcium response patterns between the three osteocyte chambers. As can be seen in Figure 2.2A, there is strong correlation between the calcium response rates and the shear stress levels experienced by osteocytes. Furthermore, we saw a similar pattern in Figure 2.2B where average magnitude of the calcium responses significantly increased with shear stress levels. There was however no positive calcium response registered in the 0.5 Pa osteocyte chamber throughout our experiments. These results not only confirms that osteocytes seeded in the co-culture device can modulate their response according to the shear stress they sense, but also demonstrated the versatile capability for our microfluidic device to be used as a live imaging platform for osteocyte mechanotransduction studies. Observed spatiotemporal patterns of calcium response curves from the microfluidic devices are very similar to those commonly seen in macroscale flow chambers (Figure 2.2C).

2.3.3 RANKL released from osteocytes

We measured extracellular secretion of RANKL protein from OFF stimulated osteocytes in our devices. From our experiments, we validated that even with a small volume reservoir in our osteocyte chambers, we could still observe a significant difference in RANKL expression between cells cultured in chambers with varying fluid shear stress. From our results, we saw a decrease in extracellular RANKL levels in chambers with higher fluid shear stress (Figure 2.3). This agrees with previously reported observations in literature [86]. Higher than expected variations in raw expression level was observed between different trials. I hypothesize that this is due to the limited volume of media we can withdraw from each channel. Standard commercial ELISA kits require 100 µL per sample and need 2-3 replicates, while total volume per channel is only 100 µL. Thus a 3-fold dilution is introduced which greatly increases the noise and variation in the data. Results are hence normalized using the 0.5 Pa chamber as the baseline expression level. No significant differences were observed between chambers in the no-flow devices, showing experimental conditions and micro-environment within the device did not alter the RANKL expression levels of osteocytes.

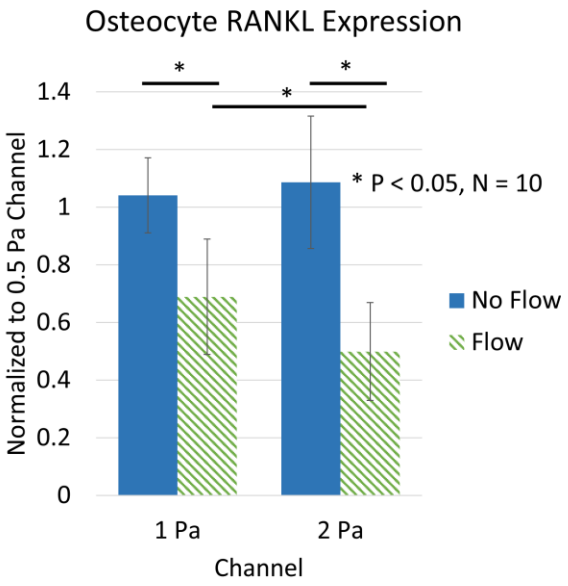

Figure 2.3: Quantification of soluble RANKL collected from osteocytes channel. After normalizing to quantities observed in each device's 0.5 Pa osteocyte chamber, there was a decrease in the level of extracellular RANKL detected when increasing the shear stress level sensed by osteocytes. No differences were seen in the no-flow devices between all three osteocyte chambers.

2.3.4 Osteoclast differentiation in co-culture

Within our co-culture experiments, we quantified osteoclast formation from RAW264.7 cells using Tartrate-resistant acid phosphatase (TRAP) staining as a positive marker for differentiation. In our devices, we observed a significant decrease in number of TRAP positive cells in osteoclast chambers adjacent to osteocytes stimulated with higher levels of fluid shear stress (Figure 2.4). This agrees with our previous results demonstrating a decrease in RANKL expression levels from osteocytes would result in lower numbers of differentiated osteoclasts [83]. We saw a significant difference in TRAP positive cells between the 0.5 Pa chamber and the other two chambers. However, only a decreasing trend was observed between the 1 Pa and 2 Pa chambers without statistical significance. From our results it seems rate of decrease is in a logarithmic relation with the level of fluid shear stress, and 1 Pa OFF could be a threshold level for the effect of mechanical stimulation on osteoclast differentiation in a co-culture environment.

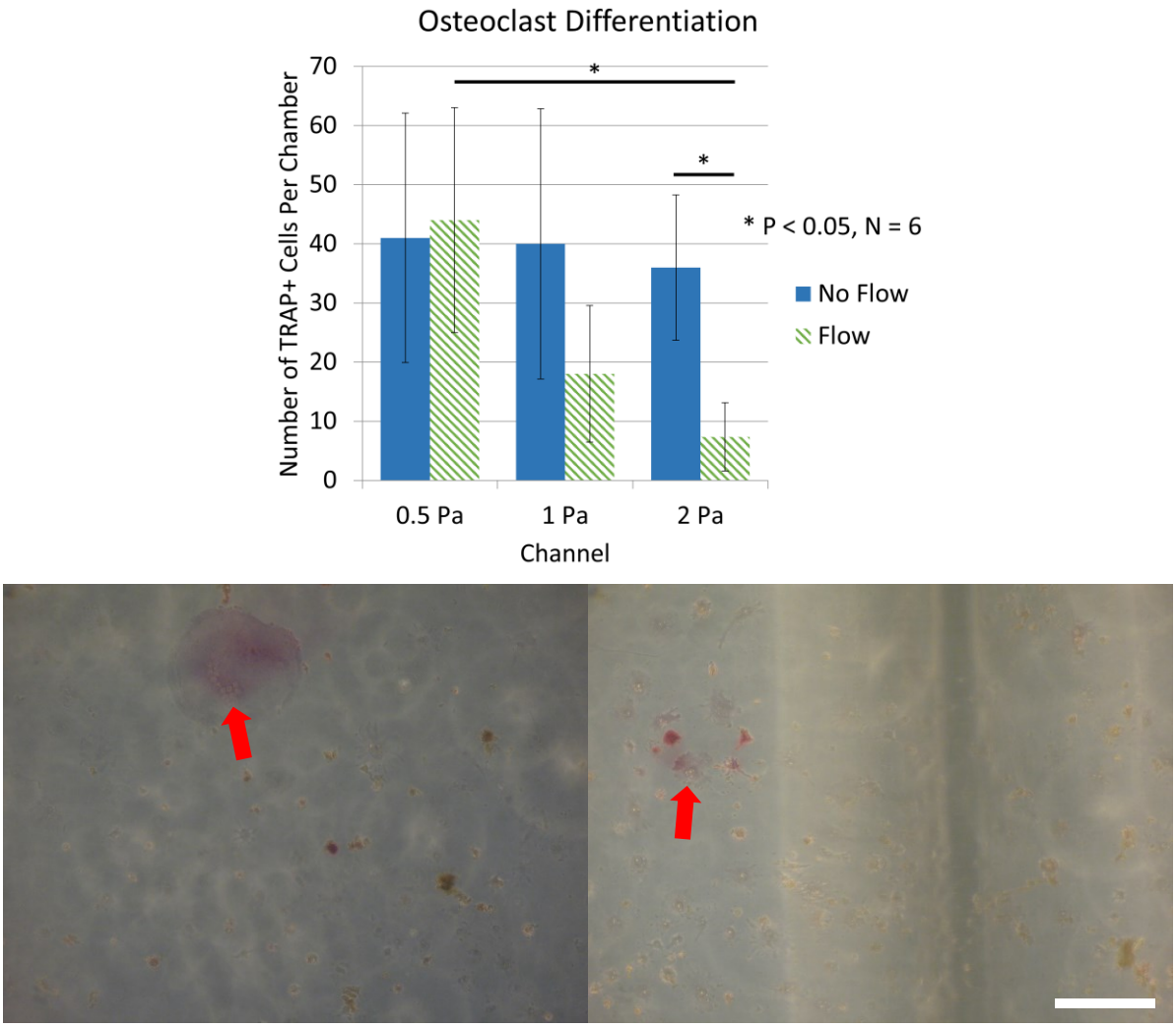

Figure 2.4: Quantification of osteoclast differentiation when co-cultured with osteocytes. After 7 day incubation in the co-culture device with bi-daily OFF stimulation of osteocytes, a significant decrease in osteoclast formation was seen when co-cultured adjacent to osteocytes in the 2 Pa chamber. A decreasing trend was also observed beside the 1 Pa chamber, but not statistically significant. No differences in osteoclast differentiation were observed in devices without mechanical stimulation of osteocytes. Sample images showing representative images of TRAP stained osteoclast in 2 Pa channel; on the left is an image from no-flow control, and on the right is an image from a flow device. Osteoclast is counted positive when there is 3 or more visible nucleus along with a pink hue. Scale bar represent 100 μm.

2.3.5 Effect of zoledronic acid on osteoclast differentiation in co-culture

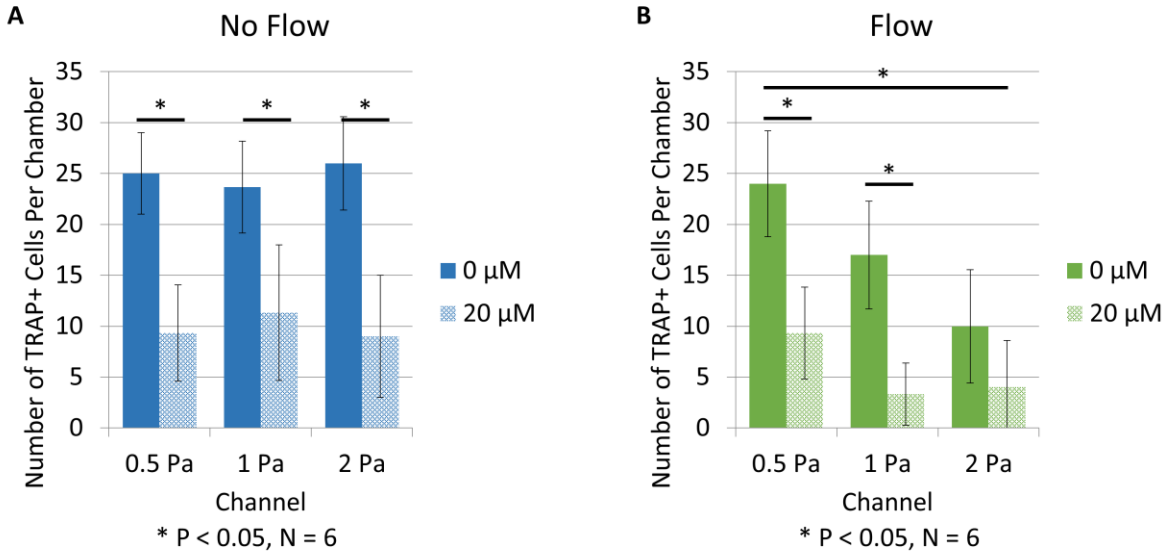

Figure 2.5: Osteoclast differentiation under the treatment of ZA. A) The effect of ZA on osteoclast differentiation was tested in the co-culture device. Under no OFF stimulation, a significant decrease in osteoclast formation was seen when treated with 20 µM ZA compared to control devices. B) A similar effect was seen in fluid flow stimulated devices, where a significant decrease was seen in devices treated with 20 µM ZA compared to devices with only fluid flow stimulation. A compounding effect is observed between OFF stimulation and ZA, where both the mechanical loading of the osteocytes and the ZA treatment of cells in the device worked together, resulting in the lowest amount of osteoclast formation observed.

After establishing our co-culture microfluidic device and validating observable differences in osteoclast differentiation when co-cultured with osteocytes stimulated under different levels of fluid shear stress, we moved on to demonstrate potential application of our device. One of the key advantages of our microfluidic device is real-time signalling between osteoclast and fluid stimulated osteocytes. Thus, it is an ideal platform to study how drugs can affect osteoclast differentiation when combined with mechanically stimulated osteocytes. We chose to study how ZA, an established bisphosphonate, can change osteoclast differentiation within our device. From our seven day co-culture experiments, we observed a significant decrease in osteoclast differentiation in all chambers of the no-flow devices when supplemented with 20 µM of ZA (Figure 2.5A), demonstrating the substantial effect ZA has on osteoclast differentiation in a co-culture environment. After applying OFF stimulation to osteocytes in adjacent microfluidic channel, we observed a compounding effect between mechanical loading and ZA, where further

decrease in osteoclast differentiation was observed when ZA-supplemented osteoclasts were co-cultured with osteocytes stimulated with 1 Pa and 2 Pa fluid shear stress (Figure 2.5B). These results demonstrated that our microfluidic device is capable of not only studying the effect of mechanical loading only on osteocyte-osteoclast signalling, but also allow studying of synergistic effect of mechanical loading and drug effect on osteoclasts within this co-culture environment.

2.4 Discussion

Through our experimental results, we have demonstrated the versatile analytical methods that can be used in our co-culture microfluidic device when studying osteocyte mechanotransduction and intercellular signaling during the bone remodeling process. Due to simple design principles and established fundamental fluid flow phenomenon, our co-culture device can be easily scaled up to larger array systems, considerably increasing the throughput of experiments. To the best of our knowledge, this is the first device that capable of integrating multi-shear stress level and co-culture micro environment in studying bone remodeling.

We have shown that standard analytics techniques used to study osteocytes-osteoclast interaction such as calcium response, extracellular RANKL expression, and TRAP staining can be easily adopted to the microfluidic device. Furthermore, the device steps away from traditional time-sensitive conditioned media experiments, and moves to a real-time intercellular signaling model, a much closer representation of the *in vivo* conditions. This is shown through our osteoclast differentiation results, where bi-daily fluid flow stimulation of osteocytes still produced a significant difference in osteoclast formation compared to the previous daily dosage of mechanical stimulation commonly used in large flow chambers. Our microfluidic devices also require significantly less media volume and cell count, making it ideal for studying large-scale drug screening as well as primary cell interactions. Although our device attempts to mimic the *in vivo* microenvironment by setting an appropriate communication channel length, due to the limitation of fabrication techniques, we are unable to design channel width closer to the lacuna-canaliculi network found *in vivo*. With 2D cultures and millimeter scale flow chambers, our device is still far from the submicron-level microstructure in the bone tissue where osteocytes reside. With future development in fabrication technology, this limitation can be eventually overcome.

We have demonstrated here that our co-culture device can be used to study other factors in combination with the impact of fluid flow stimulation on osteocyte-osteoclast interaction. Our results have shown that in a co-culture environment, ZA still decreases the differentiation of osteoclasts. Furthermore, this effect can be combined with the reduction in osteoclast formation caused by mechanically stimulated osteocytes. This agrees largely with what is previous reported in literature, where ZA inhibits osteoclast formation and activity *in vitro* [87–89]. However, there has been a study where osteocyte-mediated enhancement of osteoclast formation was observed *in vitro* using conditioned media experiments [90]. Although we added the ZA supplement to our osteoclast differentiation media, due to the diffusion channels between the two cell populations, osteocytes should also experience the effect of the drug. However, we do not see any signs of enhanced osteoclast formation within the device. This could be due to the synergistic drug effect on both the osteoclast and osteocytes. Further investigations are needed to confirm whether ZA is having any effect on osteocyte-mediated increase in osteoclast formation in our co-culture devices.

In our quantification of extracellular RANKL expression from osteocytes cultured in our devices, we saw a large trial-to-trial variation in the collected soluble RANKL protein levels. We believe this is due to the limited size of our osteocyte chamber, as the media volume extracted per sample is only enough for the minimum volume requirement of commercialized ELISA kits. This is a common issue among similar types of microfluidic devices, making it even more difficult to measure protein concentrations via ELISA with more scaled down systems. However, many researchers are now working on on-chip protein detection methods based on electrochemistry principles [91,92]. We hope to adapt these novel detection methods in the future to allow for more accurate and persistent measurement of protein concentrations. These new detection techniques will also allow for real-time tracking of expression factors, enabling our device to map variations in signaling molecules during and after mechanical stimulation of osteocytes. This will create a powerful tool that provides important insight into the bone remodeling process and enable better understanding of the type of synergies that exist in the bi-directional interaction of osteocytes and osteoclasts.

Another limitation of our current device in modelling the bone remodeling process is the lack of osteoblasts in our system. As shown in literature, communication between osteocyte and osteoblast is another crucial process during bone remodeling [93]. These interactions are difficult

to model *in vitro* due to the limitation of the existing MLO-Y4 cell line, as ongoing work is attempting to establish appropriate osteocyte cell lines suitable for studying osteocyte-osteoblast signaling [26,69]. Future experiments using our microfluidic device can mitigate this issue by using primary osteocytes, but current design still lack the capability for a tri-culture system where communications across osteocytes, osteoclasts, and osteoblasts can be modelled. Newer iterations of the design can include adaptation of a second layer to the device, allowing for culture of osteoblasts while maintaining proper diffusion channels in between all three cell types. These new devices will provide even more physiological-relevant micro-environment to study bone remodeling *in vitro*. It will also provide more comprehensive understanding to effects of drugs such as ZA, and how administering such chemical reagents can affect the interplay of all three bone cells during remodeling. Furthermore, various disease models can be adapted within our microfluidic devices in order to study changes in cell-cell communication during these defects in bone remodeling, and identify potential clinical targets that can be used as treatments.

2.5 Conclusion

Here we have shown the design of a novel co-culture microfluidic platform that can study the effect of various levels of fluid stimulation of osteocytes within the same device. We validated that osteocytes adapt their behavior to different levels of fluid shear stress, and downstream osteoclast differentiation is directly affected by the level of mechanical stimuli sensed by co-cultured osteocytes. Our microfluidic device has the capability to perform drug studies on bone remodeling, and delivers a potential platform for large scale drug screening experiments. We hope to further develop our platform to enable *in vitro* studies of a tri-culture system for bone remodeling, empowering researchers to gain a better understanding of this phenomenon and find novel clinical solutions to bone diseases. This device also has the potential to allow co-culture studies of other cellular systems that experiences significant mechanical loading like cardiovascular system.

Chapter 3

3 Validating OCY454 Cell Model for Osteocyte Mechanotransduction Studies

3.1 Introduction and Background

Current *in vitro* experimentations on osteocyte regulation of bone remodelling rely on the MLO-Y4 osteocyte-like cell-line, established by Dr. Bonewald in 1997 [94]. Isolated from mouse long bones, these osteocytes were selected based on their dendritic phenotype. The MLO-Y4 cells have been shown to be sensitive to mechanical loading, and respond by changing the secretion level of many key soluble factors [21][95]. Among all the mechanical stimuli that osteocytes are exposed to *in vivo*, loading-induced fluid flow is well-accepted as an important stimulus that osteocytes sense, [96]and is therefore used in many *in vitro* studies [97][98]. Using the MLO-Y4 cells, researchers have extensively studied the mechano-regulation of osteoclast via osteocytes [99][100], establishing a solid foundation for understanding the cross-talk between osteocytes and osteoclasts under mechanical loading. Furthermore, MLO-Y4 cells have been used in many studies of osteocyte intracellular calcium response, setting it as a major marker for measuring the mechano-sensitivity of osteocytes [101][102][103]. Other research focusing on osteocyte markers also benefited from the establishment of a stable osteocyte cell line; mechanical regulation of Wnt signalling [103] in osteocytes, as well as roles of PGE2 [104][105], are widely explored. Recently, there is even a novel study of extracellular vesicles released by osteocytes using MLO-Y4 cells [106]. These *in vitro* experiments often use osteocyte conditioned medium (CM), which is comprised of the complete osteocyte secretory response, to study the indirect effect of fluid stimulation on osteoblasts and osteoclasts via osteocytes.

However, there is a major limitation of using MLO-Y4 cells as an osteocyte cell model. *In vivo* studies have shown that osteoblasts are regulated by an important molecule released by osteocytes – sclerostin [104]. It has been revealed that sclerostin inhibits osteoblast activity and bone formation through the Wnt/Beta-Catenin pathway [107][108], and that mechanical loading on the bone leads to a reduction in sclerostin levels *in vivo* [18], thus proving sclerostin's critical role in mechanotransduction studies between osteocytes and osteoblasts. Unfortunately, this essential signalling molecule is missing from the MLO-Y4 released soluble factors, giving the

MLO-Y4 cell model a great disadvantage in studying osteocyte regulation of osteoblast function under mechanical loading.

Recently, a new cell line for osteocytes had been developed by Dr. Pajevic (Boston University), the OCY454 osteocytes [26]. Also derived from mouse long bones, these cells have been shown to secrete significant levels of soluble sclerostin and dentin matrix acidic phosphoprotein 1 (DMP1) after differentiation. They are also shown to be mechano-sensitive, significantly increasing its expression of sclerostin in response to microgravity *in vitro*. Using both 2D and 3D cultures of OCY454 cells, the authors demonstrated that mRNA expression of several important signaling molecules such as sclerostin, DMP1, and OPG were significantly affected by uni-directional laminar fluid flow with a shear stress of 0.2 Pa. These promising results suggest that OCY454 cells have the potential of serving as a new cell model for studying osteocyte mechano-regulation of osteoblasts. Nevertheless, there have yet to be any studies done on how mechanically stimulated OCY454 osteocytes can affect downstream bone cells. It is crucial to understand whether this new cell line is capable of regulating osteoblast differentiation and activities, as it has the potential to instigate considerable numbers of novel intercellular communication research on the bone remodelling process.

In this study, we aim to investigate OCY454 osteocyte's mechano-sensitivity by measuring known markers of osteocyte mechanotransduction, both immediately after oscillatory fluid flow (OFF) and 24 hrs after flow. We will also examine the response of osteoblasts and osteoclasts to the CM generated from flow-stimulated OCY454 osteocytes. These results will provide us a good indication of whether this new cell line can be used as an *in vitro* model for studying osteocyte mechano-regulation of other bone cells.

3.2 Methods

3.2.1 Cell Culture

OCY454 osteocytes were grown on collagen-coated (0.15 mg/ml Type I collagen (Corning, USA)) dishes with alpha minimum essential medium (MEM) (WISENT, Canada) containing 10% fetal bovine serum (FBS) (Gibco, USA) and 1% antibiotic-antimycotic (Gibco, USA). OCY454 cells were seeded at 10^5 cells per 100 mm diameter dish (Corning, USA), and allowed to reach 80% confluency at the permissive temperature (33 ˚C) for 3 days before passaging. Cells

were differentiated at the semi-permissive temperature (37 ˚C) for 10 days before stimulation with flow.

MLO-Y4 osteocytes were grown on collagen-coated dishes with alpha-MEM containing 2.5% calf serum (Gibco, USA), 2.5% FBS, and 1% penicillin-streptomycin (Gibco, USA). MC3T3-E1 osteoblast precursors were grown in alpha-MEM containing 10% FBS and 1% penicillin-streptomycin. MC3T3-E1s were seeded at 5 x 10^3 cells per well in 24-well plate for osteoblast conditioning experiment. RAW264.7 osteoclast precursors were grown in D-MEM media (WISENT, Canada) containing 10% FBS, 2% l-glutamine (Sigma-Aldrich, USA), and 1% penicillin-streptomycin. RAW264.7 were seeded at 2.5 x 10^3 cells per well in 24-well plate for osteoclast conditioning experiment.

3.2.2 Parallel Plate Flow Chamber Experiments

OCY454 osteocytes were seeded on collagen coated glass slides at 2 x 10^5 cells per slide and incubated in 37 ˚C overnight. Slides were then inserted into custom-made flow chambers [20] for OFF stimulation with shear stress of 1.2 Pa for 2 hours in the incubator. After flow stimulation, slides were incubated in 10mL media for 24 hours at 37 ˚C. CM was then extracted and used for osteoblast and osteoclast conditioning experiment.

3.2.3 Sclerostin and RANKL/OPG ELISA

Both sclerostin (recombinant Mouse and Rat antibody purchased as a complete ELISA kit, R&D Systems, USA) and RANKL/OPG (mouse monoclonal antibody purchased from R&D Systems, USA) ratio were quantified using standard ELISA method on CM collected 24 hrs after osteocytes were exposed to fluid stimulation. Briefly, 96-well plates were coated with capture antibodies (R&D Systems, USA) overnight and blocked with 10% BSA (Bioshop, Canada) in PBS, then incubated with media sample for 2 hrs, after which detection antibodies (R&D Systems, USA) and secondary HRP-labelled antibodies (R&D Systems, USA) were added for colorimetric detection using a Spectromax i3 Multimode Detection Platform (Molecular Devices, USA).

3.2.4 Intracellular Calcium Response Quantification

Cells were seeded into flow channels (ibidi, Germany) at a density of 2 x 10^5 per channel and incubated overnight. Cells were stained with Fura-2 AM (ThermoFisher Scientific, USA) for 45 min before imaging. Using a custom syringe pump [109], cells were stimulated with OFF at 4 Pa shear stress and 1 Hz frequency for up to 4 min. The elevated shear stress level chosen in comparison to standard MLO-Y4 protocols was due an attempt to increase the number of positive readings per experiment, as our preliminary studies suggested OCY454 cells responded to much higher shear stress levels. Fluorescent signals were read using a Nikon Eclipse Ti fluorescent microscope, and a final ratio of 340 nm/380 nm was used to generate the calcium response curves. A calcium response was quantified as having 2-times fold-change or greater compared to baseline fluctuations, and data was analyzed using custom in-house MATLAB scripts.

3.2.5 Fluid Flow and Quantification of ATP Synthesis

Differentiated OCY454 cells were seeded into flow channels (ibidi, Germany). After overnight incubation, cell numbers were quantified with bright field imaging and manual counting. The cells in the devices were then stimulated with OFF (2 Pa, 1 Hz) for 20 minutes. ATP contents within the cell lysate and in the media collected were combined together for quantification of total ATP synthesis as mentioned previously [110]. ATP levels were measured using a luciferin-luciferase reaction (Abcam, UK).

3.2.6 Osteoblast Conditioning Experiment

CM from OCY454 parallel plate flow chamber experiment was used on MC3T3-E1 osteoblasts seeded in 24-well plates. Media in sample wells consist of 50% CM and 50% MC3T3-E1 media. Media was replaced on day 4, 7, 10, and 14. Extracted media from these time points were used for measurement of extracellular ALP activity, and after which the cells were used for Alizarin Red S (ARS) quantification on day 14.

3.2.7 Quantification of extracellular ALP activity

Extracellular ALP activity levels of cultured MC3T3-E1 were quantified using colorimetric assay. Briefly, media collected (40 µL) after the 14-day osteoblast conditioning experiment was added to 40 µL of deionized water and 50 µL of 5 mM pNPP (Sigma-Aldrich, USA), followed

by a 60-minute incubation at room temperature. Finally, 20 µL of NaOH (Sigma-Aldrich, USA) was added into the mixture to stop the reaction. The resultant absorbance reading at 450 nm was detected using the Spectromax i3 Multimode Detection Platform (Molecular Devices, USA).

3.2.8 Calcium Deposit Quantification

MC3T3-E1 osteoblasts cultured for 14 days in CM were fixed with 4% formaldehyde (Sigma-Aldrich, USA) before staining with 40 mM ARS (ScienCell, USA) for 30 min. After extensive washing with DPBS, the cells were incubated in 10% acetic acid (ScienCell, USA) for 30 min before heated at 85°C for 10 min. The sample is then centrifuged at 16,000g for 20 min, after which 10% ammonium hydroxide was added to neutralize the acid. The supernatant is read at 405 nm using the Spectromax i3 Multimode Detection Platform (Molecular Devices, USA).

3.2.9 Osteoclast Conditioning Experiment and TRAP Staining

RAW264.7 osteoclasts seeded in 24-well plates were supplied with media consisting of 50% CM and 50% RAW264.7 media with a final concentration of 10 ng/mL recombinant RANKL (R&D Systems, USA). Media was changed on days 4, 5, and 6. Cells seeded on well plate were stained for osteoclast formation using Tartrate-resistant acid phosphatase (TRAP) staining on day 7 using protocol previously described [20]. Briefly, cells were fixed and stained with a leukocyte acid phosphatase kit (Sigma-Aldrich, USA). TRAP-positive cells were counted and grouped into small (2-4 nucleus) and large (5 or more nucleus) osteoclasts.

3.2.10 Statistics

A minimum of three individual experiments were ran with minimum 2 samples per experimental group. Student's t-test (2-tail, non-paired for calcium response; 2-tail, paired for all other results) was used to test significance between flow and no flow groups ($\alpha = 0.05$). The *n* value represents the total number of samples from all experiments.

3.3 Experimental Results

3.3.1 Sclerostin Expression under OFF

To establish the OCY454 cell line as an appropriate model for studying osteocyte intercellular signalling *in vitro*, there is a need to demonstrate its mechano-sensitivity under physiological flow conditions (0.8-3Pa, 1 - 9 Hz [20][111][112]). OFF (1.2 Pa, 1 Hz) was applied to stimulate

differentiated OCY454 cells, and soluble protein level was measured 24 hrs after flow. We observed that sclerostin expression by OCY454 cells decreased after exposure to fluid flow (Figure 3.1A), but no decrease in RANKL/OPG ratio was measured (Figure 3.1B). However, the secreted levels of RANKL is significantly lower than those measured from MLO-Y4 cells under the same conditioned as reported previously [95]. Under similar seeding and mechanical stimulation conditions, the raw ELISA measurement of RANKL were a whole magnitude lower that previously studied MLO-Y4 cells. However, total cell number is significantly higher for OCY454 cells due to their culturing protocol, which suggest an even lower per cell expression level of RANKL.

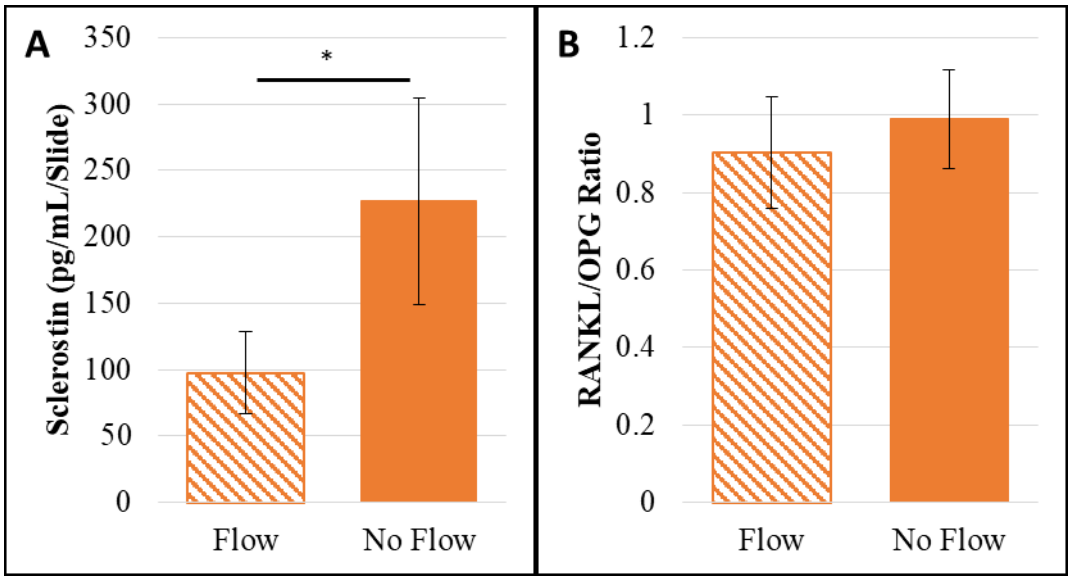

Figure 3.1: Sclerostin and RANKL/OPG Expression from OCY454 Cells. Extracellular sclerostin and RANKL/OPG concentration in media from OCY454 cells 24 hours after flow stimulation. A) Sclerostin levels measured from the flow-stimulated OCY454 cells were significantly lower compared to no flow control group ($p<0.05$, $n = 6$). B) Both RANKL and OPG secretion levels were also measured. No significant differences in RANKL/OPG ratio was observed between flow and no flow groups ($p=0.39$, $n = 12$).

3.3.2 Intracellular Calcium Response after Fluid Flow

It is well established that MLO-Y4 cells can respond to fluid flow with instantaneous intracellular calcium response [98], which is one of the major early events in the mechanotransduction cascade. Outcome variables such as responding cell percentage, response magnitude, and number of responding peaks have been used as indicators of response to flow to evaluate osteocyte mechano-sensitivity. We here applied OFF at 4 Pa peak shear stress to

differentiated OCY454 cells, showing that OCY454 cells do have calcium response to this level of flow (Figure 3.2). However, comparing to the calcium response of MLO-Y4 cells stimulated under the same flow conditions, OCY454 cells had a significant lower percentage of responding cells (Figure 3.2A). Furthermore, the OCY454 osteocytes sometimes had a much higher magnitude of response, unseen in MLO-Y4 cells (Figure 3.2B&D). These response magnitudes varied considerably between different experiments, while those from MLO-Y4 cells are known to be more stable and precise. The OCY454 cells rarely had multiple peak responses (Figure 3.2C), but characteristic multi-peak calcium responses were sometimes found in MLO-Y4 cells (Figure 3.2D). Furthermore, OCY454 cells typically had longer response durations than the MLO-Y4 cells, as can be seen in Figure 3.2D, where there is a long response curve in contrast to the sharp curve observed for MLO-Y4 cells.

3.3.3 ATP Release after Fluid Flow

One of the important markers of mechano-sensitivity of osteocytes is the immediate release of ATP upon fluid flow stimulation. After 20 min of OFF stimulation (2 Pa, 1 Hz), both media and cell lysates were extracted from the ibidi chambers to measure for total ATP contents. The results showed a significant difference in the total ATP content between OCY454 cells under fluid flow and cells in static conditions (Figure 3.3). This agreed with previously observed response from MLO-Y4 osteocytes *in vitro* [98].

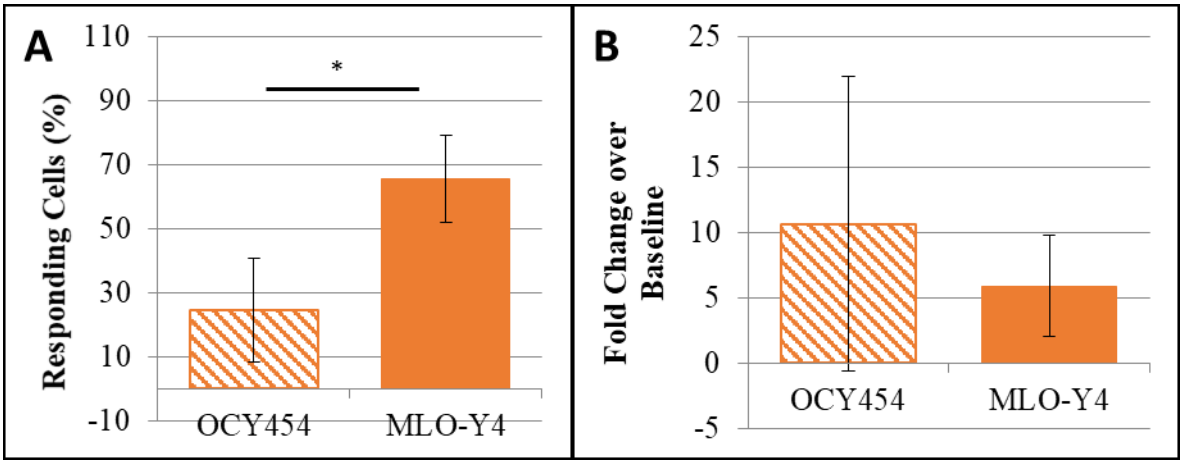

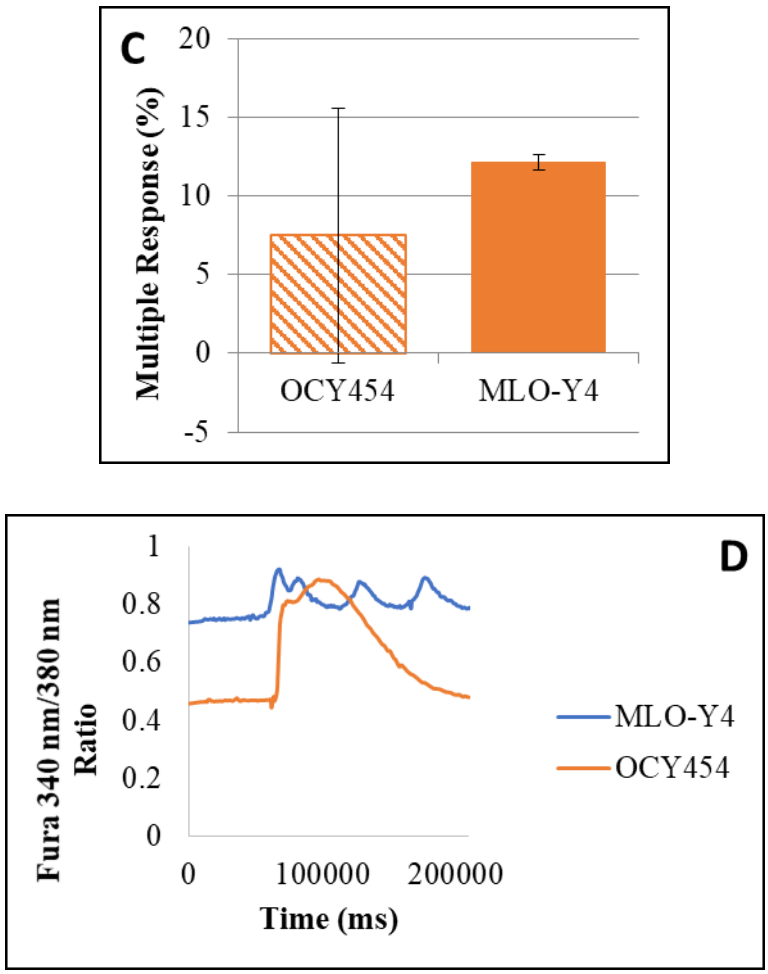

Figure 3.2: OCY454 Calcium response. Immediate intracellular calcium response measured at the onset of OFF (4 Pa, 1 Hz) stimulation. A) Significant difference in percentage of responding cells observed ($p < 0.05$, $n = 6$), however no statistically significant difference observed for B) average magnitude of response and C) percentage of cells exhibiting multiple response. D) A graph showing typical calcium response curves (flow stimulation started at 1 min) observed from the two different osteocyte cell lines, with multi-peak response shown in the MLO-Y4 curve.

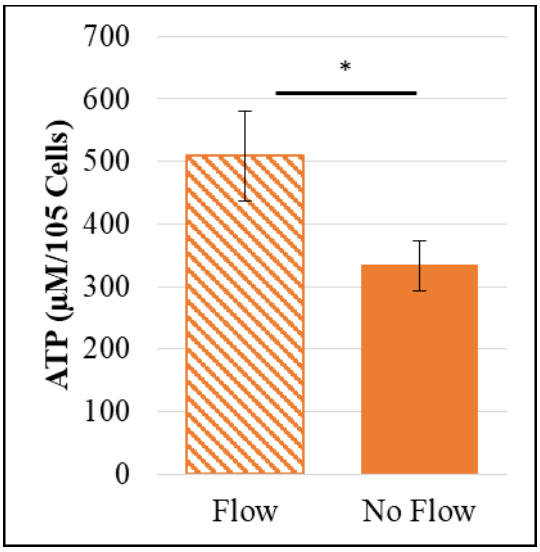

Figure 3.3: Total ATP level from OCY454. Total ATP contents were measured from OCY454 cells immediately after a 20-minute stimulation with OFF. Cell lysate and media were combined to test for total ATP. There was a significant difference observed between cells exposed to fluid flow versus no flow ($p < 0.01$, $n = 6$).

3.3.4 Flow Stimulated OCY454 Affects Osteoblast Activity

Cross-talk between mechano-sensing osteocytes and osteoblasts is essential to the loading-regulated metabolic bone remodelling process. To investigate this regulation, CM from OCY454 cells 24 hours after OFF stimulation were used to culture MC3T3-E1 osteoblasts over a period of 14 days. ALP activity was measured on day 4, 7, 10, and 14 from the cell culture media (Figure 3.4A). There was a noticeable increase in ALP activity of osteoblasts cultured in CM from flow-stimulated osteocytes in comparison to CM from static osteocytes in the first three time points (Figure 3.4A). These differences started to diminish on day 14, where the ALP activity stabilized to similar levels between osteoblasts conditioned with flow and static osteocyte media. This is expected since ALP activity is known to be an early marker for osteoblast differentiation.

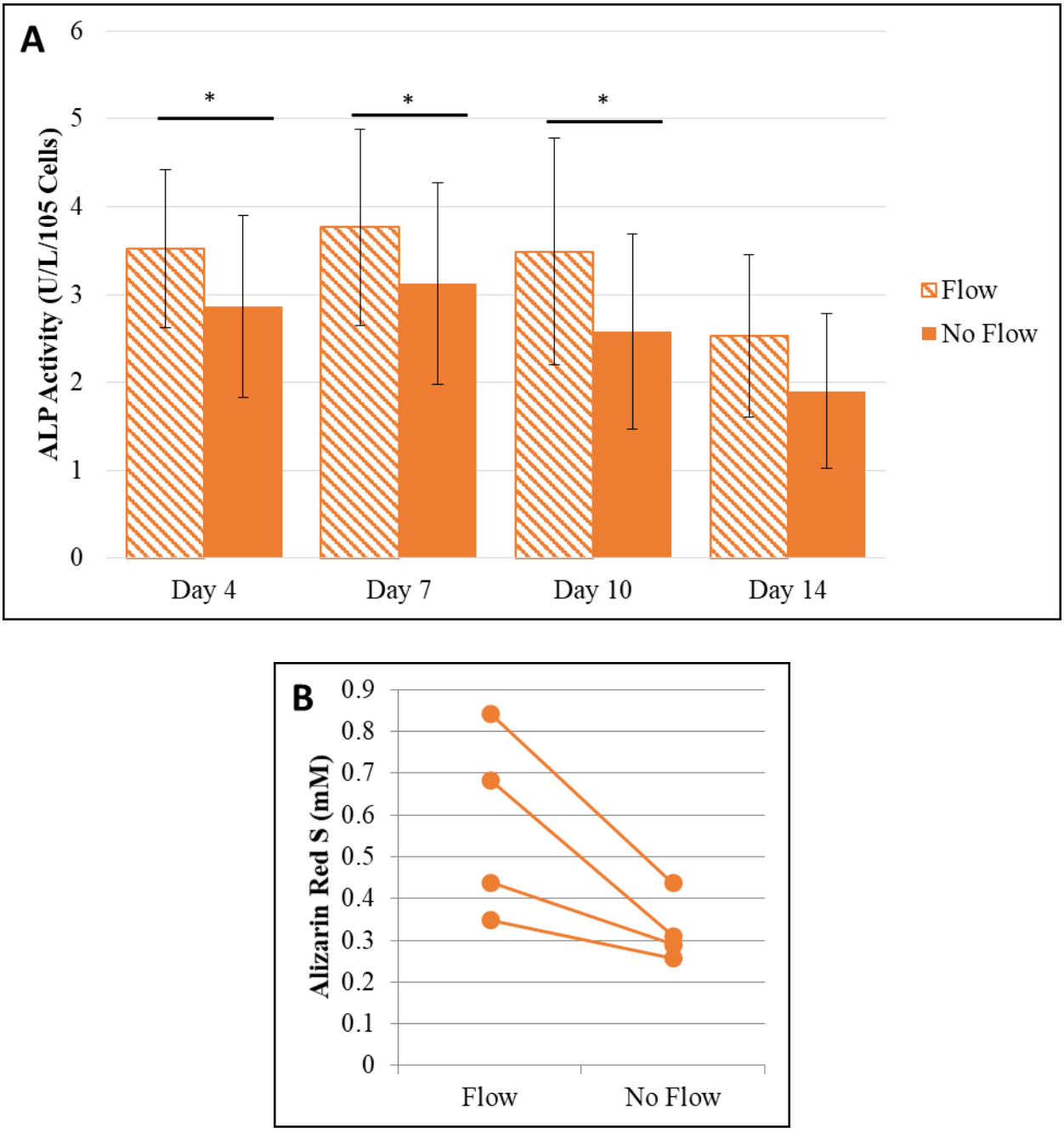

Figure 3.4: Osteoblast activity. Intracellular ALP activity and ARS stain for calcium deposition in osteoblasts conditioned in CM from static or flow-stimulated OCY454 cells. A) A significant difference in ALP activity was observed between flow and no-flow groups on days 4 ($p < 0.05$, $n = 11$), 7 ($p < 0.01$, $n = 11$) and 10 ($p < 0.01$, $n = 11$). However, this difference decreased on day 14 ($p > 0.05$, $n = 7$). B) A significant difference between flow and no flow group was observed in calcium deposition at day 14 (each line represents a separate trial, $p < 0.05$, $n = 9$). This verified that the observed differences in ALP activity does affect osteoblast functions.

In addition to intracellular ALP, calcium deposition is often used as an important indicator of osteoblast activity *in vitro* [113]. Calcium deposition levels were also measured at the end of day

14 using ARS stain. Although ALP levels started to stabilize, there was a significant difference in the final calcium deposition between osteoblasts conditioned in flow and no flow CM (Figure 3.4B). Quantitative measurement of ARS showed similar trends as those observed from day 4 to day 10 of ALP activity measurements (Figure 3.4B). These results, combined with the ALP activity assay, demonstrated that fluid flow-stimulated OCY454 cells can increase bone formation activities.

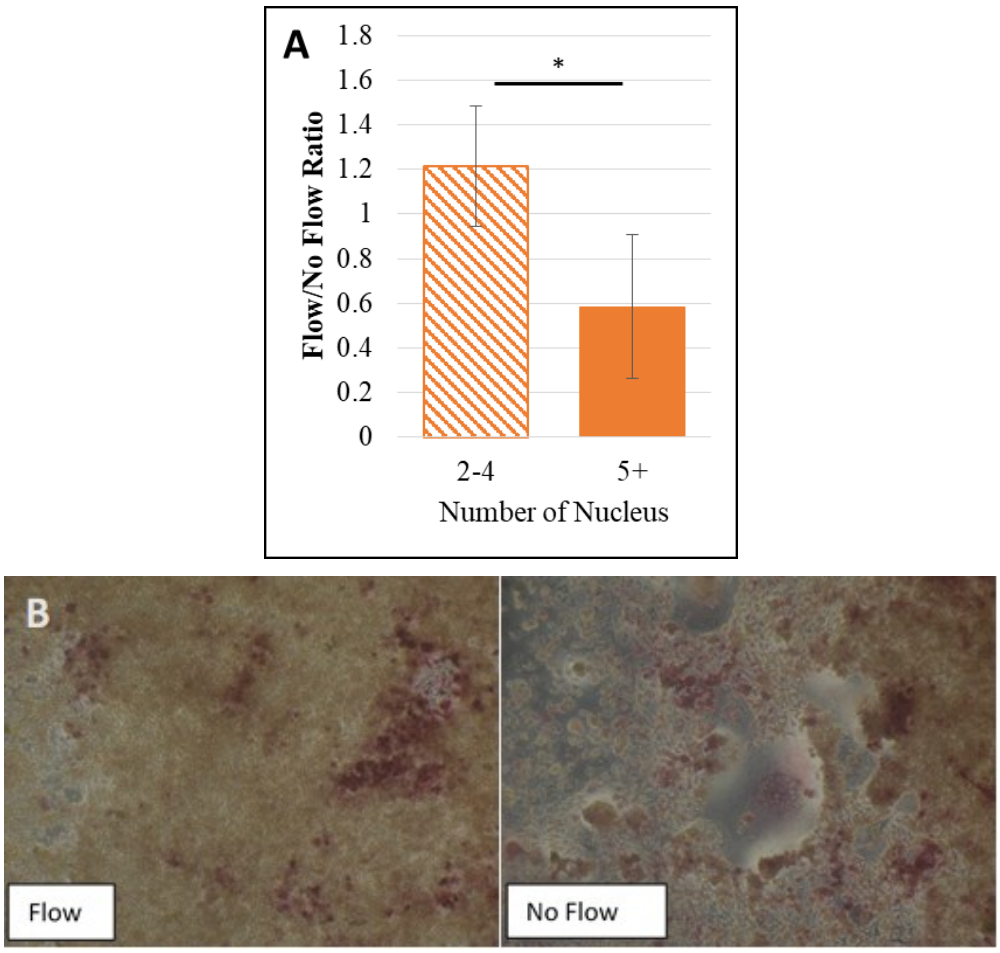

Figure 3.5: Osteoclast activity. Osteoclast activity was measured using TRAP stain on osteoclast cultured in CM from OCY454 cells for 7 days. A) There was no difference in the total number of TRAP-positive osteoclasts. However, there was a significant decrease in the number of large osteoclasts with 5 or greater nucleus when conditioned in media from the flow-stimulated OCY454 cells *($p < 0.05$, $n = 8$)*. B) Sample images showing that osteoclasts in the no flow group appeared larger in size.

3.3.5 OCY454 Affects Osteoclast Differentiation

Similarly, cross-talk between osteocytes and osteoclasts is critical in the regulation of bone resorption. CM from mechanically stimulated OCY454 osteocytes was used to culture RAW264.7 cells supplemented with RANKL. Differentiation of RAW264.7 cells into osteoclasts was measured by TRAP staining on day 7. Although no significant differences were observed between the overall numbers of differentiated osteoclasts in the flow and no flow groups (Figure 3.5A), there was a significant higher number of large osteoclasts with more than 5 nuclei in the no flow group (Figure 3.5B). This demonstrates that fluid flow experienced by OCY454 cells stimulated a change in secreted factors that altered osteoclast activity, even though the initial ELISA results showed no difference in the RANKL/OPG ratio.

3.4 Discussion

To address one of the major challenges in osteocyte mechanobiology field, the lack of secreted sclerostin from MLO-Y4 cells, we here investigated the potential of OCY454 cells as a new osteocyte model. We showed that OCY454 cells responded to physiologically relevant OFF with both immediate ATP syntheses as well as long-term sclerostin expression. Furthermore, the results from our CM experiments confirmed that the factors secreted from OCY454 cells are capable of regulating osteoblast activities. This is a significant finding since, to the best of our knowledge, there is very limited *in vitro* studies on osteocyte-osteoblast intercellular communication due to the absence of sclerostin secretion from MLO-Y4 cells [114][115]. Our results suggest that OCY454 cells have the potential to fill this gap in knowledge.

In osteoblast conditioning experiments, ALP activity of MC3T3-E1 osteoblasts conditioned with flow-stimulated osteocyte CM was consistently higher than that of the no-flow group at 4, 7, and 10 days after the start of conditioning. However, the ALP activity slightly decreased on day 14, and there was no more significant difference between the flow and no-flow groups. As we are interested in the time-lapse change of osteoblast ALP activity in response to the same group of osteocytes, all CM for a single well of osteoblasts came from one specific glass slide of osteocytes. During the conditioning experiment, vials of CM were thawed from -20 °C during media changes. Due to the length of storage, media used on day 10 might have significantly less protein content compared to when it was first collected. This will affect the ALP activity measured on day 14, and could also explain why there was an overall reduction in ALP activity

measured in both the flow and no-flow groups. However, the final ARS staining stands as a more concrete proof to the overall effect of the 14-day conditioning of osteoblasts using OCY454 CM. ARS stain from the flow group was consistently higher than that from the no-flow groups, demonstrating the lasting effect of the mechano-regulation of osteoblasts via osteocytes. Although fresh CM could be generated from new flow experiments for each media change, this would result in large variations between the CM due to differences, such as cell passages, making it difficult to isolate the effect of the osteocyte mechano-regulation of osteoblasts. The difference observed between osteoblasts conditioned in CM from static and flow-stimulated OCY454 cells is likely due to the flow-induced downregulation of sclerostin expression, though more molecular experiments will be needed to confirm this proposition.

Results from the osteoclast conditioning experiments also demonstrated a difference between the flow and no flow groups. This is unexpected as the initial ELISA quantification of RANKL/OPG ratio showed no major change when the OCY454 osteocytes were exposed to flow. Though it has been suggested that sclerostin might have a catabolic mechanism to increase osteoclast activity through a RANKL-dependent pathway [116], RANKL levels measured from OCY454 cells using standard ELISA were often very low, similar to the results obtained by the original developers of the cell line [26], indicating other pathways are at play. There is also a possibility that the decrease in osteoclast differentiation in the flow group could be due to β-catenin signals. It has been proposed in literature that β-catenin signals play a role in osteoclast differentiation [117] and, as an inhibitor of the Wnt pathway, decrease in sclerostin might also decrease osteoclast differentiation. However, this phenomenon is still widely debated in literature [118][119], and OCY454 osteocytes may be an ideal candidate to explore this pathway *in vitro*.

We have also tested the immediate response of OCY454 osteocytes to fluid flow, in an attempt to verify and quantify its mechano-sensitivity. Flow-induced ATP release is a well-known indicator of mechanotransduction for osteocytes, often coupled with autophagy [110] and transient calcium response [98][120]. Similar to results observed for MLO-Y4 cells [121], the new OCY454 osteocytes also exhibited a significant increase in total ATP expression when stimulated with flow. Interestingly, the calcium responses measured from the OCY454 cells is very different compared to the MLO-Y4 cells. Under elevated flow condition of 4 Pa shear

stress, MLO-Y4 cells exhibited consistency in percentage of responding cells, mean magnitude of response, and percentage of multiple response. But when the same flow conditions were applied to the OCY454 cells, large variations in response were observed between the different experiments. Overall, there were significantly less OCY454 cells that responded to flow. Furthermore, when applied with standard *in vitro* fluid flow condition of 2 Pa shear stress, almost no calcium response was observed from the OCY454 cells (data not shown). The large variations in response could be due to the heterogeneity of the cell line. Since it is a relatively new cell line, the OCY454 cells we have been working with are yet to be isolated to a homogeneous population. As further development of the cell line occurs, there should be a significant reduction in the variation of the response. However, this may not explain the observation that there was little to no response to the normal physiological flow condition of 2 Pa shear stress. A previous study had elicited measurable calcium responses at 0.4 and 1.6 Pa shear stress [122], using omni-directional laminar flow [123], which is very different compared to the physiological OFF used in this study. Previous literatures have shown different cell response under different flow profiles [124], prompting the speculation that OCY454 cells might also have different calcium response profiles when exposed to different flow schemes.

There is a distinct difference between the culturing methods for the OCY454 osteocytes compared to MLO-Y4 cells. The overall differentiation period of the new cell line was 14 days, which resulted in an extremely confluent layer of cells at the end of differentiation. This is very different from MLO-Y4 cells which require passaging before reaching full confluence. It is possible that traditional cell culturing techniques are not ideal for this OCY454 cells, and more novel methods that encompass a steady supply of nutrients during its differentiation stage should be explored. Furthermore, the original authors have noted to avoid passaging the cells during the differentiation period, making it difficult to culture to the full length of the differentiation period without substantial amount of cell death. As osteocytes in the bone are situated in sparse networks without direct contact between cell bodies, it is reasonable to question whether the new OCY454 cells are truly representative of the *in vivo* osteocytes. Future experimentation with the OCY454 cells should investigate whether there is a more optimal protocol for culturing these cells that can instigate a similar morphology to *in vivo* osteocytes.

In vitro studies related to many bone diseases or osteocyte-associated diseases had been limited as there was a lack of a physiologically-accurate cell line to characterize the disease. Similarly,

many diseases related to sclerostin cannot be studied using MLO-Y4 cells. Animal studies and clinical data is often used, but without proper understanding of their pathways *in vitro*, it is extremely difficult to uncover clinical solutions to these diseases. We suggest that, by demonstrating their capability to regulate osteoblast and osteoclast activities, OCY454 cells can be used *in vitro* to study diseases such as bone dysplasia and van Buchem disease [125]. The incorporation of OCY454 cells will provide insight into the imbalances between bone resorption and bone formation, leading to potential clinical solutions to disorders such as osteoporosis.

3.5 Conclusion

In summary, we showed that OCY454 osteocytes respond to flow with changes in intracellular calcium concentration, ATP contents, and sclerostin release. We also showed that soluble factors released from fluid flow-stimulated OCY454 cells can further regulate osteoblasts. Therefore, our findings suggest that OCY454 is a promising new cell model for *in vitro* osteocyte mechanotransduction studies. We hope that, by demonstrating these traits, OCY454 cells will be recognized as a new cell line capable of tackling intercellular signalling studies between bone cells and unveil molecular targets that are key to future clinical solutions.

Chapter 4

4 Magnetically Actuated Beam for Osteocyte Stimulation

4.1 Introduction and Background

Mechanotransduction is an important process for basic cell functions, affecting key cellular mechanisms such as protein signalling and DNA transcription. Physical cues act as fundamental inputs to mechanotransduction, ranging from mechanical stimulation of the cell surface to unique physical properties embedded in the surrounding extracellular matrix [126,127]. Although observed in a variety of organ systems, these physical cues are most prominent in load-bearing tissues such as the bone.

In bone tissue, osteocytes, the major mechano-sensory cells, are embedded within the lacunar-canalicular network exposing them to high levels of fluid shear stress upon bone tissue compression [128]. This mechanical stimulus is important for bone tissue function, as it activates key signalling pathways that regulate the bone remodelling process [3,129]. Osteocytes seeded within *in vitro* fluid flow systems have demonstrated their sensitivity to different levels of fluid shear stress [130–132]. However, current typical *in vitro* systems rely on macro-scale devices that stimulate a monolayer cell culture with uniform shear stress, in contrast with the pockets of shear stress gradients experienced by osteocytes in the lacuna-canaliculi network [133,134]. The rise of microfluidic systems has filled this gap by introducing cell culturing platforms with dimensions closer to that of the lacunar-canalicular network, therefore demanding development of newer fluid stimulation mechanisms beyond traditional parallel flow chambers to mimic more physiologically accurate mechanical stimulation of osteocytes.

One of the early stage cell responses to flow in the form of intracellular calcium fluctuations have been successfully detected from both osteocytes cultured using *in vitro* fluid flow systems [135–137], as well as *in vivo* models [16,138,139]. These calcium fluxes were measured with either the average response from a population of osteocytes or the single-cell calcium fluctuation pattern. However, it is still very difficult to differentiate the cellular responses that result from intercellular signalling transport from mechanically stimulated cells. Both *in vitro* experiments using patterned cell networks [140] and *ex vivo* studies using bone tissue [141] have

demonstrated the key role calcium fluctuations play in propagation of signals between mechanically stimulated and non-stimulated osteocytes; however these studies rely on membrane disturbance and tissue strain as the mechanical stimulus, lacking the capability to study how fluid shear stress influences this type of signal propagation. Existing tools such as atomic force microscopy (AFM) can only provide point-force membrane disturbances to the cell and lack the capability to generate localized fluid shear stress representative of the different levels of shear stress experienced by osteocytes within the lacuna-canaliculi network. Hence there is a need for the development of a platform to locally stimulate a selected region of osteocyte culture with a shear stress gradient to measure the varying response of osteocytes to mechanical stimulation, as well as response from intracellular signalling to non-stimulated cells.

While local stimulation of cells has been attempted in the past [142], no study has attempted to quantify the shear stress gradient that can be generated through local non-contact cell manipulation. Contact cell manipulation involves direct physical contact between the cell wall and external tools or forces whereas non-contact cell manipulation is the indirect manipulation of cells through remote actuation methods such as magnetic fields [20], acoustics [145–147], fluid forces [148,149], and dielectrophoresis [150–152]. Contact manipulation allows for precise control of single cells using techniques such as optics or optical tweezers [153–155], magnetic fields [156–158] or bio-actuation [159,160]. These techniques can be embedded into a microfluidic chip and allow for cutting, injecting and stimulation of individual cells with a high degree of selectivity and accuracy [161–163]. Non-contact cell manipulation has the capability to manipulate a larger number of cells in a multitude of environments but loses some of the accuracy and specificity of contact manipulation. They are, however, less likely to damage cells as a result. Magnetically actuated micro-robotic tools have been used in the past for cell manipulation tasks such as transportation [143,144] or proposed for other biomedical applications [164].

This study aims to design a platform which can enable local cell mechanical stimulation by fluid shear stress in a targeted region. A magnetically-actuated beam is placed above adherent MLO-Y4 osteocyte-like cells and oscillated at a frequency of 1 Hz in order to apply fluid shear stresses to the cells. The shear stress is localized to the region surrounding the beam, while cells further away from the stimulated region experience minimal shear stress. Finite element simulations are performed in order to quantify the shear stress values that can be generated by the oscillating

magnetic beam. An experimental protocol is established with a specifically designed coil system and driving electronics integrated into an optical inverted microscope. Live imaging of intracellular calcium fluctuations is used to quantify cell response during magnetic actuation. A shear stress map is plotted along with the locations of all stimulated cells in order to illustrate the working principles of the device and to understand how future studies with local cell stimulation can be performed more reliably.

4.2 Methods

4.2.1 Design and fabrication

Local stimulation of cells is achieved through the placement of a magnetically-actuated flexible beam above the adherent cell surface, which can generate localized shear stress regions [165]. The beam is manufactured as a flexible polymer with magnetic material embedded inside. It consists of a mixture of polydimethylsiloxane (PDMS, Sylgard 184, Dow Corning) which comes in two parts with a polymer base and curing agent that are combined in a 10:1 ratio by mass. This mixture is then combined with permanent magnetic particles (MQFP-15-7, NdPrFeB, Magnequench) in a 1:1 mass ratio. This mixture is poured into a negative mold of the beam that was created using photolithography. The excess is scraped off with a razor blade. This mixture is fully cured on an 85°C hot plate for 4 hours and the beam is subsequently removed from the mold using a needle. After the beam has been removed, the magnetic particles inside the beam are magnetized before assembly by placing the beam in a uniform magnetic field of 1.1 T created by two permanent magnets (1-inch cube, NdFeB, N40, Magnet4US) placed 3 mm apart (Figure 4.1).

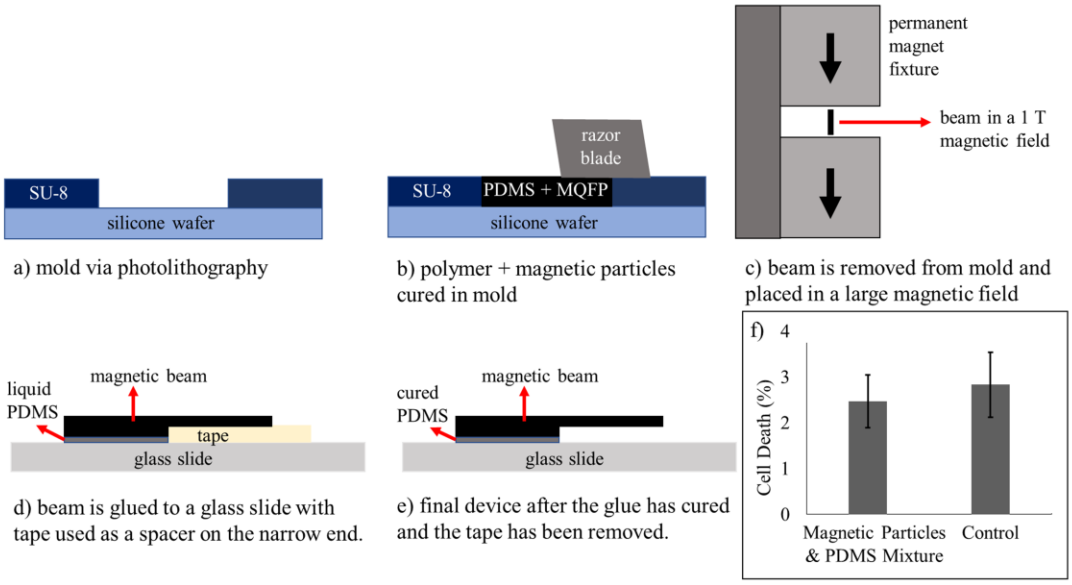

Figure 4.1: The fabrication process for the magnetically-actuated beam. a) a negative mold for the beam is created via photolithography, b) A mixture of PDMS with magnetic particles is cured in the mold with any excess removed via a razor blade, c) the beam is removed after curing and magnetized in a large magnetic field generated by two permanent magnets, d) the magnetic beam is then glued to a glass slide using liquid PDMS and tape as a spacer and again cured, e) the final device when the spacer is removed after the device has been fully cured. f) Experiment demonstrating that the magnetic mixture has no effect on cell death compared to conventional plastic cultureware. N = 3.

The beam is then glued using liquid PDMS to a glass slide with a spacer added to prevent the sinking of the beam. This is again cured on an 85°C hot plate for 4 hours. After curing, the spacer is removed. Separately, an adhesive film is added as a border to another glass slide on which cells are cultured. The slide with the beam is then flipped and placed on top of the cell surface. A small gap between the beam and the cell surface is necessary to ensure non-contact manipulation. Two different types of adhesives films are used to leave a gap height of 10 and 25 µm respectively. However, we will show in our results that cell stimulation was likely not achieved until the gap height was 5 µm as shear stress levels at higher gap heights are not sufficient. The small gap heights are achieved coincidentally in these set of experiments, but future experiments can be designed to repeatedly achieve this gap height. The most common reasons for the experimental gap height to be smaller than the theoretical gap height is because of gravity, which pulls the tip of the beam down when the device is assembled or a thick layer of glue that pushes the whole structure downward (see Figure 4.2). The former would also result in an uneven shear stress gradient resulting in cells closer to the tip of the beam to be more easily

stimulated due to higher shear stress levels while the latter would increase the shear stress uniformly across the localized region.

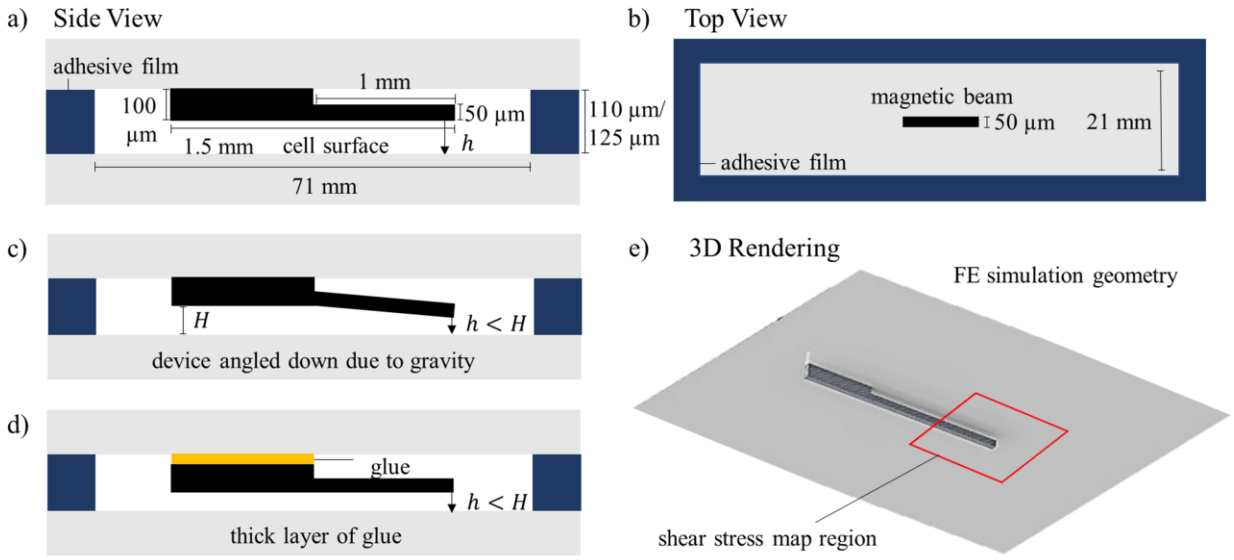

Figure 4.2: Schematics showing the magnetic actuator. a) Side view of the fully assembled device where the magnetic beam sits a distance h above the cell surface, b) top view of the device is shown with the adhesive film border on the bottom slide and the magnetic device glued to the top glass slide. c) and d) show scenarios where the gap height h can be coincidentally reduced either due to the device being angled downwards due to gravity (c) or as a result of thick spacer or a thick layer of glue pushing the whole structure downwards (d). e) A 3D rendering of the geometry is shown. This is the geometry used in the finite element analysis. The red square shows the region where shear stress calculations were performed.

4.2.2 Experimental design

A pair of electromagnetic coils (Figure 4.3) were designed to fit around a fluorescence microscope. A large set of coils were designed with a 17 cm radius, 300 turns of a 7 AWG copper wire mounted on a wooden structure that generates 10 mT in the center of the workspace. The device is placed in the center of the workspace such that the magnetization direction of the beam is perpendicular to the external magnetic flux density. An oscillating magnetic flux density of 10 mT at 1 Hz (Figure 4.4b) causes the beam to oscillate in the x-y plane [165] that results in fluid shear stress on the cell surface. From previous literature, commonly accepted range of fluid shear stress sensed by osteocytes in the lacuna-canaliculi network is estimated to be around 0.8 –

3 Pa [133], with our previous work showing a response from MLO-Y4 osteocytes at a minimum of 0.5 Pa [130].

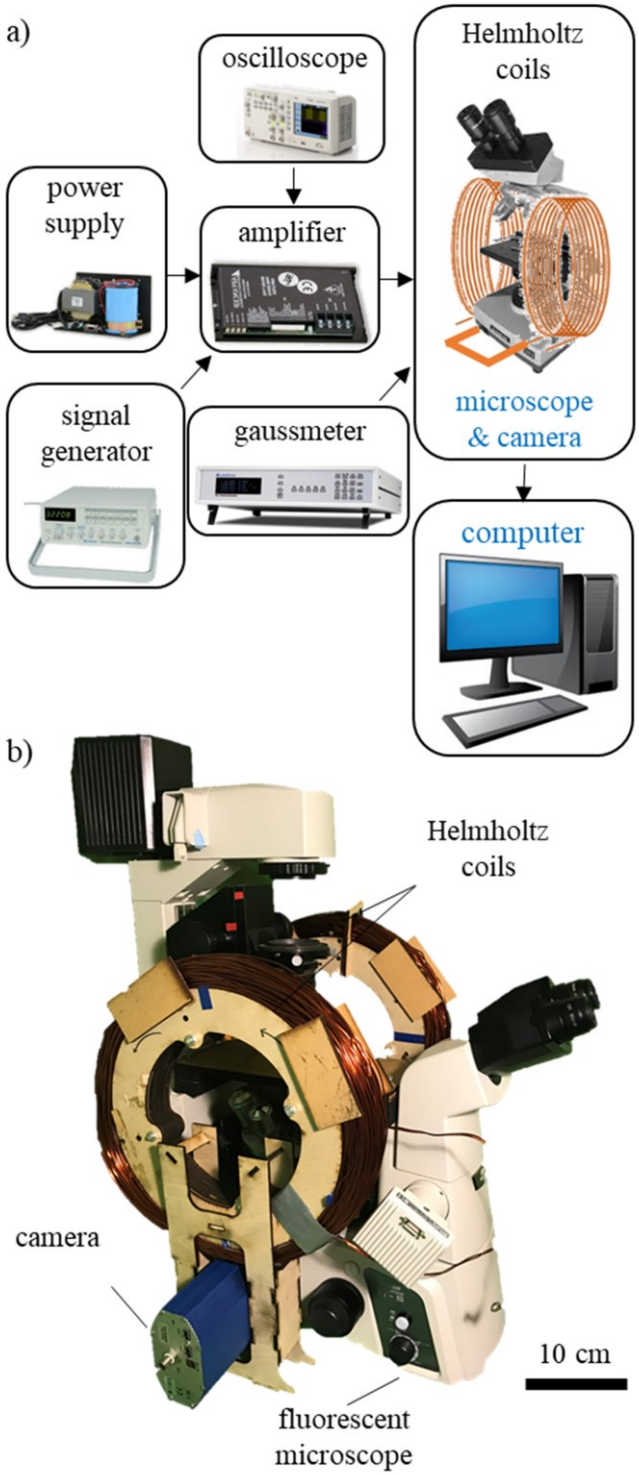

Figure 4.3: Experimental setup to test magnetic actuator. a) A schematic of the experimental setup is shown, b) the actual coils when placed around the microscope are shown. The 1D Helmholtz coils are specifically designed to fit around a fluorescent

microscope. The coils are connected to an amplifier and power supply for current generation.

Hence, the magnitude of the shear stress must be greater than 0.5 Pa to result in cell stimulation, which occurs for very small beam-surface gap heights. The coil system is connected to an analog servo driver (30A8, Advanced Motion Controls) and power supply for tunable field generation. A signal generator is used to generate a 1 Hz sinusoidal waveform. The sinusoidal waveform was chosen because it is the most well-accepted stimulus pattern for osteocytes in literature [166,167]. The external magnetic flux density (B) results in a torque on the magnetic beam since the direction of magnetization (m) is placed perpendicular to the field direction. The magnetization of the beam is 48 kA/m [168] . The resulting magnetic torque (T) is described by Eq. 1.

$$T = m \times B = mBsin\theta \quad (1)$$

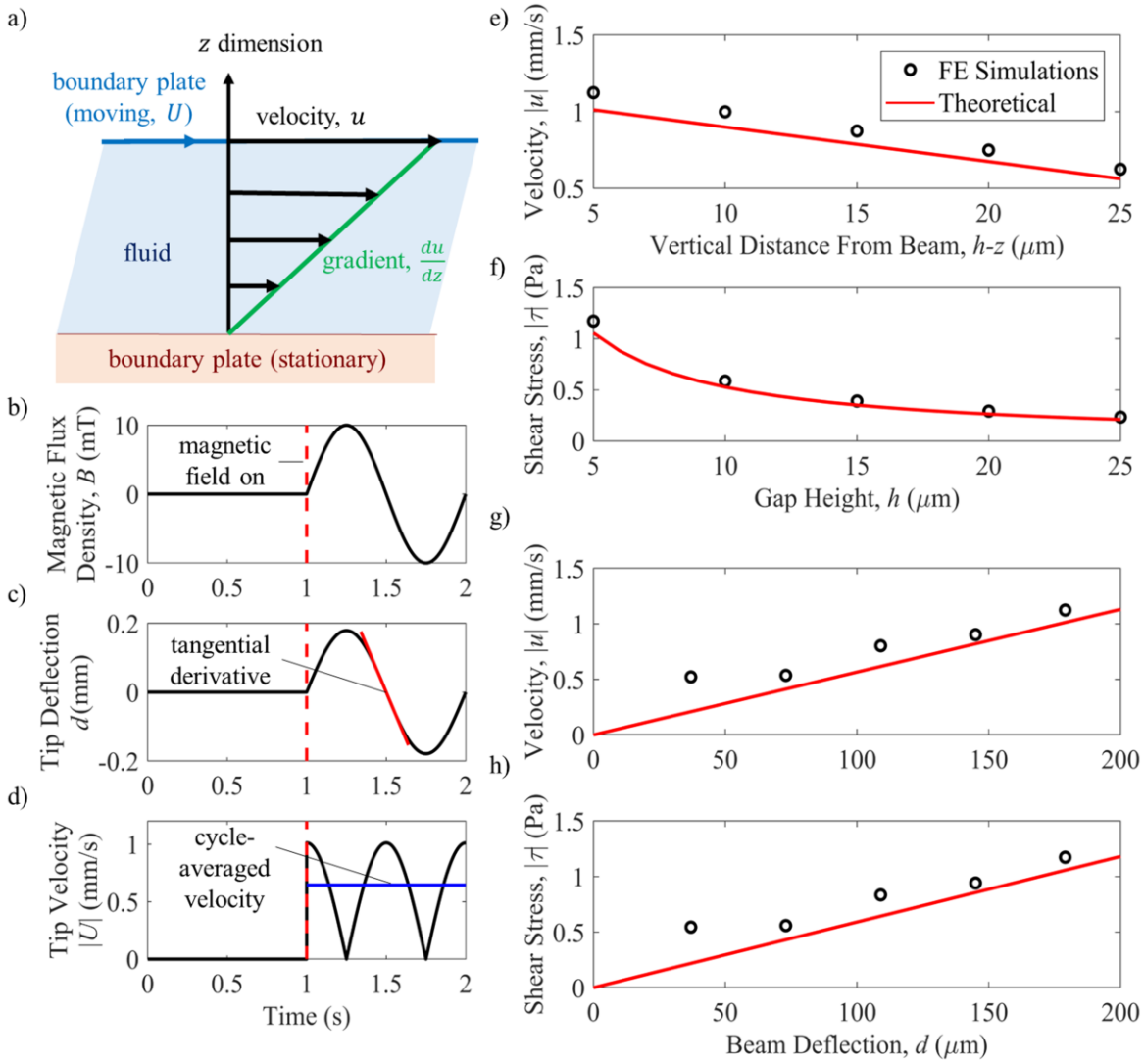

Figure 4.4: Simulation results for magnetic beam flow generation. a) 2D Couette flow principle; b) magnetic flux density generated by the coils (shown for 2 s for posterity but this takes place over several minutes); c) the resulting theoretical deflection profile of the beam if the magnetic flux density in (b) is applied. This is also the profile used in the finite element analysis and the tangential derivative is used to determine the theoretical velocities shown in parts (e) and (g). d) The theoretical beam tip velocity magnitude as well as the cycle averaged velocity is shown for the deflection profile seen in (c). e) and g) are plotted using Eq. 7 with theoretical velocities determined using the tangential derivative of the deflection profile and the numerical velocities determined from the finite element simulations. f) and h) show the shear stress with varying gap heights and beam tip deflection based on Eq. 6 using theoretical and numerical velocities.

4.2.3 Finite element simulations and analysis

To determine the shear stress that is applied to the cells and to understand how the results can be made reproducible, a set of fluid-structure interaction simulations were performed in ANSYS Workbench 17.1. These were repeated for different deflections with a gap height of 50 µm. The results of these simulations can be seen in Figures 4.4 and 4.5. A 3D geometry was constructed as shown in Figure 4.2e in ANSYS Workbench 17.1 with Transient Structural and Fluent components coupled together. A tip force was applied to the magnetic beam to match the average deflection seen in experiments. Note that the devices are all manually fabricated where small variations can result in large changes to the deflection profile of the beam. This simulation uses an average observed deflection, but this can be higher or lower for individual experiments resulting in higher or lower shear stress values. The magnetic physics were not modelled here since magnetic actuation is only used to deflect the beam, which is easily observed experimentally, and therefore a model is not necessary to determine beam deflection or other parameters for estimation of the shear stress. A sinusoidally oscillating force is applied to the beam which induces motion in the fluid. The resulting velocity data from the fluid domain was extracted from CFD-Post for the 1 mm square shown in red in Figure 4.2e. For a 2D geometry, a spatial gradient of the velocity (u) data can be used to generate the shear stress (τ) results as shown in Eq. 2 where μ is the fluid viscosity.

$$\tau(z) = \mu \frac{\partial u}{\partial z} \tag{2}$$

For our 3D geometry with all 3 components of velocity, we need to use a spatial gradient of the velocity vector, which results in a 2nd order stress tensor as seen in Eqs. 3 and 4 where the diagonal elements correspond to the normal stresses and the rest are shear stress components.

$$\tau(\vec{u}) = \mu \nabla \vec{u} \tag{3}$$

$$\nabla\vec{u} = \begin{bmatrix} \frac{\partial u_x}{\partial x} & \frac{\partial u_x}{\partial y} & \frac{\partial u_x}{\partial z} \\ \frac{\partial u_y}{\partial x} & \frac{\partial u_y}{\partial y} & \frac{\partial u_y}{\partial z} \\ \frac{\partial u_z}{\partial x} & \frac{\partial u_z}{\partial y} & \frac{\partial u_z}{\partial z} \end{bmatrix} \tag{4}$$

When all components of the shear stress tensor were plotted, we observed that the results of the tensor are asymmetric, and this is likely a result of the vortices created by the beam oscillation and that τ_{xz} is the largest component of the shear stress. This is in line with the design of our device where the magnetic beam is placed a certain gap height above the cell surface and oscillates in the *x* direction resulting in a large spatial gradient. Finding the principal stresses of an asymmetric tensor is computationally intensive [169]. For our purposes, it is sufficient to conclude that all other elements are negligible and concentrate on the τ_{xz} component as the primary shear stress component leading to cell stimulation.

$$\tau_{xz} = \mu \frac{\partial u_x}{\partial z} \tag{5}$$

4.2.4 Analytical model

A Couette flow model is used as a simplified model of the system fluid dynamics. The Couette flow model is the flow of viscous fluid between two infinite plates separated by a distance h with one plate moving at a velocity *U* and the other plate held stationary as shown in Figure 4.4b. The shear stress for this simplified model is determined by Eq. (2) (the spatial gradient of the velocity). The geometry of motion in the experimental setup of this paper differs from the Couette assumption in two main ways: 1) oscillating flow generated due to the back and forth motions and 2) edge effects of the beam. A correction factor for the oscillatory Couette flow is found in Nalim *et al* [170]. However, since the Reynolds number for our flow is very small (with a peak of around 1.0), the oscillating flow correction is found to have negligible impact on the shear stress and does not need to be accounted for. Regarding the infinite plate assumption in the Couette flow model, our beam has defined edges and we see from the finite element model that some of the largest shear stress values occur near the edges of the beam. It has been shown in the past that edge effects increase the shear stress locally [170], and so we investigated the accuracy

of the simple Couette flow model (Eq. 6) for our setup to obtain the shear stress values plotted in Figure 4.4f and h. Here, U is the plate velocity (or the tip velocity of the beam in our specific case), h is the gap height and z is the vertical distance from the stationary wall. The velocities used in the calculation of the shear stress using this model are determined using 1) finite element simulations and 2) theoretical velocities determined based on the tangential derivative of a sinusoidal wave of the beams' deflection profile as shown in Figure 4.4c. The theoretical velocity profile of the beam is also illustrated in Figure 4.4d. The fluid velocity at different vertical distances from the beam (as shown by Eq. 7) is plotted in Figure 4.4e to show that the analytical Couette flow model and numerical simulations are in agreement and thus accurately captures the dominant fluid effects. The in-plane component of the fluid velocity is also plotted versus varying beam tip deflections in Figure 4.4g.

$$\tau = \frac{\mu U}{h} \tag{6}$$

$$u(z) = \frac{Uz}{h} \tag{7}$$

4.2.5 Cell culture

MLO-Y4 osteocytes (courtesy of Dr. Bonewald, Indiana University School of Medicine) are cultured in growth media composed of 2.5% calf serum (CS, Gibco, USA), 2.5% fetal bovine serum (FBS, Gibco, USA), 1% penicillin-streptomycin (PS, Gibco, USA), and 94% Alpha Minimum Essential Medium (MEM) (WISENT, Canada). Cells are seeded during passage 29 at 10^5 cells per 100 mm diameter collagen-coated (0.15 mg/ml Type I collagen (Corning, USA)) culture dishes and expanded until they achieve 80% confluency. The cells are then transferred onto collagen-coated experimental slides (75x25 mm) at a density of 500k cells per slide for overnight incubation untill they reach 80% confluence again before imaging. MLO-Y4 cells are passaged between P29 and P35 while maintained in an incubator at 37 ˚C and 5% CO_2. Cell death was quantified using Trypan Blue Stain (Sigma-Aldrich, USA) and counted under a standard light microscope.

4.2.6 Intracellular calcium imaging

Calcium imaging protocols are based on previously existing studies in literature [58,83,171]. Briefly, MLO-Y4 cells are stained with Fura-2 AM intracellular calcium dye (ThermoFisher

Scientific, USA) for 45 min at room temperature in darkness. After rinsing with phosphate-buffered saline (PBS, Sigma-Aldrich, USA) and resting on a heated imaging stage for 15 min, experimental slides seeded with stained cells are imaged by a Nikon Eclipse fluorescence microscope for 1-2 minutes before the magnetic field is turned on to oscillate the beam for up to 10 minutes. During experiments, cells are seeded in regular growth media supplemented with 4.6 mg/mL Dextran (500k MW) (Sigma–Aldrich) to achieve the needed shear stress value without significantly increasing the size of the beam. This results in an increase in the viscosity of the media which is directly proportional to shear stress. It has been previously shown that the addition of Dextran to flow experiments using MLO-Y4 osteocytes does not affect their calcium response [25]. Fluorescence signals are read, and a ratio between signals produced from exposure to 340 nm and 380 nm wavelength light is used to generate the calcium response curves. A point in an empty space is used to check for any background imaging noise; due to the ratiometric nature of the Fura-2 AM dye, no additional manual correction for noise is necessary if no imaging noise in the empty space is observed.. A calcium response is quantified as having 2-fold-change or greater compared to baseline average response peak magnitudes measured in the initial 2 minutes of non-stimulated cells.

4.3 Contribution to Overall Project

This was a collaborative project with Dr. Eric Diller's lab here at University of Toronto. Both co-first authors of the publication had specific contributions to the project. For my part, I was first involved in the experimental design for the validation of the device, where I helped setup the prototype device as well as the imaging system we used for all our validation experiments. I was then responsible for carrying out all the cellular experiments, where I was responsible for measuring intracellular calcium fluctuation of osteocytes under magnetically actuated micro-beams, and associated maintenance and preparation of osteocytes for these experiments. Both co-first authors equally contributed to the data analysis and manuscript writing related to the project.

4.4 Experimental Results and Discussion

We see from the analytical and numerical results of the shear stress values with different gap heights that large shear stress values are only obtained for very small gap heights (below 10 μm) and large beam tip deflection (greater than 150 μm). In Figure 4.5a, we have plotted the maximum shear stress map resulting from the oscillation of the beam over 10 cycles (the flow

has stabilized within 1 cycle as differences between the 1 cycle and 10 cycle simulations appear negligible) in the 1 mm square region of interest around the beam tip, along with all responding cells recorded from multiple experimental trials. A sample microscope view of the beam and osteocytes is shown in Figure 4.5b. The maximum shear stress occurs in small areas around the beam oscillation which we refer to as the 'local stimulation region' (LSR). We see that cells in and around the LSR are stimulated. This is confirmed to be a response due to the magnetic actuator, as cells seeded in the magnetic field without the actuator elicited no quantifiable calcium response. We also observed cells being stimulated outside of the LSR where the shear stress magnitude was below the threshold required for cell stimulation. We have two hypotheses as to why this is the case; first, this could be the result of some form of cell response due to prolonged low magnitude shear stress, or secondly, a release of signalling factors from the stimulated cells in the LSR cross talk with cells outside the LSR that lead to their response through intercellular communication. Also plotted here are the results of stimulated cells colour coded with a time stamp. It is observed that the response time of the cells is correlated with the distance of that cell from the tip of the beam (Figure 4.5c and 4.6a). The linear coefficient between these two variables is calculated to be 0.59, demonstrating a trend between distance and response time. We believe a higher coefficient can be achieved once we adopt the experimental setup in an enclosed microfluidic device, where we will have more control over the gap height between the osteocytes and the magnetic beam, as well as the reproducibility of device fabrication and thus the setup. This corroborates our earlier prediction that gravity is pulling down the tip of the beam resulting in higher shear stress levels near the tip and lower shear stress levels in the remaining LSR. The effect of gravity on the beam was also visually observed on multiple devices. The detailed calcium response of three cells is shown in Figure 4.6b.

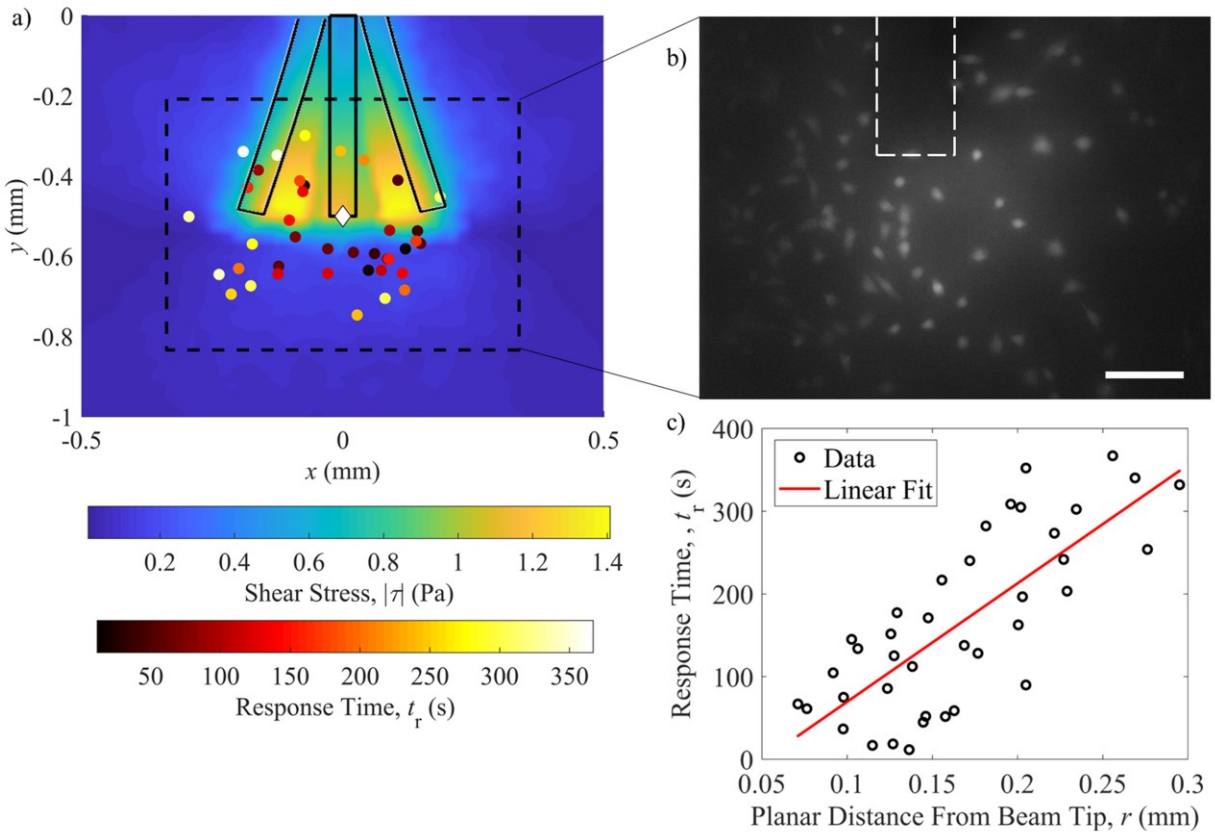

Figure 4.5: Osteocyte calcium response under magnetic actuator stimulation. a) The shear stress map obtained using Eq. 6 with velocities obtained from finite element simulations is overlaid with the locations of all responding cells from multiple trials that are coded with the time it takes to respond. The dotted line shows the typical viewing window in experiments and the range of the beam oscillation is also overlaid on the map. b) A representative image obtained of the Fura-2 AM stained cells along with the beam is shown which corresponds to the dotted lines on the shear stress map. Scale bar = 50 μm. c) A plot of the cell response time vs distance from the tip of the beam with a linear regression performed is shown, showing an increase in response time for cells further away from the stimulated region. A total of 3 trials and 39 cells were recorded, with an r^2 value of 0.59 for the linear regression.

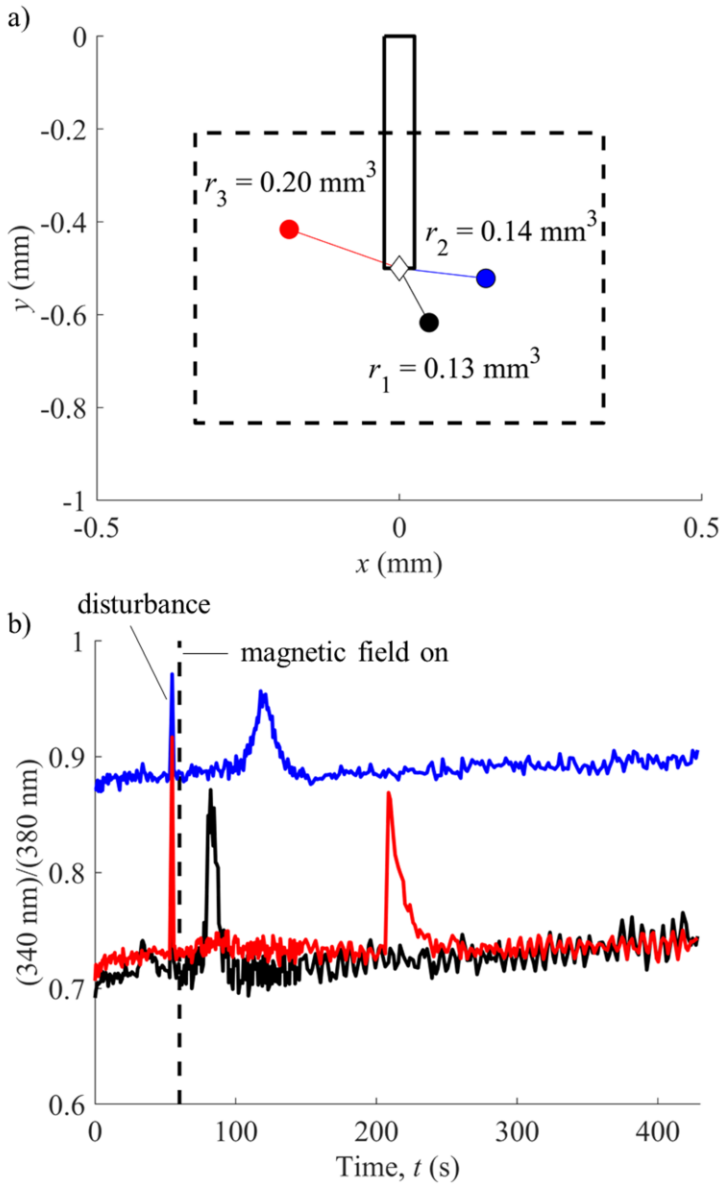

Figure 4.6: Sample calcium response curves resulting from magnetic actuation. a) Three cells are plotted with respect to their positions from the tip of the beam, positioned in regions with different shear stress values; b) the calcium response of the corresponding cells from part (a) are shown.

As established in the literature, signals propagate within an osteocyte network through key molecules such as ATP and calcium. It is interesting to note that despite the relatively far distance between the LSR and responding cells further away (100-250 µm) from the magnetic actuator, previous work has reported that extracellular vesicles could play a key role in delivering signals at a distance [141,171]. Since *in vitro* studies using cell indentation tools have shown it is difficult for calcium signals alone to propagate intracellular signalling beyond its neighbouring cells [140], we speculate that exosomes could be a potential explanation for

responding cells outside of LSR. Furthermore, first peak response time of up to 300 s has been observed from distant cells. As this time is much longer than standard calcium fluctuation response time due to mechanical stimulation [172,173], it can be implied that cellular response seen at this time scale is due to signal propagation from previously stimulated cells. However, future experiments involving fluorescent tracing of signal molecules will be required to confirm this hypothesis. Interestingly, except the time of initial response, there was no distinct difference in other response characteristics such as peak response magnitude and frequency of multi-peak response between mechanically stimulated osteocytes and osteocytes outside of the LSR with a registered calcium response. However, there was a slight, statistically non-significant trend towards higher response rate closer to the magnetic actuator (as can be seen by density of dots in Figure 4.5c). The above similarity in response magnitude is different from previous studies using cell membrane indentation technique, where a decrease in response magnitude was observed between stimulated and neighbouring non-stimulated cells [140]. With a prolonged stimulation time, it is possible that the concentration of signalling molecules increased to a threshold level capable of generating a comparable cellular response as fluid shear stress [174]. As there is an inherent difference between types of forces applied to the cell during fluid shear stress vs. cell membrane indentation, it is difficult to draw appropriate conclusions.

4.5 Conclusion

A device design is proposed and fabricated in order to locally stimulate cells. The device was employed experimentally, and cells under direct beam oscillation induced shear stress were found to respond with an intracellular calcium concentration increase. A set of finite element simulations were performed in order to obtain a shear stress map and a small LSR was found at a gap height of 5 μm. Over time, cells outside the LSR also respond. We postulate that this could be the result of communication between cells from the LSR or due to prolonged application of low magnitude shear stress. Future experiments can be made more reproducible by controlling the gap height more precisely in device fabrication. Another easy way of increasing the shear stress is to further increase the viscosity of the fluid which has been shown to increase the shear stress on the cells [175]. This is a straightforward path to achieve higher levels of stimulatory shear stress observed in bone tissue during loading [176]. Future studies will aim to place the beam inside microfluidic channels in order to do more in depth molecular analysis. A

microfluidic device will allow for future studies of osteocyte network signalling with physiologically accurate localized shear stress gradient.

Chapter 5

5 Summary

5.1 Contributions

Throughout all of my thesis projects, I had made significant contribution to the field of osteocyte mechanobiology, particularly in the design and validation of microfluidic platforms for osteocyte mechanotransduction studies. Using the multi-shear stress, co-culture microfluidic devices, I was able to demonstrate that osteocyte response to mechanical loading is tiered, where different levels of fluid shear stress changed the expression levels of signalling protein from osteocytes, as well as key mechanotransduction events such as intracellular calcium fluctuations. Furthermore, I demonstrated that using microfluidic platforms, I was able to test effects of both a chemical cue (zoledronic acid) and a physical cue (fluid shear stress) together with ease. It can be seen that the combined effect was not necessarily directly additive. Through my experiments and results, not only have I confirmed the importance of mechanical stimulation to osteocytes, but I had further proven that microfluidic devices were a useful tool in studying bone remodelling, and varying adaptations of its design could generate very beneficial tools for the bone field.

To improve *in vitro* experimental tools for osteocyte mechanotransduction studies, I partnered with a collaborator and developed a novel magnetically actuated micro-beam that can generate localized shear stress regions. This was an extremely useful platform, as the current standard *in vitro* mechanical loading model for osteocytes relied heavily on the parallel flow chamber concept, where an entire network of osteocytes all experienced the same fluid shear stress. The localized shear stress region produced by our micro-beams mimicked the *in vivo* fluid shear stress pockets in the lacuna-canalicular space, offering a more accurate representation of mechanical loading on osteocytes. Using this model, we were able to for the first time observe propagation of calcium signals from stimulated osteocytes to surrounding non-stimulated cells *in vitro*, and correlated this response time to the distance from center of stimulation. This was very important for the field as it allowed for study of more physiologically-relevant calcium signalling in osteocyte networks, and potentially help us understand how localized shear stress can affect distant osteocyte networks to produce an overall systemic cellular response.

The work I have done for the validation of novel OCY454 osteocyte cell line was pivotal for the *in vitro* study of bone remodelling. For many years, *in vitro* studies looking at osteocyte-osteoblast interactions, particular under mechanical loading conditions, had been scarce mainly due to a lack of stable osteocyte cell line with proper extracellular sclerostin expression. Using the novel OCY454 cell line, I confirmed its sensitivity to mechanical loading, and demonstrated its capability to regulate osteoblast activity. To the best of my knowledge, this was the first time mechanically stimulate osteocytes were used to induce increase in osteoblast activity *in vitro*. The results I obtained layout the foundation for future adaptations of OCY454 osteocytes to *in vitro* studies of bone remodelling, allowing for a more complete picture of the process as well as open the opportunity to create next-generation tri-culture systems of osteocyte, osteoblast, and osteoclasts.

5.2 Limitations

Even though I had successfully demonstrated the intercellular communication between mechanically stimulated osteocytes and osteoclasts, there are still significant limitations to the current microfluidic device, particularly during the experimental setup phase. Currently, to prevent mixing of cells between the two chambers, cell loading was conducted in two separate days. This allowed for selected chambers to be pressurized in order to minimize cells travelling through the communication pores during cell loading. However, this was not a robust method as many attempts resulted in failure due to difficulty in maintaining proper pressure with our inlet/outlet plugs. Any leakages in these inlets/outlets would result in failed cell loading, and often meant a restart to the experiment. This limitation could be resolved in the next iteration of the design, paying particular attention to developing new cell loading methods to achieve more robust co-culture of osteocytes and osteoclasts. Another limitation of the microfluidic device is issue caused by the interconnected channels. Although channel length was designed so that signalling molecules did not have enough time to diffuse to other co-culture units in between daily media changes, I had ran into significant problems when one of the co-culture units either had a defect, leakage, or minor infection. In traditional flow chamber experiments, since each chamber was separated, failure in one chamber only reduced the sample number by one. However, the co-culture microfluidic device I designed here resulted in three failed co-culture units whenever one of them had a problem. This drastically reduced the success rate of the experiments, hence more robust designs are needed. One way to resolve this issue is to integrate

microfluidic flow control valves into the design [177–179]. By advancing to a multilayer microfluidic device, I can introduce these control valves which allows for temporary closure of each co-culture unit. Valves can remained closed for the entire duration of the experience once problems arise from one of the sub-units, essentially saving two other co-culture units for experimentation. These valves can also help with the cell loading limitation in the current device, where flow control valves can temporarily seal the communication pores so that cells can be seeded without mixing prior to the beginning of the experiments.

As for the OCY454 osteocytes, although I had demonstrated their potential for osteocyte-osteoblast intercellular communication studies, they are currently not at a stage where they could be implemented into microfluidic devices. One of the biggest issue with the OCY454 cells was their need for over-confluent culture before they expressed significant levels of sclerostin. This was problematic for microfluidic devices since its physiologically-relevant volume-to-cell ratio did not allow for prolonged culture of over-confluent cells. Even perfusion of media was not enough to maintain proper cell health, and large layers of cultured OCY454 osteocytes would detach and flow out with the perfusion. This limited the application of OCY454 cells to traditional macro-scale flow chambers, and newer subclones of the cells were needed to have improved culturing properties before their use in microfluidic devices could be explored. Furthermore, since they did not express significant levels of RANKL protein, they could not be used for osteocyte-osteoclast experiments, which meant microfluidic devices looking at bone remodelling will need two different types of osteocyte cell line. This would present an obstacle for the tri-culture studies of bone remodelling.

Finally, for the magnetically actuated micro-beam project, we were limited by our current prototype in terms of the type of cellular analysis we could conduct on the osteocytes. This limitation could be resolved when we are designing the next generation of devices, where a sealed microfluidic device could be used to house the micro-beams, allowing for more accurate fixed-positioning of the localized shear stress region. Another challenging factor in the setup of next generation devices would be the re-design of the magnetic coils. These coils needed to reduce in size so that they could be used in the incubator along with the microfluidic devices. This posed as a challenge since the micro-beams might also need to be re-designed so that the same degree of actuated strength could be achieved with a potentially weaker magnetic field.

5.3 Future Directions

Although I had shown significant proof of osteocyte-osteoclast interaction with the multi-shear stress device, there are still a lot of experiments that can be carried out within the current device to further validate the device's application to bone remodelling. One of the immediate topic of research will be studying osteocyte-osteoblast intercellular communication during mechanical stimulation. To achieve this, one can either use the established MLO-Y4 cells to look at other signalling molecules outside of sclerostin, or utilize the small feature advantage of microfluidic devices and use primary osteocytes from digested animal bone samples. This will allow us to gain a better understanding of osteocyte-osteoblast interaction, as well as test various clinically relevant drug targets such as bisphosphonates to understand its effect on intercellular signalling during bone remodelling. If newer sub-cultures of OCY454 cells without previously discussed limitations become available, they will be an ideal, easy to adapt cell line model for this study as well.

Further work can also be continued on the development of the microfluidic device itself. Current prototype devices are designed for initial validation experiments, but many features can be adjusted and new features implemented to improve functionality. Chamber sizes can be significantly reduced since future experiments can rely on imaging based cellular analysis instead of using ELISA to measure for cell secretion. This will significantly increase the number of chambers we can fit on a single chip, increasing the experimental throughput. Furthermore, sizes of device inlets and outlets can be reduced to fit smaller tubing and needle pins, reducing their footprint on the device layout. A third channel in between the two culture chambers can be designed to assist during the cell seeding phase, where better fluid control of the middle channel can create a fluid barrier so that we can achieve dual cell seeding instead of seeding osteocyte and osteoclasts on separate days. These new design features will allow easier setup and increase the number of experiments that can be done simultaneously. Another class of improvements that can be made to the microfluidic device is on-chip nano-wire sensors that can track real-time concentration of signalling proteins post mechanical stimulation [180]. This would make up for the reduced chamber size in the new designs, where standard ELISA kits will not be applicable due to the low sample volume.

In terms of the magnetically actuated micro-beam, after our initial validation of its effect on cultured osteocytes, the next step will be to implement this device in a sealed microfluidic prototype to conduct more cellular analysis via imaging based techniques. The current prototype setup does not allow for long-term mechanical stimulation of osteocytes, which can be resolved by the new microfluidic device. This would require a re-design of the magnetic coil system so that we can generate the same magnetic field in the incubator, allowing for longer culture times for the cells. Dosage-dependent response can then be analyzed based on the frequency and duration of the mechanical stimulation on these cells. Furthermore, with fixed micro-beam locations, we can now look at the long term effects of adjacent pockets of fluid shear stress and how they affect osteocyte mechanotransduction in regions between the different shear stress pockets. Extensive analysis can be done using immunostaining techniques to look at different protein expression levels and how they correlate with distance to locally stimulated osteocytes. This will greatly improve our understanding of how osteocytes communicate to each other, and how *in vivo* shear stress pockets influence the mechanotransduction of an entire osteocyte network.

References

[1] X. Feng, J.M. McDonald, Disorders of bone remodeling., Annu. Rev. Pathol. 6 (2011) 121–145. https://doi.org/10.1146/annurev-pathol-011110-130203.

[2] A. Santos, A.D. Bakker, J. Klein-Nulend, The role of osteocytes in bone mechanotransduction, Osteoporos. Int. 20 (2009) 1027–1031. https://doi.org/10.1007/s00198-009-0858-5.

[3] J.C. Crockett, M.J. Rogers, F.P. Coxon, L.J. Hocking, M.H. Helfrich, Bone remodelling at a glance, J. Cell Sci. 124 (2011) 991–998. https://doi.org/10.1242/jcs.063032.

[4] S.L. Teitelbaum, F.P. Ross, Genetic regulation of osteoclast development and function., Nat. Rev. Genet. 4 (2003) 638–649. https://doi.org/10.1038/nrg1122.

[5] Z. Chen, H. Lv, J. Jiang, LTB4 can stimulate human osteoclast differentiation dependent of RANKL., Artif. Cells. Blood Substit. Immobil. Biotechnol. 38 (2010) 52–56. https://doi.org/10.3109/10731190903495785.

[6] M.M. Guerrini, C. Sobacchi, B. Cassani, M. Abinun, S.S. Kilic, A. Pangrazio, D. Moratto, E. Mazzolari, J. Clayton-Smith, P. Orchard, F.P. Coxon, M.H. Helfrich, J.C. Crockett, D. Mellis, A. Vellodi, I. Tezcan, L.D. Notarangelo, M.J. Rogers, P. Vezzoni, A. Villa, A. Frattini, Human osteoclast-poor osteopetrosis with hypogammaglobulinemia due to TNFRSF11A (RANK) mutations., Am. J. Hum. Genet. 83 (2008) 64–76. https://doi.org/10.1016/j.ajhg.2008.06.015.

[7] S. Marcellini, J.P. Henriquez, A. Bertin, Control of osteogenesis by the canonical Wnt and BMP pathways in vivo: cooperation and antagonism between the canonical Wnt and BMP pathways as cells differentiate from osteochondroprogenitors to osteoblasts and osteocytes., Bioessays. 34 (2012) 953–962. https://doi.org/10.1002/bies.201200061.

[8] G. Lombardi, C. Di Somma, M. Rubino, A. Faggiano, L. Vuolo, E. Guerra, P. Contaldi, S. Savastano, A. Colao, The roles of parathyroid hormone in bone remodeling: prospects for novel therapeutics., J. Endocrinol. Invest. 34 (2011) 18–22.

[9] S. Tatsumi, K. Ishii, N. Amizuka, M. Li, T. Kobayashi, K. Kohno, M. Ito, S. Takeshita, K.

Ikeda, Targeted ablation of osteocytes induces osteoporosis with defective mechanotransduction., Cell Metab. 5 (2007) 464–475. https://doi.org/10.1016/j.cmet.2007.05.001.

[10] R.L. van Bezooijen, B.A.J. Roelen, A. Visser, L. van der Wee-Pals, E. de Wilt, M. Karperien, H. Hamersma, S.E. Papapoulos, P. ten Dijke, C.W.G.M. Löwik, Sclerostin is an osteocyte-expressed negative regulator of bone formation, but not a classical BMP antagonist., J. Exp. Med. 199 (2004) 805–14. https://doi.org/10.1084/jem.20031454.

[11] S.A. Al-Dujaili, E. Lau, H. Al-Dujaili, K. Tsang, A. Guenther, L. You, Apoptotic osteocytes regulate osteoclast precursor recruitment and differentiation in vitro., J. Cell. Biochem. 112 (2011) 2412–2423. https://doi.org/10.1002/jcb.23164.

[12] B. Cheng, S. Zhao, L.F. Luo, E. Sprague, L.F. Bonewald, J.X. Jiang, Expression of functional gap junctions and regulation by fluid flow in osteocyte-like MLO-Y4 cells, J. Bone Miner. Res. 16 (2001) 249–259. https://doi.org/10.1359/jbmr.2001.16.2.249.

[13] X. Wang, Y. He, S. Tian, F. Zhu, B. Huang, J. Zhang, Z. Chen, H. Wang, Fluid shear stress increases osteocyte and inhibits osteoclasts via downregulating receptor-activator of nuclear factor kb (RANK)/osteoprotegerin expression in myeloma microenvironment, Med. Sci. Monit. 25 (2019) 5961–5968. https://doi.org/10.12659/MSM.915986.

[14] S.D. Tan, T.J. de Vries, A.M. Kuijpers-Jagtman, C.M. Semeins, V. Everts, J. Klein-Nulend, Osteocytes subjected to fluid flow inhibit osteoclast formation and bone resorption, Bone. 41 (2007) 745–751. https://doi.org/10.1016/j.bone.2007.07.019.

[15] W.Y. Cheung, C. Liu, R.M.L. Tonelli-Zasarsky, C.A. Simmons, L. You, Osteocyte apoptosis is mechanically regulated and induces angiogenesis in vitro, J. Orthop. Res. 29 (2011) 523–530. https://doi.org/10.1002/jor.21283.

[16] I. Kalajzic, B.G. Matthews, E. Torreggiani, M.A. Harris, P. Divieti Pajevic, S.E. Harris, In vitro and in vivo approaches to study osteocyte biology, Bone. 54 (2013) 296–306. https://doi.org/10.1016/j.bone.2012.09.040.

[17] J.I. Aguirre, L.I. Plotkin, S.A. Stewart, R.S. Weinstein, A.M. Parfitt, S.C. Manolagas, T.

Bellido, Osteocyte apoptosis is induced by weightlessness in mice and precedes osteoclast recruitment and bone loss, J. Bone Miner. Res. (2006). https://doi.org/10.1359/jbmr.060107.

[18] A.G. Robling, P.J. Niziolek, L.A. Baldridge, K.W. Condon, M.R. Allen, I. Alam, S.M. Mantila, J. Gluhak-Heinrich, T.M. Bellido, S.E. Harris, C.H. Turner, Mechanical Stimulation of Bone *in Vivo* Reduces Osteocyte Expression of Sost/Sclerostin, J. Biol. Chem. 283 (2008) 5866–5875. https://doi.org/10.1074/jbc.M705092200.

[19] C. Lin, X. Jiang, Z. Dai, X. Guo, T. Weng, J. Wang, Y. Li, G. Feng, X. Gao, L. He, Sclerostin mediates bone response to mechanical unloading through antagonizing Wnt/beta-catenin signaling., J. Bone Miner. Res. Off. J. Am. Soc. Bone Miner. Res. 24 (2009) 1651–1661. https://doi.org/10.1359/jbmr.090411.

[20] N. Lara-Castillo, N.A. Kim-Weroha, M.A. Kamel, B. Javaheri, D.L. Ellies, R.E. Krumlauf, G. Thiagarajan, M.L. Johnson, In vivo mechanical loading rapidly activates β-catenin signaling in osteocytes through a prostaglandin mediated mechanism, Bone. 76 (2015) 58–66. https://doi.org/10.1016/j.bone.2015.03.019.

[21] L.F. Bonewald, Establishment and characterization of an osteocyte-like cell line, MLO-Y4., J. Bone Miner. Metab. 17 (1999) 61–5. https://doi.org/10.1007/s007740050066.

[22] Y. Kato, A. Boskey, L. Spevak, M. Dallas, M. Hori, L.F. Bonewald, Establishment of an Osteoid Preosteocyte-like Cell MLO-A5 That Spontaneously Mineralizes in Culture, J. Bone Miner. Res. 16 (2001) 1622–1633. https://doi.org/10.1359/jbmr.2001.16.9.1622.

[23] T. Nakashima, M. Hayashi, T. Fukunaga, K. Kurata, M. Oh-hora, J.Q. Feng, L.F. Bonewald, T. Kodama, A. Wutz, E.F. Wagner, J.M. Penninger, H. Takayanagi, Evidence for osteocyte regulation of bone homeostasis through RANKL expression, Nat. Med. 17 (2011) 1231–1234. https://doi.org/10.1038/nm.2452.

[24] J.-N. Zhang, Y. Zhao, C. Liu, E.S. Han, X. Yu, D. Lidington, S.-S. Bolz, L. You, The role of the sphingosine-1-phosphate signaling pathway in osteocyte mechanotransduction, Bone. 79 (2015) 71–78. https://doi.org/10.1016/j.bone.2015.05.017.

[25] S.E. Papanicolaou, R.J. Phipps, D.P. Fyhrie, D.C. Genetos, Modulation of sclerostin expression by mechanical loading and bone morphogenetic proteins in osteogenic cells., Biorheology. 46 (2009) 389–99. https://doi.org/10.3233/BIR-2009-0550.

[26] J.M. Spatz, M.N. Wein, J.H. Gooi, Y. Qu, J.L. Garr, S. Liu, K.J. Barry, Y. Uda, F. Lai, C. Dedic, M. Balcells-Camps, H.M. Kronenberg, P. Babij, P.D. Pajevic, The Wnt inhibitor sclerostin is up-regulated by mechanical unloading in osteocytes in vitro, J. Biol. Chem. 290 (2015) 16744–16758. https://doi.org/10.1074/jbc.M114.628313.

[27] J. Klein-Nulend, R.G. Bacabac, A.D. Bakker, Mechanical loading and how it affects bone cells: the role of the osteocyte cytoskeleton in maintaining our skeleton., Eur. Cell. Mater. 24 (2012) 278–91. http://www.ncbi.nlm.nih.gov/pubmed/23007912 (accessed September 23, 2018).

[28] A.L. Rath, L.F. Bonewald, J. Ling, J.X. Jiang, M.E. Van Dyke, D.P. Nicolella, Correlation of cell strain in single osteocytes with intracellular calcium, but not intracellular nitric oxide, in response to fluid flow, J. Biomech. 43 (2010) 1560–1564. https://doi.org/10.1016/j.jbiomech.2010.01.030.

[29] D.P. Nicolella, D.E. Moravits, A.M. Gale, L.F. Bonewald, J. Lankford, Osteocyte lacunae tissue strain in cortical bone, J. Biomech. 39 (2006) 1735–1743. https://doi.org/10.1016/j.jbiomech.2005.04.032.

[30] A. Rath Bonivtch, L.F. Bonewald, D.P. Nicolella, Tissue strain amplification at the osteocyte lacuna: A microstructural finite element analysis, J. Biomech. 40 (2007) 2199–2206. https://doi.org/10.1016/j.jbiomech.2006.10.040.

[31] J. You, C.E. Yellowley, H.J. Donahue, Y. Zhang, Q. Chen, C.R. Jacobs, Substrate deformation levels associated with routine physical activity are less stimulatory to bone cells relative to loading-induced oscillatory fluid flow, J. Biomech. Eng. 122 (2000) 387–393. https://doi.org/10.1115/1.1287161.

[32] L. You, S.C. Cowin, M.B. Schaffler, S. Weinbaum, A model for strain amplification in the actin cytoskeleton of osteocytes due to fluid drag on pericellular matrix, J. Biomech. 34 (2001) 1375–1386. https://doi.org/10.1016/S0021-9290(01)00107-5.

[33] L.D. You, S. Weinbaum, S.C. Cowin, M.B. Schaffler, Ultrastructure of the osteocyte process and its pericellular matrix, Anat. Rec. - Part A Discov. Mol. Cell. Evol. Biol. 278 (2004) 505–513. https://doi.org/10.1002/ar.a.20050.

[34] L.M. McNamara, R.J. Majeska, S. Weinbaum, V. Friedrich, M.B. Schaffler, Attachment of osteocyte cell processes to the bone matrix, Anat. Rec. 292 (2009) 355–363. https://doi.org/10.1002/ar.20869.

[35] C.S. Yee, C.A. Schurman, C.R. White, T. Alliston, Investigating Osteocytic Perilacunar/Canalicular Remodeling, Curr. Osteoporos. Rep. 17 (2019) 157–168. https://doi.org/10.1007/s11914-019-00514-0.

[36] M.L. Hagan, K. Yu, J. Zhu, B.N. Vinson, R.L. Roberts, M. Montesinos Cartagena, M.H. Johnson, L. Wang, C.M. Isales, M.W. Hamrick, P.L. McNeil, M.E. McGee-Lawrence, Decreased pericellular matrix production and selection for enhanced cell membrane repair may impair osteocyte responses to mechanical loading in the aging skeleton, Aging Cell. 19 (2020). https://doi.org/10.1111/acel.13056.

[37] S. Temiyasathit, C.R. Jacobs, Osteocyte primary cilium and its role in bone mechanotransduction, in: Ann. N. Y. Acad. Sci., Blackwell Publishing Inc., 2010: pp. 422–428. https://doi.org/10.1111/j.1749-6632.2009.05243.x.

[38] M. Spasic, C.R. Jacobs, Lengthening primary cilia enhances cellular mechanosensitivity, Eur. Cells Mater. 33 (2017) 158–168. https://doi.org/10.22203/eCM.v033a12.

[39] K.L. Lee, M.D. Guevarra, A.M. Nguyen, M.C. Chua, Y. Wang, C.R. Jacobs, The primary cilium functions as a mechanical and calcium signaling nexus, Cilia. 4 (2015). https://doi.org/10.1186/s13630-015-0016-y.

[40] T.R. Coughlin, M. Voisin, M.B. Schaffler, G.L. Niebur, L.M. McNamara, Primary cilia exist in a small fraction of cells in trabecular bone and marrow, Calcif. Tissue Int. 96 (2014) 65–72. https://doi.org/10.1007/s00223-014-9928-6.

[41] A.E. Morrell, G.N. Brown, S.T. Robinson, R.L. Sattler, A.D. Baik, G. Zhen, X. Cao, L.F. Bonewald, W. Jin, L.C. Kam, X.E. Guo, Mechanically induced Ca2+ oscillations in

osteocytes release extracellular vesicles and enhance bone formation, Bone Res. 6 (2018). https://doi.org/10.1038/s41413-018-0007-x.

[42] A. Siddique, T. Meckel, R.W. Stark, S. Narayan, Improved cell adhesion under shear stress in PDMS microfluidic devices, Colloids Surfaces B Biointerfaces. 150 (2017) 456–464. https://doi.org/10.1016/j.colsurfb.2016.11.011.

[43] P.A. Galie, D.H.T. Nguyen, C.K. Choi, D.M. Cohen, P.A. Janmey, C.S. Chen, Fluid shear stress threshold regulates angiogenic sprouting, Proc. Natl. Acad. Sci. U. S. A. 111 (2014) 7968–7973. https://doi.org/10.1073/pnas.1310842111.

[44] S.K. Mahto, J. Tenenbaum-Katan, A. Greenblum, B. Rothen-Rutishauser, J. Sznitman, Microfluidic shear stress-regulated surfactant secretion in alveolar epithelial type II cells in vitro, Am. J. Physiol. - Lung Cell. Mol. Physiol. 306 (2014). https://doi.org/10.1152/ajplung.00106.2013.

[45] G.J. Mahler, C.M. Frendl, Q. Cao, J.T. Butcher, Effects of shear stress pattern and magnitude on mesenchymal transformation and invasion of aortic valve endothelial cells, Biotechnol. Bioeng. 111 (2014) 2326–2337. https://doi.org/10.1002/bit.25291.

[46] K. Hattori, Y. Munehira, H. Kobayashi, T. Satoh, S. Sugiura, T. Kanamori, Microfluidic perfusion culture chip providing different strengths of shear stress for analysis of vascular endothelial function, J. Biosci. Bioeng. 118 (2014) 327–332. https://doi.org/10.1016/j.jbiosc.2014.02.006.

[47] Z.Z. Chen, W.M. Yuan, C. Xiang, D.P. Zeng, B. Liu, K.R. Qin, A microfluidic device with spatiotemporal wall shear stress and ATP signals to investigate the intracellular calcium dynamics in vascular endothelial cells, Biomech. Model. Mechanobiol. 18 (2019) 189–202. https://doi.org/10.1007/s10237-018-1076-x.

[48] J. Lee, Z. Estlack, H. Somaweera, X. Wang, C.M.R. Lacerda, J. Kim, A microfluidic cardiac flow profile generator for studying the effect of shear stress on valvular endothelial cells, Lab Chip. 18 (2018) 2946–2954. https://doi.org/10.1039/c8lc00545a.

[49] D.Y. Park, T.H. Kim, J.M. Lee, C.D. Ahrberg, B.G. Chung, Circular-shaped microfluidic

device to study the effect of shear stress on cellular orientation, Electrophoresis. 39 (2018) 1816–1820. https://doi.org/10.1002/elps.201800109.

[50] X. Zhang, D.J. Huk, Q. Wang, J. Lincoln, Y. Zhao, A microfluidic shear device that accommodates parallel high and low stress zones within the same culturing chamber, Biomicrofluidics. 8 (2014) 054106. https://doi.org/10.1063/1.4894783.

[51] S.K. Dash, R.S. Verma, S.K. Das, Long range microfluidic shear device for cellular mechanotransduction studies, in: Proc. Annu. Int. Conf. IEEE Eng. Med. Biol. Soc. EMBS, Institute of Electrical and Electronics Engineers Inc., 2015: pp. 3209–3212. https://doi.org/10.1109/EMBC.2015.7319075.

[52] S. Arora, A.J.Y. Lam, C. Cheung, E.K.F. Yim, Y.C. Toh, Determination of critical shear stress for maturation of human pluripotent stem cell-derived endothelial cells towards an arterial subtype, Biotechnol. Bioeng. 116 (2019) 1164–1175. https://doi.org/10.1002/bit.26910.

[53] K.W. Oh, K. Lee, B. Ahn, E.P. Furlani, Design of pressure-driven microfluidic networks using electric circuit analogy, Lab Chip. 12 (2012) 515–545. https://doi.org/10.1039/c2lc20799k.

[54] B.D. Riehl, J.Y. Lim, Macro and microfluidic flows for skeletal regenerative medicine., Cells. 1 (2012) 1225–45. https://doi.org/10.3390/cells1041225.

[55] S.L. York, A.R. Arida, K.S. Shah, P. Sethu, M.M. Saunders, Osteocyte Characterization on Polydimethylsiloxane Substrates for Microsystems Applications, J. Biomim. Biomater. Tissue Eng. 16 (2012) 27–42. https://doi.org/10.4028/www.scientific.net/JBBTE.16.27.

[56] C. Wei, B. Fan, D. Chen, C. Liu, Y. Wei, B. Huo, L. You, J. Wang, J. Chen, Osteocyte culture in microfluidic devices, Biomicrofluidics. 9 (2015). https://doi.org/10.1063/1.4905692.

[57] L. You, S. Temiyasathit, S.R. Coyer, A.J. García, C.R. Jacobs, Bone Cells Grown on Micropatterned Surfaces are More Sensitive to Fluid Shear Stress, Cell. Mol. Bioeng. 1 (2008) 182–188. https://doi.org/10.1007/s12195-008-0017-7.

[58] X.L. Lu, B. Huo, V. Chiang, X.E. Guo, Osteocytic network is more responsive in calcium signaling than osteoblastic network under fluid flow, J. Bone Miner. Res. 27 (2012) 563–574. https://doi.org/10.1002/jbmr.1474.

[59] J. Li, E. Rose, D. Frances, Y. Sun, L. You, Effect of oscillating fluid flow stimulation on osteocyte mRNA expression, J. Biomech. 45 (2012) 247–251. https://doi.org/10.1016/j.jbiomech.2011.10.037.

[60] L. You, S. Temiyasathit, E. Tao, F. Prinz, C.R. Jacobs, 3D Microfluidic Approach to Mechanical Stimulation of Osteocyte Processes, Cell. Mol. Bioeng. 1 (2008) 103–107. https://doi.org/10.1007/s12195-008-0010-1.

[61] Y. Gu, W. Zhang, Q. Sun, Y. Hao, J. Zilberberg, W.Y. Lee, Microbead-guided reconstruction of the 3D osteocyte network during microfluidic perfusion culture, J. Mater. Chem. B. 3 (2015) 3625–3633. https://doi.org/10.1039/c5tb00421g.

[62] K. Middleton, L. You, A Microfluidic System To Study the Effects of Mechanically Loaded Osteocytes on Osteoclast Recruitment and Formation, 18th Int. Conf. Miniaturized Syst. Chem. Life Sci. 4 (2014) 627–629.

[63] B. Roy, T. Das, D. Mishra, T.K. Maiti, S. Chakraborty, Oscillatory shear stress induced calcium flickers in osteoblast cells., Integr. Biol. (Camb). 6 (2014) 289–299. https://doi.org/10.1039/c3ib40174j.

[64] S. Kou, L. Pan, D. van Noort, G. Meng, X. Wu, H. Sun, J. Xu, I. Lee, A multishear microfluidic device for quantitative analysis of calcium dynamics in osteoblasts, Biochem. Biophys. Res. Commun. 408 (2011) 350–355. https://doi.org/10.1016/j.bbrc.2011.04.044.

[65] C.W. Wei, J.Y. Cheng, T.H. Young, Elucidating in vitro cell-cell interaction using a microfluidic coculture system, Biomed. Microdevices. 8 (2006) 65–71. https://doi.org/10.1007/s10544-006-6384-8.

[66] R.S.W. Thomas, P.D. Mitchell, R.O.C. Oreffo, H. Morgan, Trapping single human osteoblast-like cells from a heterogeneous population using a dielectrophoretic microfluidic device, Biomicrofluidics. 4 (2010). https://doi.org/10.1063/1.3406951.

[67] J.J. Cody, A.A. Rivera, J. Liu, J.M. Liu, J.T. Douglas, X. Feng, A simplified method for the generation of human osteoclasts in vitro., Int. J. Biochem. Mol. Biol. 2 (2011) 183–189.

[68] E. Lau, S. Al-Dujaili, A. Guenther, D. Liu, L. Wang, L. You, Effect of low-magnitude, high-frequency vibration on osteocytes in the regulation of osteoclasts, Bone. 46 (2010) 1508–1515. https://doi.org/10.1016/j.bone.2010.02.031.

[69] L.H. Xu, H. Shao, Y.H. V. Ma, L. You, OCY454 Osteocytes as an in Vitro Cell Model for Bone Remodeling Under Mechanical Loading, J. Orthop. Res. 37 (2019) 1681–1689. https://doi.org/10.1002/jor.24302.

[70] O. Onaizah, L. Xu, K. Middleton, L. You, E. Diller, Local stimulation of osteocytes using a magnetically actuated oscillating beam, PLoS One. 15 (2020) e0235366. https://doi.org/10.1371/journal.pone.0235366.

[71] P. V. Hinton, S.M. Rackard, O.D. Kennedy, In Vivo Osteocyte Mechanotransduction: Recent Developments and Future Directions, Curr. Osteoporos. Rep. 16 (2018) 746–753. https://doi.org/10.1007/s11914-018-0485-1.

[72] W. Yang, I. Kalajzic, Y. Lu, D. Guo, M.A. Harris, J. Gluhak-Heinrich, L.F. Bonewald, J.Q. Feng, D.W. Rowe, S.E. Harris, In vitro and in vivo study on osteocyte-specific mechanical signaling pathways, J. Musculoskelet. Neuronal Interact. 4 (2004) 386–387. https://europepmc.org/article/med/15758272 (accessed July 1, 2020).

[73] R. Owen, G.C. Reilly, In vitro models of bone remodelling and associated disorders, Front. Bioeng. Biotechnol. 6 (2018) 134. https://doi.org/10.3389/fbioe.2018.00134.

[74] T. Nakashima, M. Hayashi, T. Fukunaga, K. Kurata, M. Oh-hora, J.Q. Feng, L.F. Bonewald, T. Kodama, A. Wutz, E.F. Wagner, J.M. Penninger, H. Takayanagi, Evidence for osteocyte regulation of bone homeostasis through RANKL expression, Nat. Med. 17 (2011) 1231–1234. https://doi.org/10.1038/nm.2452.

[75] J. Li, E. Rose, D. Frances, Y. Sun, L. You, Effect of oscillating fluid flow stimulation on osteocyte mRNA expression, J. Biomech. 45 (2012) 247–251.

https://doi.org/10.1016/j.jbiomech.2011.10.037.

[76] J.L. Pathak, N. Bravenboer, F.P. Luyten, P. Verschueren, W.F. Lems, J. Klein-Nulend, A.D. Bakker, Mechanical Loading Reduces Inflammation-Induced Human Osteocyte-to-Osteoclast Communication, Calcif. Tissue Int. 97 (2015) 169–178. https://doi.org/10.1007/s00223-015-9999-z.

[77] Y.H. V. Ma, C. Lam, S. Dalmia, P. Gao, J. Young, K. Middleton, C. Liu, H. Xu, L. You, Mechanical regulation of breast cancer migration and apoptosis via direct and indirect osteocyte signaling, J. Cell. Biochem. 119 (2018) 5665–5675. https://doi.org/10.1002/jcb.26745.

[78] Y.H.V. Ma, L. Xu, X. Mei, K. Middleton, L. You, Mechanically stimulated osteocytes reduce the bone-metastatic potential of breast cancer cells in vitro by signaling through endothelial cells, J. Cell. Biochem. 120 (2019) 7590–7601. https://doi.org/10.1002/jcb.28034.

[79] S. Trkov, G. Eng, R. Di Liddo, P.P. Parnigotto, G. Vunjak-Novakovic, Micropatterned three-dimensional hydrogel system to study human endothelial-mesenchymal stem cell interactions, J. Tissue Eng. Regen. Med. 4 (2010) 205–215. https://doi.org/10.1002/term.231.

[80] O.F. Khan, M.D. Chamberlain, M. V. Sefton, Toward an in vitro vasculature: Differentiation of mesenchymal stromal cells within an endothelial cell-seeded modular construct in a microfluidic flow chamber, Tissue Eng. - Part A. 18 (2012) 744–756. https://doi.org/10.1089/ten.tea.2011.0058.

[81] D. Huh, B.D. Matthews, A. Mammoto, M. Montoya-Zavala, H. Yuan Hsin, D.E. Ingber, Reconstituting organ-level lung functions on a chip, Science (80-.). 328 (2010) 1662–1668. https://doi.org/10.1126/science.1188302.

[82] K.H. Benam, R. Villenave, C. Lucchesi, A. Varone, C. Hubeau, H.H. Lee, S.E. Alves, M. Salmon, T.C. Ferrante, J.C. Weaver, A. Bahinski, G.A. Hamilton, D.E. Ingber, Small airway-on-a-chip enables analysis of human lung inflammation and drug responses in vitro, Nat. Methods. 13 (2016) 151–157. https://doi.org/10.1038/nmeth.3697.

[83] K. Middleton, S. Al-Dujaili, X. Mei, A. Günther, L. You, Microfluidic co-culture platform for investigating osteocyte-osteoclast signalling during fluid shear stress mechanostimulation, J. Biomech. 59 (2017) 35–42. https://doi.org/10.1016/j.jbiomech.2017.05.012.

[84] S.W. Donahue, C.R. Jacobs, H.J. Donahue, Flow-induced calcium oscillations in rat osteoblasts are age, loading frequency, and shear stress dependent, Am. J. Physiol. - Cell Physiol. 281 (2001). https://doi.org/10.1152/ajpcell.2001.281.5.c1635.

[85] J. Friend, L. Yeo, Fabrication of microfluidic devices using polydimethylsiloxane, Biomicrofluidics. 4 (2010). https://doi.org/10.1063/1.3259624.

[86] L. You, S. Temiyasathit, P. Lee, C.H. Kim, P. Tummala, W. Yao, W. Kingery, A.M. Malone, R.Y. Kwon, C.R. Jacobs, Osteocytes as mechanosensors in the inhibition of bone resorption due to mechanical loading, Bone. 42 (2008) 172–179. https://doi.org/10.1016/j.bone.2007.09.047.

[87] X.L. Huang, L.Y. Huang, Y.T. Cheng, F. Li, Q. Zhou, C. Wu, Q.H. Shi, Z.Z. Guan, J. Liao, W. Hong, Zoledronic acid inhibits osteoclast differentiation and function through the regulation of NF-κB and JNK signalling pathways, Int. J. Mol. Med. 44 (2019) 582–592. https://doi.org/10.3892/ijmm.2019.4207.

[88] K. Kimachi, H. Kajiya, S. Nakayama, T. Ikebe, K. Okabe, Zoledronic acid inhibits RANK expression and migration of osteoclast precursors during osteoclastogenesis, Naunyn. Schmiedebergs. Arch. Pharmacol. 383 (2011) 297–308. https://doi.org/10.1007/s00210-010-0596-4.

[89] M. Li, P. Wan, W. Wang, K. Yang, Y. Zhang, Y. Han, Regulation of osteogenesis and osteoclastogenesis by zoledronic acid loaded on biodegradable magnesium-strontium alloy, Sci. Rep. 9 (2019) 1–12. https://doi.org/10.1038/s41598-018-37091-8.

[90] H.J. Kim, H.J. Kim, Y. Choi, M.K. Bae, D.S. Hwang, S.H. Shin, J.Y. Lee, Zoledronate enhances osteocyte-mediated osteoclast differentiation by IL-6/RANKL axis, Int. J. Mol. Sci. 20 (2019). https://doi.org/10.3390/ijms20061467.

[91] S. Sun, M. Yang, Y. Kostov, A. Rasooly, ELISA-LOC: Lab-on-a-chip for enzyme-linked immunodetection, Lab Chip. 10 (2010) 2093–2100. https://doi.org/10.1039/c003994b.

[92] X. Li, C. Zhao, X. Liu, A paper-based microfluidic biosensor integrating zinc oxide nanowires for electrochemical glucose detection, Microsystems Nanoeng. 1 (2015) 15014. https://doi.org/10.1038/micronano.2015.14.

[93] Y. Han, X. You, W. Xing, Z. Zhang, W. Zou, Paracrine and endocrine actions of bone - The functions of secretory proteins from osteoblasts, osteocytes, and osteoclasts, Bone Res. 6 (2018) 1–11. https://doi.org/10.1038/s41413-018-0019-6.

[94] Y. Kato, J.J. Windle, B.A. Koop, G.R. Mundy, L.F. Bonewald, Establishment of an Osteocyte-like Cell Line, MLO-Y4, J. Bone Miner. Res. 12 (2010) 2014–2023. https://doi.org/10.1359/jbmr.1997.12.12.2014.

[95] S. Zhao, Y. Kato, Y. Zhang, S. Harris, S.S. Ahuja, L.F. Bonewald, MLO-Y4 Osteocyte-Like Cells Support Osteoclast Formation and Activation, J. Bone Miner. Res. 17 (2002) 2068–2079. https://doi.org/10.1359/jbmr.2002.17.11.2068.

[96] S.W. Verbruggen, T.J. Vaughan, L.M. McNamara, Fluid flow in the osteocyte mechanical environment: a fluid–structure interaction approach, Biomech. Model. Mechanobiol. 13 (2014) 85–97. https://doi.org/10.1007/s10237-013-0487-y.

[97] J. Li, E. Rose, D. Frances, Y. Sun, L. You, Effect of oscillating fluid flow stimulation on osteocyte mRNA expression, J. Biomech. 45 (2012) 247–251. https://doi.org/10.1016/j.jbiomech.2011.10.037.

[98] X.L. Lu, B. Huo, M. Park, X.E. Guo, Calcium response in osteocytic networks under steady and oscillatory fluid flow, Bone. 51 (2012) 466–473. https://doi.org/10.1016/j.bone.2012.05.021.

[99] L. You, S. Temiyasathit, P. Lee, C.H. Kim, P. Tummala, W. Yao, W. Kingery, A.M. Malone, R.Y. Kwon, C.R. Jacobs, Osteocytes as mechanosensors in the inhibition of bone resorption due to mechanical loading, Bone. 42 (2008) 172–179. https://doi.org/10.1016/j.bone.2007.09.047.

[100] S.D. Tan, T.J. de Vries, A.M. Kuijpers-Jagtman, C.M. Semeins, V. Everts, J. Klein-Nulend, Osteocytes subjected to fluid flow inhibit osteoclast formation and bone resorption, Bone. 41 (2007) 745–751. https://doi.org/10.1016/j.bone.2007.07.019.

[101] X.L. Lu, B. Huo, V. Chiang, X.E. Guo, Osteocytic network is more responsive in calcium signaling than osteoblastic network under fluid flow, J. Bone Miner. Res. 27 (2012) 563–574. https://doi.org/10.1002/jbmr.1474.

[102] Y. Gu, M.R. Preston, J. Magnay, A.J. El Haj, S.J. Publicover, Hormonally-Regulated Expression of Voltage-Operated Ca2+ Channels in Osteocytic (MLO-Y4) Cells, Biochem. Biophys. Res. Commun. 282 (2001) 536–542. https://doi.org/10.1006/bbrc.2001.4615.

[103] D. Jing, X.L. Lu, E. Luo, P. Sajda, P.L. Leong, X.E. Guo, Spatiotemporal properties of intracellular calcium signaling in osteocytic and osteoblastic cell networks under fluid flow., Bone. 53 (2013) 531–40. https://doi.org/10.1016/j.bone.2013.01.008.

[104] M.A. Riquelme, S. Burra, R. Kar, P.D. Lampe, J.X. Jiang, Mitogen-activated Protein Kinase (MAPK) Activated by Prostaglandin E $_2$ Phosphorylates Connexin 43 and Closes Osteocytic Hemichannels in Response to Continuous Flow Shear Stress, J. Biol. Chem. 290 (2015) 28321–28328. https://doi.org/10.1074/jbc.M115.683417.

[105] Y. Kitase, L. Barragan, H. Qing, S. Kondoh, J.X. Jiang, M.L. Johnson, L.F. Bonewald, Mechanical induction of PGE2 in osteocytes blocks glucocorticoid-induced apoptosis through both the β-catenin and PKA pathways, J. Bone Miner. Res. 25 (2010) 2657–2668. https://doi.org/10.1002/jbmr.168.

[106] A.E. Morrell, G.N. Brown, S.T. Robinson, R.L. Sattler, A.D. Baik, G. Zhen, X. Cao, L.F. Bonewald, W. Jin, L.C. Kam, X.E. Guo, Mechanically induced Ca2+ oscillations in osteocytes release extracellular vesicles and enhance bone formation, Bone Res. 6 (2018) 6. https://doi.org/10.1038/s41413-018-0007-x.

[107] X. Li, Y. Zhang, H. Kang, W. Liu, P. Liu, J. Zhang, S.E. Harris, D. Wu, Sclerostin Binds to LRP5/6 and Antagonizes Canonical Wnt Signaling, J. Biol. Chem. 280 (2005) 19883–19887. https://doi.org/10.1074/jbc.M413274200.

[108] M. van Dinther, J. Zhang, S.E. Weidauer, V. Boschert, E.-M. Muth, A. Knappik, D.J.J. de Gorter, P.B. van Kasteren, C. Frisch, T.D. Mueller, P. ten Dijke, Anti-Sclerostin antibody inhibits internalization of Sclerostin and Sclerostin-mediated antagonism of Wnt/LRP6 signaling., PLoS One. 8 (2013) e62295. https://doi.org/10.1371/journal.pone.0062295.

[109] K. Middleton, A. Kondiboyina, M. Borrett, Y. Cui, X. Mei, L. You, Microfluidics approach to investigate the role of dynamic similitude in osteocyte mechanobiology, J. Orthop. Res. 36 (2017) 663–671. https://doi.org/10.1002/jor.23773.

[110] B. Zhang, R. Hou, Z. Zou, T. Luo, Y. Zhang, L. Wang, B. Wang, Mechanically induced autophagy is associated with ATP metabolism and cellular viability in osteocytes in vitro, Redox Biol. 14 (2018) 492–498. https://doi.org/10.1016/j.redox.2017.10.021.

[111] Y. Han, S.C. Cowin, M.B. Schaffler, S. Weinbaum, Mechanotransduction and strain amplification in osteocyte cell processes., Proc. Natl. Acad. Sci. U. S. A. 101 (2004) 16689–94. https://doi.org/10.1073/pnas.0407429101.

[112] R.G. Bacabac, T.H. Smit, M.G. Mullender, J. Saskia, J. Klein-Nulend, M. Technology, S.J. Dijcks, J.J.W.. Van Loon, J. Klein-Nulend, Chapter 3 nitric oxide production by bone cells is fluid shear stress rate dependent, Biochem. Biophys. Res. Commun. 315 (2004) 823–829. https://doi.org/10.1016/j.bbrc.2004.01.138.

[113] E.-J. Kim, S.-Y. Bu, M.-K. Sung, M.-K. Choi, Effects of Silicon on Osteoblast Activity and Bone Mineralization of MC3T3-E1 Cells, Biol. Trace Elem. Res. 152 (2013) 105–112. https://doi.org/10.1007/s12011-012-9593-4.

[114] A.D. Bakker, R.N. Kulkarni, J. Klein-Nulend, W.F. Lems, IL-6 alters osteocyte signaling toward osteoblasts but not osteoclasts, J. Dent. Res. 93 (2014) 394–399. https://doi.org/10.1177/0022034514522485.

[115] P.S. Vezeridis, C.M. Semeins, Q. Chen, J. Klein-Nulend, Osteocytes subjected to pulsating fluid flow regulate osteoblast proliferation and differentiation, Biochem. Biophys. Res. Commun. 348 (2006) 1082–1088. https://doi.org/10.1016/j.bbrc.2006.07.146.

[116] A.R. Wijenayaka, M. Kogawa, H.P. Lim, L.F. Bonewald, D.M. Findlay, G.J. Atkins, Sclerostin Stimulates Osteocyte Support of Osteoclast Activity by a RANKL-Dependent Pathway, PLoS One. 6 (2011) e25900. https://doi.org/10.1371/journal.pone.0025900.

[117] W. Wei, D. Zeve, J.M. Suh, X. Wang, Y. Du, J.E. Zerwekh, P.C. Dechow, J.M. Graff, Y. Wan, Biphasic and dosage-dependent regulation of osteoclastogenesis by β-catenin., Mol. Cell. Biol. 31 (2011) 4706–19. https://doi.org/10.1128/MCB.05980-11.

[118] K. Maeda, Y. Kobayashi, N. Udagawa, S. Uehara, A. Ishihara, T. Mizoguchi, Y. Kikuchi, I. Takada, S. Kato, S. Kani, M. Nishita, K. Marumo, T.J. Martin, Y. Minami, N. Takahashi, Wnt5a-Ror2 signaling between osteoblast-lineage cells and osteoclast precursors enhances osteoclastogenesis, Nat. Med. 18 (2012) 405–412. https://doi.org/10.1038/nm.2653.

[119] S. Hayashi, P.L. Witte, L.D. Shultz, P.W. Kincade, H. Niwa, S. Takada, S.-I. Hayashi, Lymphohemopoiesis in culture is prevented by interaction with adherent bone marrow cells from mutant viable motheaten mice., J. Immunol. 140 (1988) 2139–47. https://doi.org/10.4049/jimmunol.167.2.765.

[120] B. Huo, X.L. Lu, K.D. Costa, Q. Xu, X.E. Guo, An ATP-dependent mechanism mediates intercellular calcium signaling in bone cell network under single cell nanoindentation, Cell Calcium. 47 (2010) 234–241. https://doi.org/10.1016/j.ceca.2009.12.005.

[121] Z. Seref-Ferlengez, S. Maung, M.B. Schaffler, D.C. Spray, S.O. Suadicani, M.M. Thi, P2X7R-Panx1 Complex Impairs Bone Mechanosignaling under High Glucose Levels Associated with Type-1 Diabetes, PLoS One. 11 (2016) e0155107. https://doi.org/10.1371/journal.pone.0155107.

[122] J.S. Lyons, H.C. Joca, R.A. Law, K.M. Williams, J.P. Kerr, G. Shi, R.J. Khairallah, S.S. Martin, K. Konstantopoulos, C.W. Ward, J.P. Stains, Microtubules tune mechanotransduction through NOX2 and TRPV4 to decrease sclerostin abundance in osteocytes., Sci. Signal. 10 (2017). https://doi.org/10.1126/scisignal.aan5748.

[123] J.S. Lyons, S.R. Iyer, R.M. Lovering, C.W. Ward, J.P. Stains, Novel multi-functional fluid flow device for studying cellular mechanotransduction., J. Biomech. 49 (2016) 4173–

4179. https://doi.org/10.1016/j.jbiomech.2016.11.051.

[124] S.M. Ponik, J.W. Triplett, F.M. Pavalko, Osteoblasts and osteocytes respond differently to oscillatory and unidirectional fluid flow profiles, J. Cell. Biochem. 100 (2007) 794–807. https://doi.org/10.1002/jcb.21089.

[125] R.L. van Bezooijen, A.L. Bronckers, R.A. Gortzak, P.C.W. Hogendoorn, L. van der Wee-Pals, W. Balemans, H.J. Oostenbroek, W. Van Hul, H. Hamersma, F.G. Dikkers, N.A.T. Hamdy, S.E. Papapoulos, C.W.G.M. Löwik, Sclerostin in Mineralized Matrices and van Buchem Disease, J. Dent. Res. 88 (2009) 569–574. https://doi.org/10.1177/0022034509338340.

[126] C. Uhler, G. V. Shivashankar, Regulation of genome organization and gene expression by nuclear mechanotransduction, Nat. Rev. Mol. Cell Biol. 18 (2017) 717–727. https://doi.org/10.1038/nrm.2017.101.

[127] S. Dupont, L. Morsut, M. Aragona, E. Enzo, S. Giulitti, M. Cordenonsi, F. Zanconato, J. Le Digabel, M. Forcato, S. Bicciato, N. Elvassore, S. Piccolo, Role of YAP/TAZ in mechanotransduction, Nature. 474 (2011) 179–183. https://doi.org/10.1038/nature10137.

[128] H. Hemmatian, A.D. Bakker, J. Klein-Nulend, G.H. van Lenthe, Aging, Osteocytes, and Mechanotransduction, Curr. Osteoporos. Rep. 15 (2017) 401–411. https://doi.org/10.1007/s11914-017-0402-z.

[129] L. You, S. Temiyasathit, P. Lee, C.H. Kim, P. Tummala, W. Yao, W. Kingery, A.M. Malone, R.Y. Kwon, C.R. Jacobs, Osteocytes as mechanosensors in the inhibition of bone resorption due to mechanical loading, Bone. 42 (2008) 172–179. https://doi.org/10.1016/J.BONE.2007.09.047.

[130] J. Li, E. Rose, D. Frances, Y. Sun, L. You, Effect of oscillating fluid flow stimulation on osteocyte mRNA expression, J. Biomech. 45 (2012) 247–251. https://doi.org/10.1016/j.jbiomech.2011.10.037.

[131] F. Meng, G.F. Murray, L. Kurgan, H.J. Donahue, Functional and structural characterization of osteocytic MLO-Y4 cell proteins encoded by genes differentially

expressed in response to mechanical signals in vitro, Sci. Rep. 8 (2018) 6716. https://doi.org/10.1038/s41598-018-25113-4.

[132] C. Wittkowske, G.C. Reilly, D. Lacroix, C.M. Perrault, In Vitro Bone Cell Models: Impact of Fluid Shear Stress on Bone Formation, Front. Bioeng. Biotechnol. 4 (2016) 87. https://doi.org/10.3389/fbioe.2016.00087.

[133] S. Weinbaum, S.C. Cowin, Y. Zeng, A model for the excitation of osteocytes by mechanical loading-induced bone fluid shear stresses, J. Biomech. 27 (1994) 339–360. https://doi.org/10.1016/0021-9290(94)90010-8.

[134] M.L. Knothe Tate, R. Steck, M.R. Forwood, P. Niederer, In vivo demonstration of load-induced fluid flow in the rat tibia and its potential implications for processes associated with functional adaptation., J. Exp. Biol. 203 (2000) 2737–45. http://www.ncbi.nlm.nih.gov/pubmed/10952874 (accessed August 31, 2019).

[135] X.L. Lu, B. Huo, M. Park, X.E. Guo, Calcium response in osteocytic networks under steady and oscillatory fluid flow, Bone. 51 (2012) 466–473. https://doi.org/10.1016/j.bone.2012.05.021.

[136] H.C. Blair, Q.C. Larrouture, Y. Li, H. Lin, D. Beer-Stoltz, L. Liu, R.S. Tuan, L.J. Robinson, P.H. Schlesinger, D.J. Nelson, Osteoblast Differentiation and Bone Matrix Formation In Vivo and In Vitro., Tissue Eng. Part B. Rev. 23 (2017) 268–280. https://doi.org/10.1089/ten.TEB.2016.0454.

[137] V. Deepak, P. Kayastha, L.M. McNamara, Estrogen deficiency attenuates fluid flow-induced [Ca2+]i oscillations and mechanoresponsiveness of MLO-Y4 osteocytes, FASEB J. 31 (2017) 3027–3039. https://doi.org/10.1096/fj.201601280R.

[138] K.J. Lewis, D. Frikha-Benayed, J. Louie, S. Stephen, D.C. Spray, M.M. Thi, Z. Seref-Ferlengez, R.J. Majeska, S. Weinbaum, M.B. Schaffler, Osteocyte calcium signals encode strain magnitude and loading frequency in vivo, Proc. Natl. Acad. Sci. 114 (2017) 11775–11780. https://doi.org/10.1073/pnas.1707863114.

[139] M. Hu, G.-W. Tian, D.E. Gibbons, J. Jiao, Y.-X. Qin, Dynamic fluid flow induced

mechanobiological modulation of in situ osteocyte calcium oscillations, Arch. Biochem. Biophys. 579 (2015) 55–61. https://doi.org/10.1016/j.abb.2015.05.012.

[140] X.E. Guo, E. Takai, X. Jiang, Q. Xu, G.M. Whitesides, J.T. Yardley, C.T. Hung, E.M. Chow, T. Hantschel, K.D. Costa, Intracellular calcium waves in bone cell networks under single cell nanoindentation., Mol. Cell. Biomech. 3 (2006) 95–107. http://www.ncbi.nlm.nih.gov/pubmed/17263256 (accessed August 14, 2019).

[141] A.E. Morrell, G.N. Brown, S.T. Robinson, R.L. Sattler, A.D. Baik, G. Zhen, X. Cao, L.F. Bonewald, W. Jin, L.C. Kam, X.E. Guo, Mechanically induced Ca2+ oscillations in osteocytes release extracellular vesicles and enhance bone formation, Bone Res. 6 (2018) 6. https://doi.org/10.1038/s41413-018-0007-x.

[142] M. Hagiwara, T. Kawahara, F. Arai, Local streamline generation by mechanical oscillation in a microfluidic chip for noncontact cell manipulations Related Articles, Cit. Appl. Phys. Lett. 101 (2012) 74102. https://doi.org/10.1063/1.4746247.

[143] S. Jeon, S. Kim, S. Ha, S. Lee, E. Kim, S.Y. Kim, S.H. Park, J.H. Jeon, S.W. Kim, C. Moon, B.J. Nelson, J. young Kim, S.W. Yu, H. Choi, Magnetically actuated microrobots as a platform for stem cell transplantation, Sci. Robot. 4 (2019). https://doi.org/10.1126/scirobotics.aav4317.

[144] W. Hu, Q. Fan, A.T. Ohta, An opto-thermocapillary cell micromanipulator, Lab Chip. 13 (2013) 2285–2291. https://doi.org/10.1039/c3lc50389e.

[145] L.Y. Yeo, J.R. Friend, Ultrafast microfluidics using surface acoustic waves, in: Biomicrofluidics, American Institute of Physics Inc., 2009: p. 012002. https://doi.org/10.1063/1.3056040.

[146] L. Meng, F. Cai, P. Jiang, Z. Deng, F. Li, L. Niu, Y. Chen, J. Wu, H. Zheng, On-chip targeted single cell sonoporation with microbubble destruction excited by surface acoustic waves, Appl. Phys. Lett. 104 (2014) 073701. https://doi.org/10.1063/1.4865770.

[147] J. Shi, D. Ahmed, X. Mao, S.C.S. Lin, A. Lawit, T.J. Huang, Acoustic tweezers: Patterning cells and microparticles using standing surface acoustic waves (SSAW), Lab

Chip. 9 (2009) 2890–2895. https://doi.org/10.1039/b910595f.

[148] A.A.S. Bhagat, H.W. Hou, L.D. Li, C.T. Lim, J. Han, Pinched flow coupled shear-modulated inertial microfluidics for high-throughput rare blood cell separation, Lab Chip. 11 (2011) 1870–1878. https://doi.org/10.1039/c0lc00633e.

[149] H.A. Nieuwstadt, R. Seda, D.S. Li, J.B. Fowlkes, J.L. Bull, Microfluidic particle sorting utilizing inertial lift force, Biomed. Microdevices. 13 (2011) 97–105. https://doi.org/10.1007/s10544-010-9474-6.

[150] S. Grilli, P. Ferraro, Dielectrophoretic trapping of suspended particles by selective pyroelectric effect in lithium niobate crystals, Appl. Phys. Lett. 92 (2008) 232902. https://doi.org/10.1063/1.2943319.

[151] S.K. Srivastava, A. Gencoglu, A.R. Minerick, DC insulator dielectrophoretic applications in microdevice technology: A review, Anal. Bioanal. Chem. 399 (2011) 301–321. https://doi.org/10.1007/s00216-010-4222-6.

[152] W.A. Braff, A. Pignier, C.R. Buie, High sensitivity three-dimensional insulator-based dielectrophoresis, Lab Chip. 12 (2012) 1327–1331. https://doi.org/10.1039/c2lc21212a.

[153] W. Hu, K.S. Ishii, A.T. Ohta, Micro-assembly using optically controlled bubble microrobots, Appl. Phys. Lett. 99 (2011) 094103. https://doi.org/10.1063/1.3631662.

[154] Y. Sun, J.S. Evans, T. Lee, B. Senyuk, P. Keller, S. He, I.I. Smalyukh, Optical manipulation of shape-morphing elastomeric liquid crystal microparticles doped with gold nanocrystals, Appl. Phys. Lett. 100 (2012) 241901. https://doi.org/10.1063/1.4729143.

[155] K. Onda, F. Arai, Multi-beam bilateral teleoperation of holographic optical tweezers, Opt. Express. 20 (2012) 3633. https://doi.org/10.1364/oe.20.003633.

[156] M. Selman Sakar, E.B. Steager, D. Hyung Kim, M. Jun Kim, G.J. Pappas, E. Steager, D. Kim, M. Kim, G. Pappas, V. Kumar, V. Kumar, S. Cell, Single Cell Manipulation using Ferromagnetic Composite Microtransporters, Appl. Phys. Lett. 96 (2010) 43705. https://doi.org/10.1063/1.3293457.

[157] E. Diller, S. Floyd, C. Pawashe, M. Sitti, Control of multiple heterogeneous magnetic microrobots in two dimensions on nonspecialized surfaces, IEEE Trans. Robot. 28 (2012) 172–182. https://doi.org/10.1109/TRO.2011.2170330.

[158] S. Tottori, L. Zhang, F. Qiu, K.K. Krawczyk, A. Franco-Obregõn, B.J. Nelson, Magnetic helical micromachines: Fabrication, controlled swimming, and cargo transport, Adv. Mater. 24 (2012) 811–816. https://doi.org/10.1002/adma.201103818.

[159] D.H. Kim, U.K. Cheang, L. Khidai, D. Byun, M.J. Kim, Artificial magnetotactic motion control of Tetrahymena pyriformis using ferromagnetic nanoparticles: A tool for fabrication of microbiorobots, Appl. Phys. Lett. 97 (2010) 173702. https://doi.org/10.1063/1.3497275.

[160] Y. Akiyama, K. Iwabuchi, Y. Furukawa, K. Morishima, Long-term and room temperature operable bioactuator powered by insect dorsal vessel tissue, Lab Chip. 9 (2009) 140–144. https://doi.org/10.1039/b809299k.

[161] Y. Murayama, C.E. Constantinou, S. Omata, Micro-mechanical sensing platform for the characterization of the elastic properties of the ovum via uniaxial measurement, J. Biomech. 37 (2004) 67–72. https://doi.org/10.1016/S0021-9290(03)00242-2.

[162] T. Wakayama, A.C.F. Perry, M. Zuccotti, K.R. Johnson, R. Yanagimachi, Full-term development of mice from enucleated oocytes injected with cumulus cell nuclei, Nature. 394 (1998) 369–374. https://doi.org/10.1038/28615.

[163] X. Liu, R. Fernandes, A. Jurisicova, R.F. Casper, Y. Sun, In situ mechanical characterization of mouse oocytes using a cell holding device, Lab Chip. 10 (2010) 2154. https://doi.org/10.1039/c004706f.

[164] C. Bi, M. Guix, B. Johnson, W. Jing, D. Cappelleri, Design of Microscale Magnetic Tumbling Robots for Locomotion in Multiple Environments and Complex Terrains, Micromachines. 9 (2018) 68. https://doi.org/10.3390/mi9020068.

[165] J. Zhang, O. Onaizah, A. Sadri, E. Diller, A generic label-free microfluidic microobject sorter using a magnetic elastic diverter, Biomed. Microdevices. 19 (2017) 43.

https://doi.org/10.1007/s10544-017-0183-2.

[166] L. Wang, J. Dong, C.J. Xian, Strain amplification analysis of an osteocyte under static and cyclic loading: A finite element study, Biomed Res. Int. 2015 (2015). https://doi.org/10.1155/2015/376474.

[167] G.C. Goulet, D. Coombe, R.J. Martinuzzi, R.F. Zernicke, Poroelastic evaluation of fluid movement through the lacunocanalicular system, Ann. Biomed. Eng. 37 (2009) 1390–1402. https://doi.org/10.1007/s10439-009-9706-1.

[168] J. Zhang, O. Onaizah, K. Middleton, L. You, E. Diller, Reliable Grasping of Three-Dimensional Untethered Mobile Magnetic Microgripper for Autonomous Pick-and-Place, IEEE Robot. Autom. Lett. 2 (2017) 835–840. https://doi.org/10.1109/LRA.2017.2657879.

[169] B. Lautrup, Physics of continuous matter : exotic and everyday phenomena in the macroscopic world, Taylor & Francis, 2011. https://www.crcpress.com/Physics-of-Continuous-Matter-Exotic-and-Everyday-Phenomena-in-the-Macroscopic/Lautrup/p/book/9781420077001 (accessed August 14, 2019).

[170] R. Nalim, K. Pekkan, H. Bin Sun, H. Yokota, Oscillating Couette flow for in vitro cell loading, J. Biomech. 37 (2004) 939–942. https://doi.org/10.1016/j.jbiomech.2003.11.004.

[171] B. Huo, X.L. Lu, X.E. Guo, Intercellular calcium wave propagation in linear and circuit-like bone cell networks, Philos. Trans. R. Soc. A Math. Phys. Eng. Sci. 368 (2010) 617–633. https://doi.org/10.1098/rsta.2009.0221.

[172] K.J. Lewis, D. Frikha-Benayed, J. Louie, S. Stephen, D.C. Spray, M.M. Thi, Z. Seref-Ferlengez, R.J. Majeska, S. Weinbaum, M.B. Schaffler, Osteocyte calcium signals encode strain magnitude and loading frequency in vivo, Proc. Natl. Acad. Sci. 114 (2017) 11775–11780. https://doi.org/10.1073/PNAS.1707863114.

[173] X.L. Lu, B. Huo, M. Park, X.E. Guo, Calcium response in osteocytic networks under steady and oscillatory fluid flow, Bone. 51 (2012) 466–473. https://doi.org/10.1016/j.bone.2012.05.021.

[174] R. Hambli, R. Rieger, R. Hambli, · R Rieger, Physiologically based mathematical model

of transduction of mechanobiological signals by osteocytes, Biomech Model Mechanobiol. 11 (2012) 83–93. https://doi.org/10.1007/s10237-011-0294-2.

[175] K. Middleton, A. Kondiboyina, M. Borrett, Y. Cui, X. Mei, L. You, Microfluidics approach to investigate the role of dynamic similitude in osteocyte mechanobiology, J. Orthop. Res. 36 (2017) 663–671. https://doi.org/10.1002/jor.23773.

[176] D. Jing, A.D. Baik, X.L. Lu, B. Zhou, X. Lai, L. Wang, E. Luo, X.E. Guo, In situ intracellular calcium oscillations in osteocytes in intact mouse long bones under dynamic mechanical loading., FASEB J. 28 (2014) 1582–92. https://doi.org/10.1096/fj.13-237578.

[177] X. Zhang, Z. Zhang, Microfluidic passive flow regulatory device with an integrated check valve for enhanced flow control, Micromachines. 10 (2019). https://doi.org/10.3390/mi10100653.

[178] Y. Arango, Y. Temiz, O. Gökçe, E. Delamarche, Electro-actuated valves and self-vented channels enable programmable flow control and monitoring in capillary-driven microfluidics, Sci. Adv. 6 (2020) eaay8305. https://doi.org/10.1126/sciadv.aay8305.

[179] M.E. Brett, S. Zhao, J.L. Stoia, D.T. Eddington, Controlling flow in microfluidic channels with a manually actuated pin valve, Biomed. Microdevices. 13 (2011) 633–639. https://doi.org/10.1007/s10544-011-9533-7.

[180] P. Song, C. Chen, J. Qu, P. Ou, M.H.T. Dastjerdi, Z. Mi, J. Song, X. Liu, Rolled-up SiO_x/SiN_x microtubes with an enhanced quality factor for sensitive solvent sensing, Nanotechnology. 29 (2018) 415501. https://doi.org/10.1088/1361-6528/aad0b1.

[181] Y. Jing, J. Jing, L. Ye, X. Liu, S.E. Harris, R.J. Hinton, J.Q. Feng, Chondrogenesis and osteogenesis are one continuous developmental and lineage defined biological process, Sci. Rep. 7 (2017). https://doi.org/10.1038/s41598-017-10048-z.

[182] Y. Jing, J. Jing, K. Wang, K. Chan, S.E. Harris, R.J. Hinton, J.Q. Feng, Vital roles of β-catenin in trans-differentiation of chondrocytes to bone cells, Int. J. Biol. Sci. 14 (2018) 1–9. https://doi.org/10.7150/ijbs.23165.

Appendices

Appendix I: Mechanical Stimulation of Tendon Cells

In a collaboration with Dr. Feng from Texas A&M, we did some work on the characterization of tendon cell mechanical property, as well as their behaviour under mechanical stimulation. This is within an effort to understand the role mechanical stimulation plays in the differentiation of tendon cells. Previously, it is well understood that cartilage differentiation (chondrogenesis) and bone differentiation (osteogenesis) are two different processes. However, recent work done by Dr. Feng and other groups have suggested a new dogma where the two processes is continuous where chondrogenesis eventually leads to osteogenesis [181][182]. This is a ground-breaking discovery, as it provides a potential solution to source cartilage cells from reversed osteogenesis. Similarly, it is observed that tendon cells might have similar relations with bone cells (unpublished work). Due to the function of tendon in the joint, it is suspected that different degree of mechanical stimulation of tendon might result in different stages of differentiation in between tendon cell and bone cell. Our work focused on the *in vitro* experiments where we analyzed the effect of mechanical stimulation on primary tendon cells.

The first step is to understand the mechanical loading experienced by tendon cells *in vivo*. We designed a simple strain sensor circuit equipped with a commercial strain sensor that is able to measure the tendon strain during regular joint movement. We fitted the strain sensor to a dissected dog limb using biocompatible glue and measured the strain while simulating regular joint movement *ex vivo*. The resistance of the strain sensor was tuned so that the range of joint movement resulted in an observable change in strain sensor feedback. Sample data is plotted in Figure I.1, were we simulated several normal joint movements and recorded the strain values during these mechanical loading. The next step is to correlate these strain values to the force readings in order to understand the level of mechanical loading the tendon is experiencing.

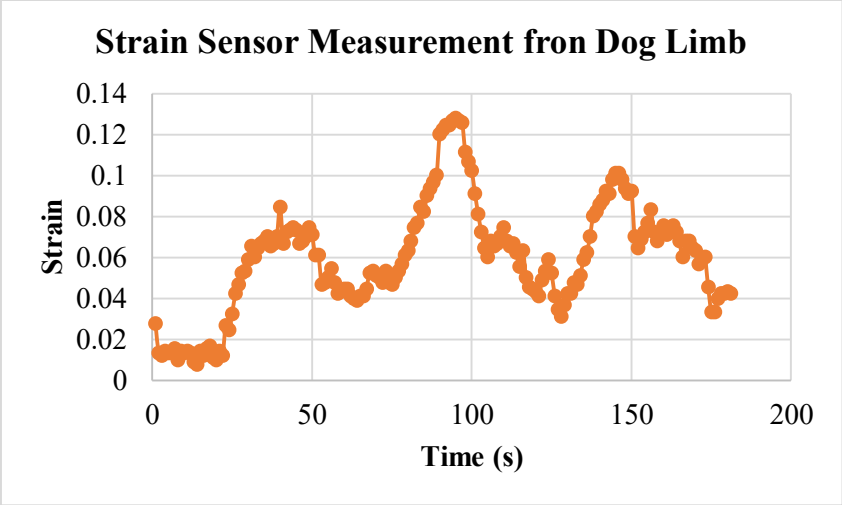

Figure I.1: Sample data from strain sensor. Raw data from the strain sensor plotted against time. Various joint movement was simulated on the god limb while sensor was collecting data.

Very limited literature is available that provides a modulus value for tendons, hence we needed to measure the mechanical properties of tendon *ex vivo*. Using dog knee tendon as the animal model, we measured the stress-strain curve from tendon explants using a mechanical stretcher equip with a force sensor module. The tendons were pulled until they failed and the relation between stress and strain was recorded (Figure I.2). We were able to derive a correlation between force and strain, which can be used to translate data from figure I.1 into force values that can be used in future *in vitro* mechanical loading experiments of tendon cells.

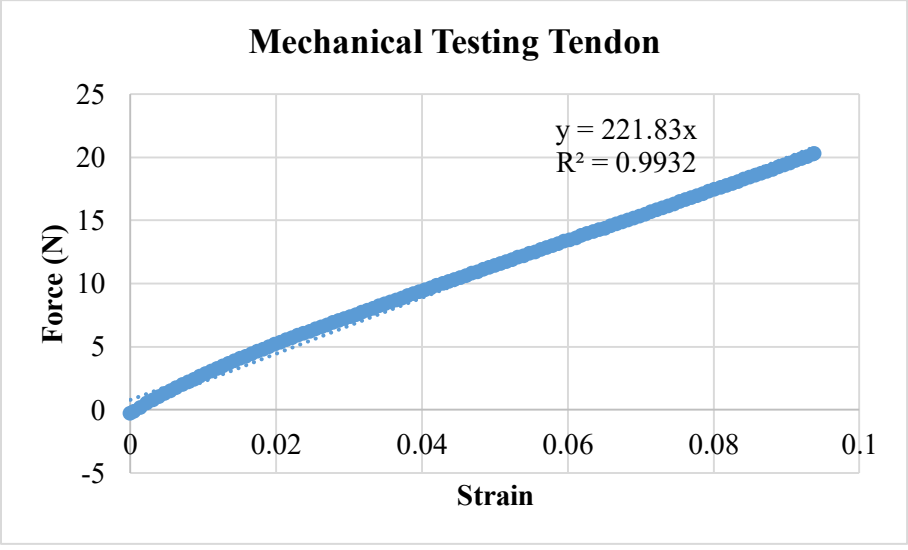

Figure I2: Example of mechanical testing result for a dog tendon. Stress-strain curve recorded from a mechanical stretcher testing of dog tendons. Plotted the linear segment of the data to obtain a correlation between the two variables.

We also worked with primary tendon cells *in vitro* to look at changes in gene expression levels when these cells are exposed to mechanical loading. Using the Flexcell membrane stretching system, we exposed the primary tendon cells to 10% strain for 2 hrs before extracting mRNA to quantify gene expression 24 hrs after stimulation. From the gene expression changes observed from the initial experiments, there is a decrease in cartilage genes and an increase in hard-tissue related gene expression (Figure I.3). This suggests that mechanical loading might be a key factor in the trans-differentiation of tendon cells into bone cells. However, there are large variations within the current data, and more extensive experiments will be needed to validate the changes we observed after mechanical stretching.

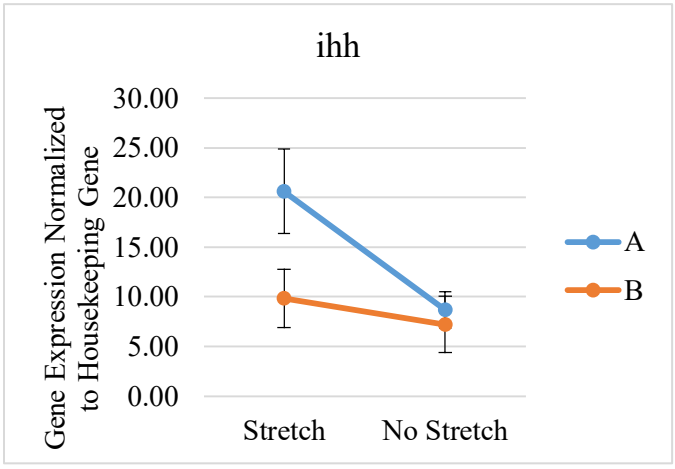

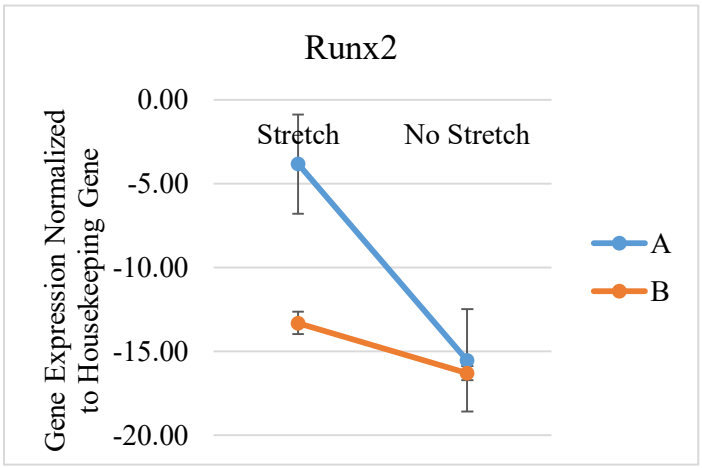

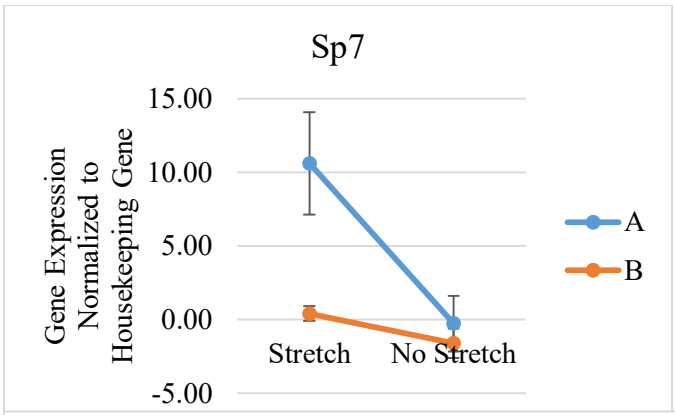
Sp7
Gene Expression Normalized to Housekeeping Gene
15.00
10.00
5.00
0.00
-5.00
Stretch
No Stretch
A
B

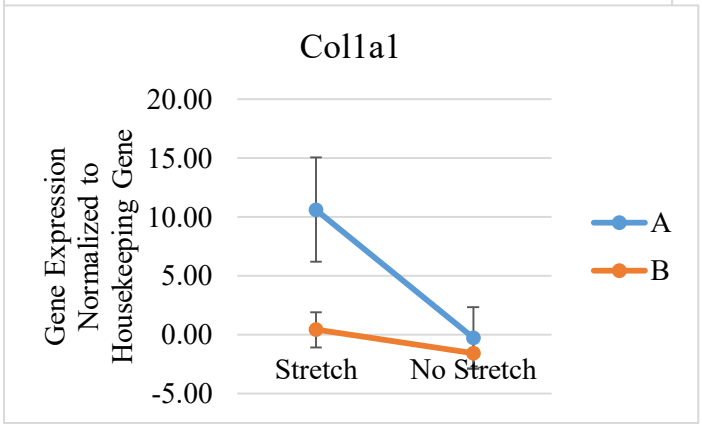
Col1a1
Gene Expression Normalized to Housekeeping Gene
20.00
15.00
10.00
5.00
0.00
-5.00
Stretch
No Stretch
A
B

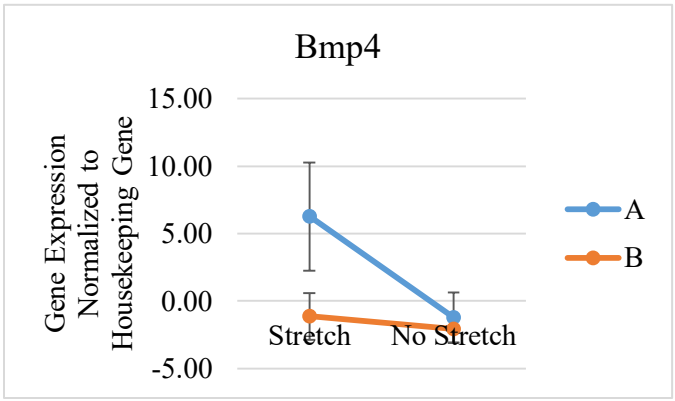
Bmp4
Gene Expression Normalized to Housekeeping Gene
15.00
10.00
5.00
0.00
-5.00
Stretch
No Stretch
A
B

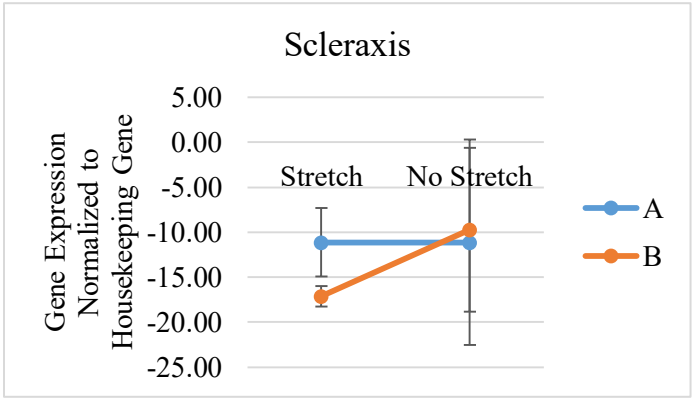
Scleraxis
Gene Expression Normalized to Housekeeping Gene
5.00
0.00
-5.00
-10.00
-15.00
-20.00
-25.00
Stretch
No Stretch
A
B

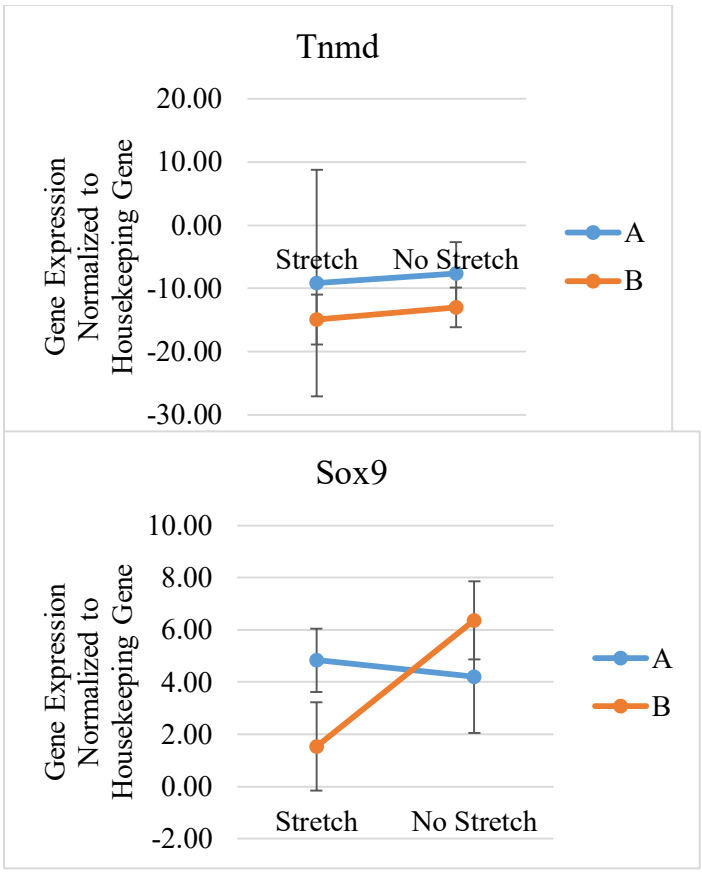

Figure I.3: Gene expression changes for primary tendon cells. Normalized gene expression level from Flexcell testing of primary tendon cells seeded on elastic membranes. Ihh, Runx2, Sp7, Col1a1, and Bmp4 are genes related to hard tissue, showing an increase after cells experienced mechanical loading. Scleraxis, Tnmd, and Sox9 are genes related to tendon differentiation, and saw a decrease after exposure to mechanical loading. Large variations in data collected can be seen from the error bars. A and B represent two separate trials.

Copyright Acknowledgements

All contents in Chapter 2 have been submitted for publication in Integrative Biology.

All contents in Chapter 3 have been published in Journal of Orthopaedic Research.

All contents in Chapter 4 have been published in PLOS One.